

The background of the slide is a light blue and white illustration of the Earth from space. Several satellites are shown in various orbits around the planet. Yellow beams of light emanate from each satellite, pointing towards the Earth's surface, symbolizing remote sensing or data collection. The overall aesthetic is clean and technical.

An On-Orbit Calibration Procedure For Spaceborne Microwave Radiometers Using Special Spacecraft Attitude Maneuvers

*Spencer Lee Farrar
Central Florida Remote Sensing Lab
University of Central Florida*

*PhD Defense
April 7th, 2015*

Presentation Outline

- Purpose of this Dissertation
- TRMM, TMI, & the Inertial Hold
- Analyses Discussed:
 - Reflector Emissivity
 - Second Stokes Analysis using a Nadir-Look
- Recommendations
- Conclusion
- Future Work

Dissertation Objectives

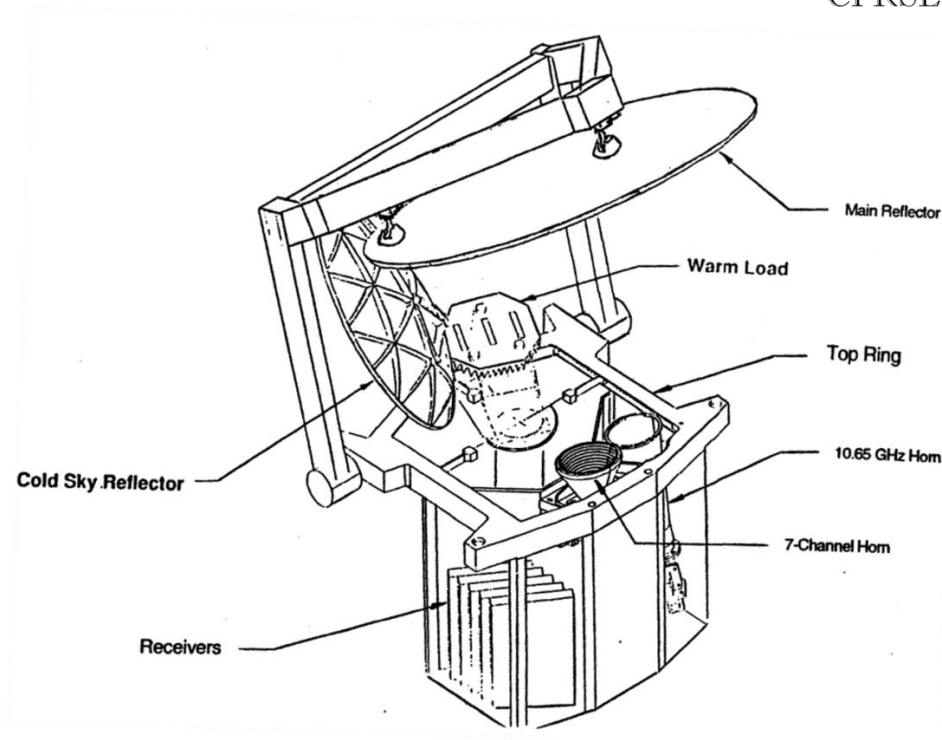
- Develop & document methods for post-launch calibration of spaceborne microwave radiometers
 - Using Calibration Attitude Maneuvers (CAM)
 - Use pre-existing & new CAMs
- Use TRMM Deep Space Calibration (DSC) maneuvers for developing this plan
 - Jan & Sept 1998 (7 maneuvers) and July 2014 (3 maneuvers)
- Calibrate TRMM Microwave Imager (TMI)
 - Use this information for the final version of the TB data product (Archived/Legacy)

Why CAMs?

- Common post-launch calibration methods:
 - Uses Earth observations which requires months of the instrument observations to detect biases
 - Inter-satellite calibration requires the other instrument to be stable
 - Heavily dependent on (imperfect) radiative transfer models that require ancillary data (weather models)
- Calibration Attitude Maneuvers (CAMs):
 - Provide early & accurate results on the performance of the instrument
 - Deep Space Calibration (DSC) Maneuvers (DSCM) use the known homogenous non-polarized cosmic microwave background (CMB)
 - Sharp transitions in TB at Earth's Horizon
 - Nadir-Look: Instruments Line of sight aligned to geodetic vector
- Overall, uses simpler well known scenes

TMI

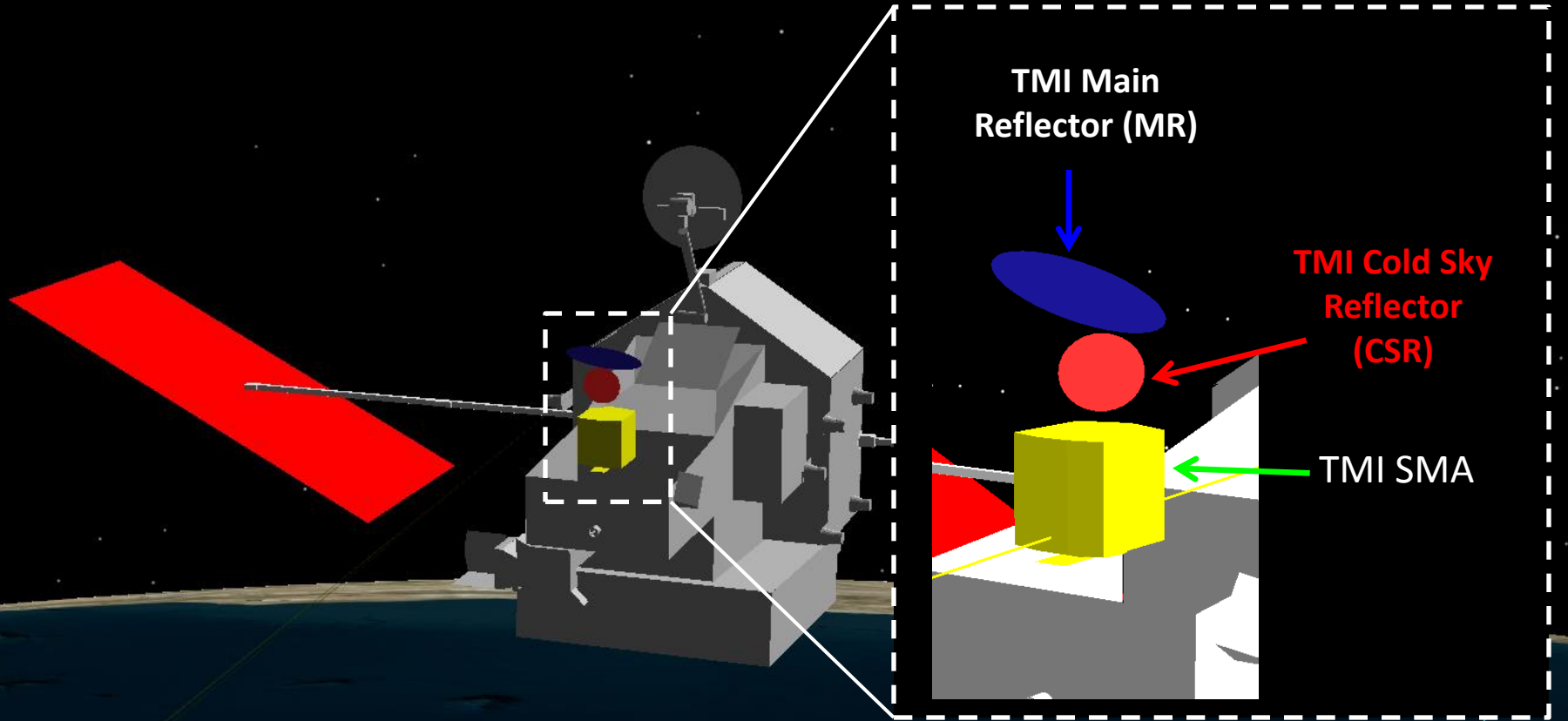
- TRMM Microwave Imager (TMI)
 - TRMM was launched on Nov 28, 1997
 - Conically scanning radiometer
 - Main reflector is emissive
 - Over 17 Years of operation
 - Will be turned off on April 8, 2015
 - Re-enters Earth atmosphere on June 11, 2015



Red Boxes: Channels we can confidently reconstruct T_A

Center Frequencies(GHz)	10.65	10.65	19.35	19.35	21.3	37.0	37.0	85.5	85.5
Polarization	V	H	V	H	V	V	H	V	H
Bandwidth (MHz)	100	100	500	500	200	2000	2000	3000	3000
Sensitivity (K)	0.63	0.54	0.50	0.47	0.71	0.36	0.31	0.52	0.93
IFOV (km x km)	63 x 37	63 x 37	30 x 18	30 x 18	23 x 18	16 x 9	16 x 9	7 x 5	7 x 5
Sampling Interval (km x km)	13.9x9.1	13.9x9.1	13.9x9.1	13.9x9.1	13.9x9.1	13.9x9.1	13.9x9.1	13.9x4.6	13.9x4.6
Integration Time (msec)	6.6	6.6	6.6	6.6	6.6	6.6	6.6	3.3	3.3

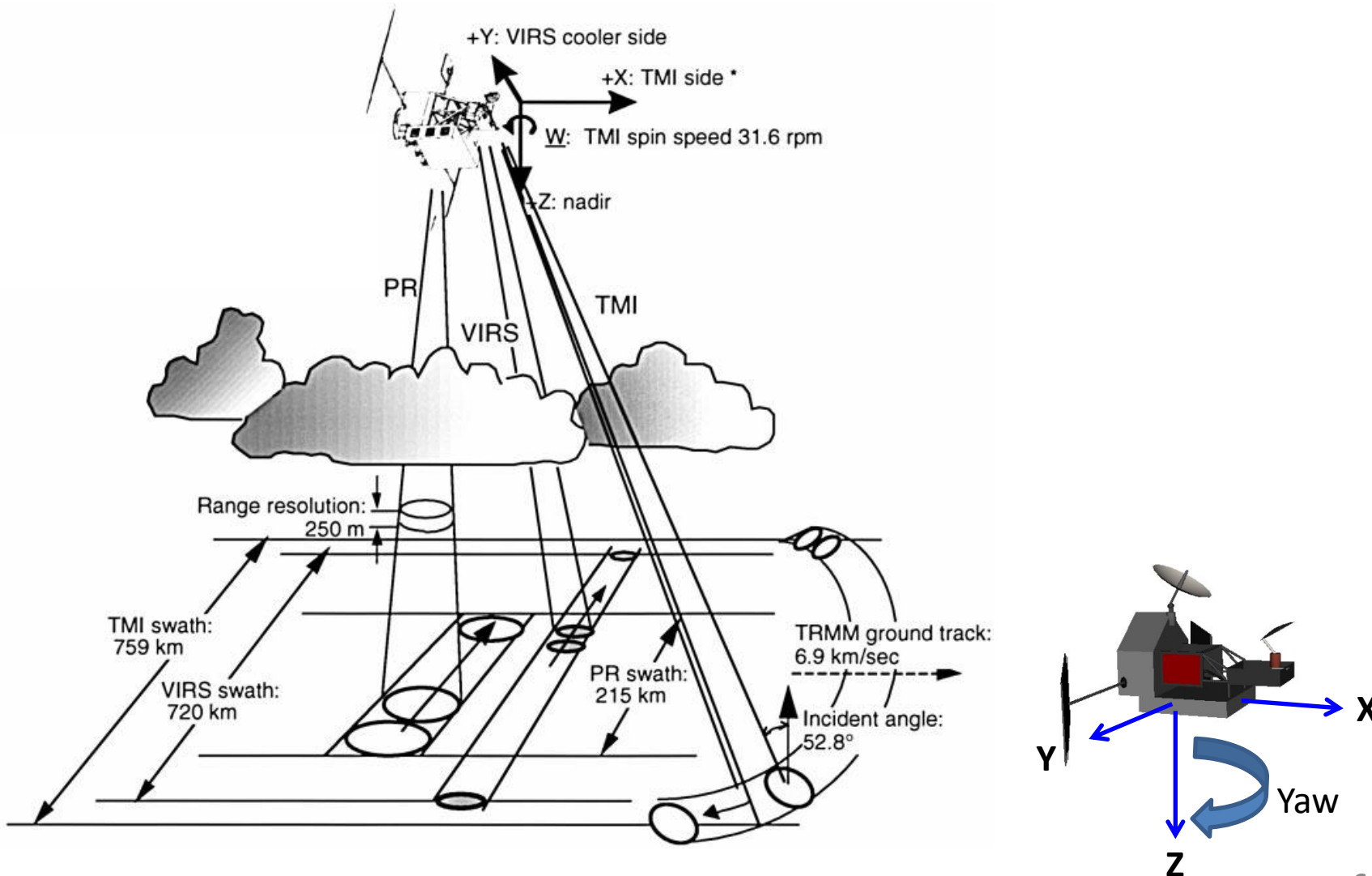
Tropical Rainfall Measuring Mission (TRMM) Spacecraft



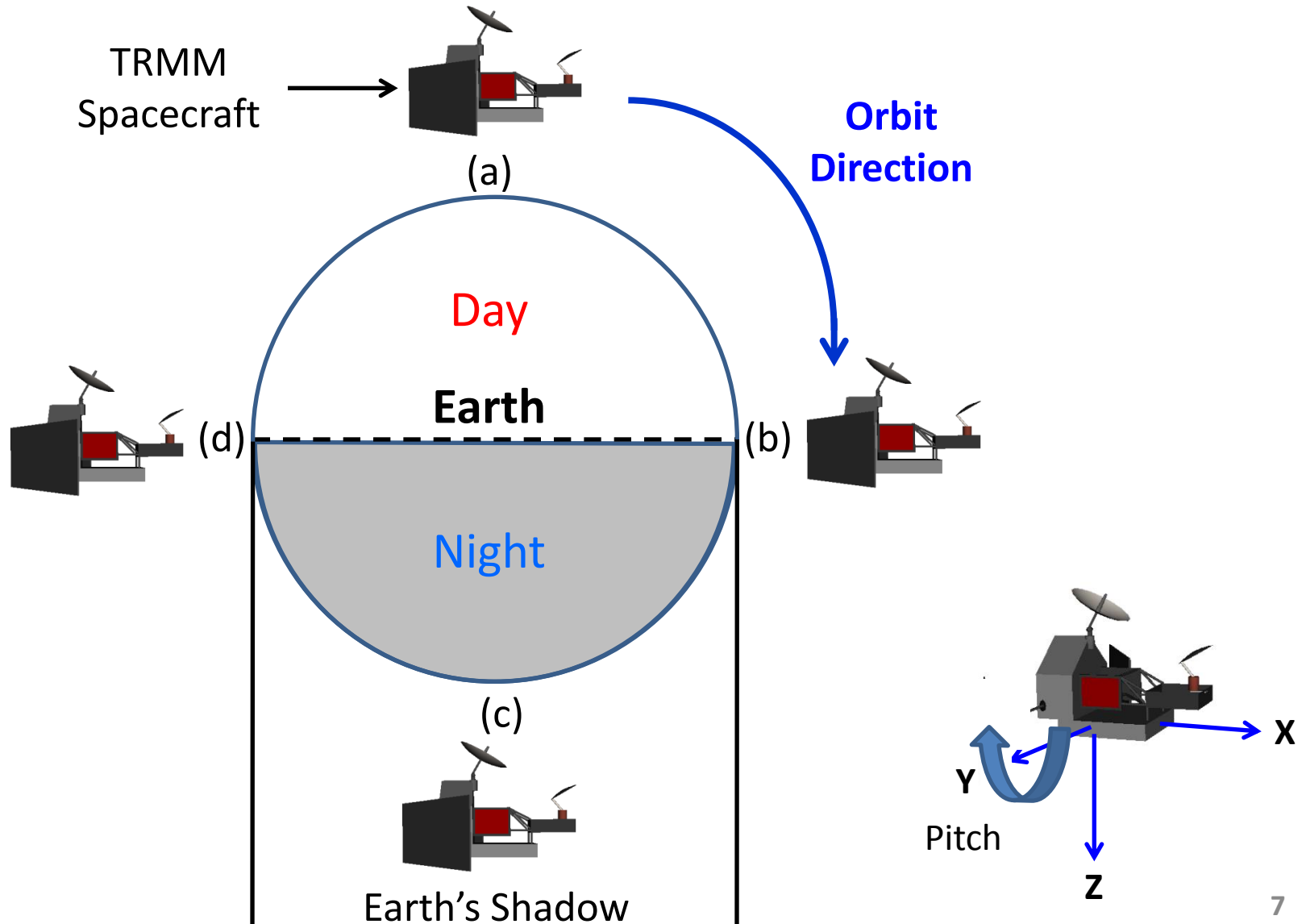
0.001 sec



TMI Scanning Geometry

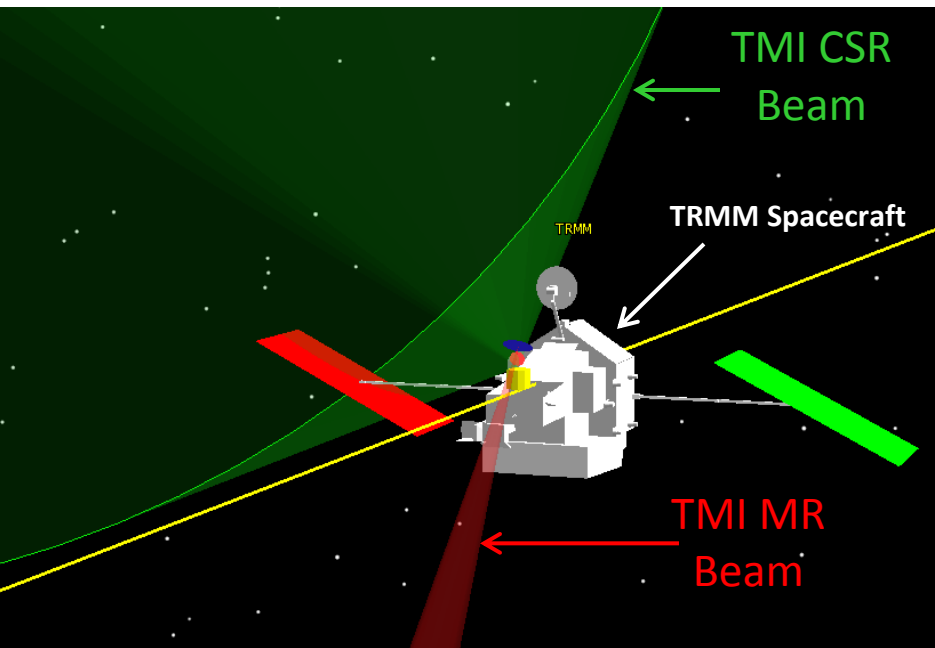


Example of an Inertial Hold at Yaw=0°



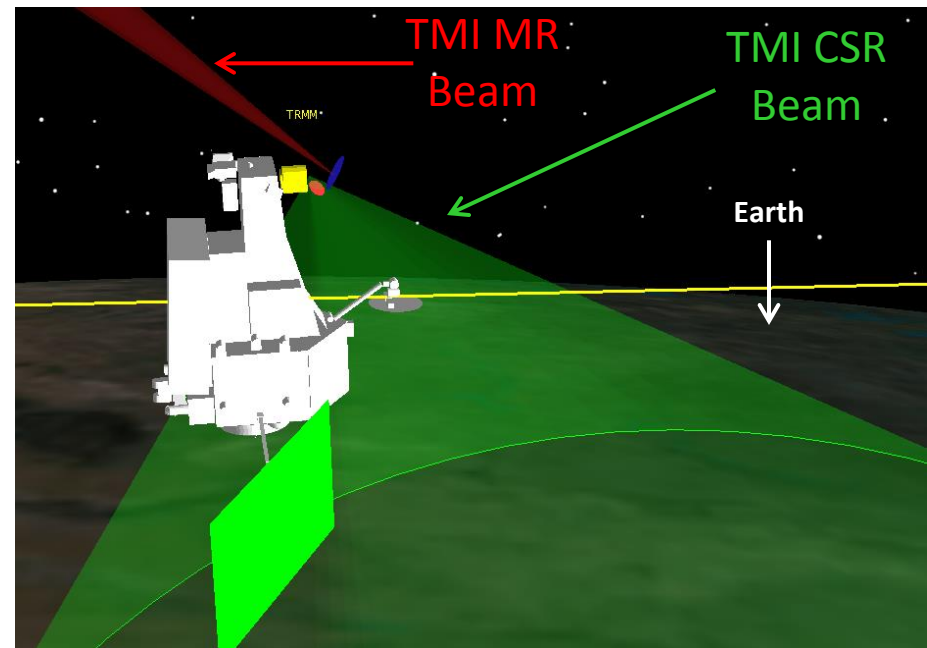
Main Reflector & Cold Sky Reflector Beams

Earth Pointing Mode



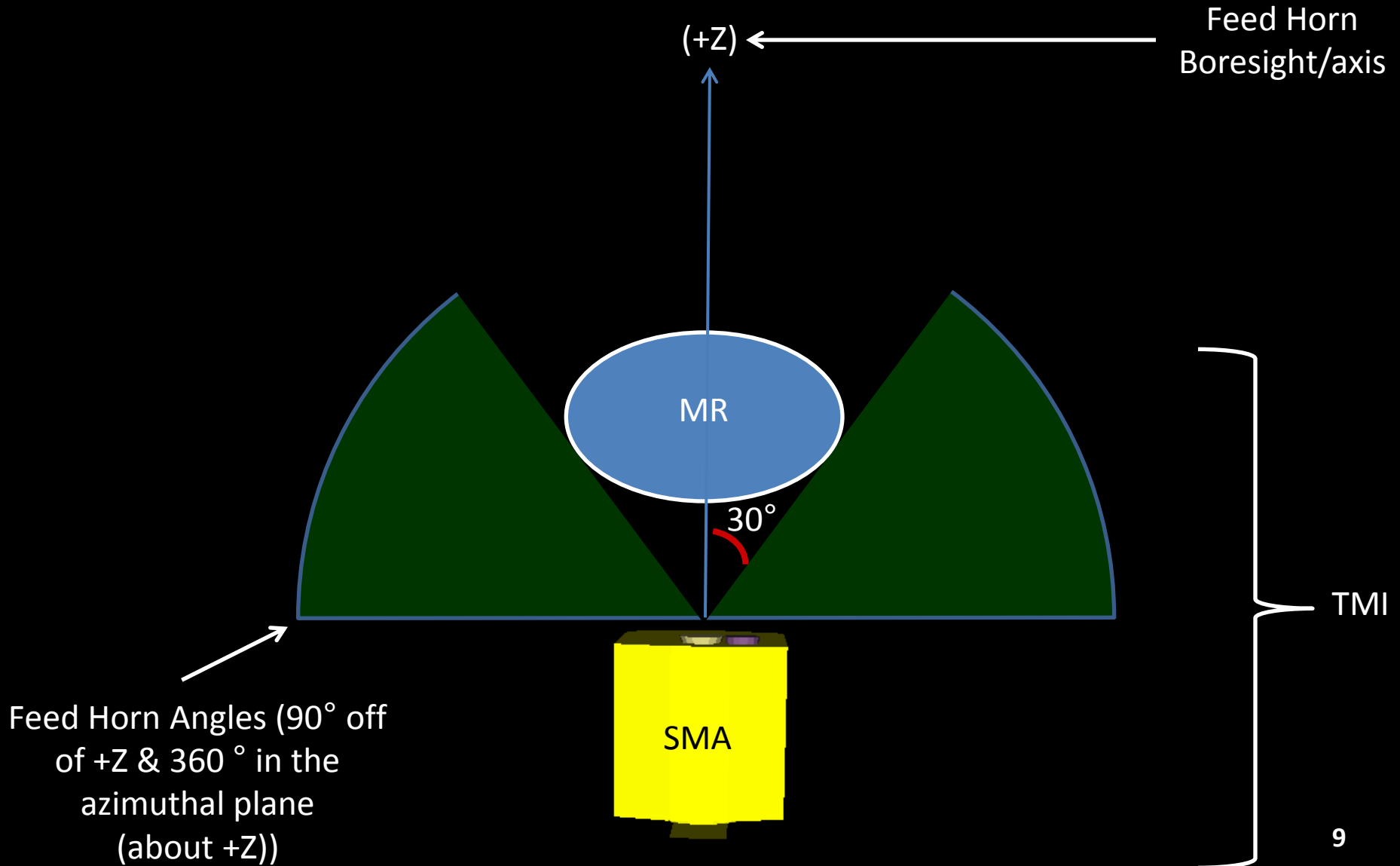
(a)

DSC Mode



(b)

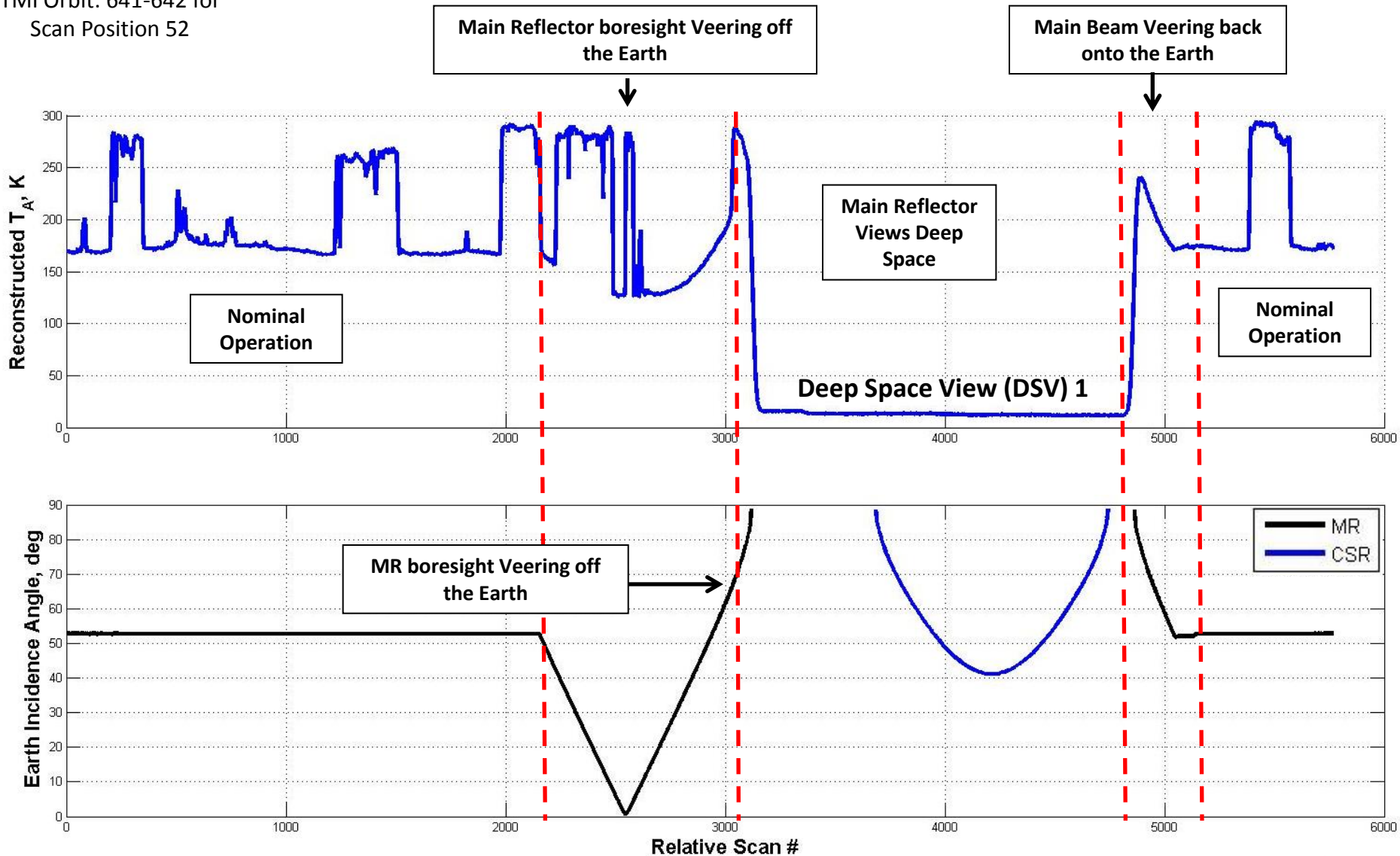
Depicting Spillover Region



Time Series During T_A (10 V-pol) & EIA



TMI Orbit: 641-642 for
Scan Position 52



Analyses Performed

- Data Products Used:

- TMI 1A11 & Base files: radiometric counts, temperature sensors, geolocation purposes
- ERA-I from CSU for RTM

- Dissertation Covers:

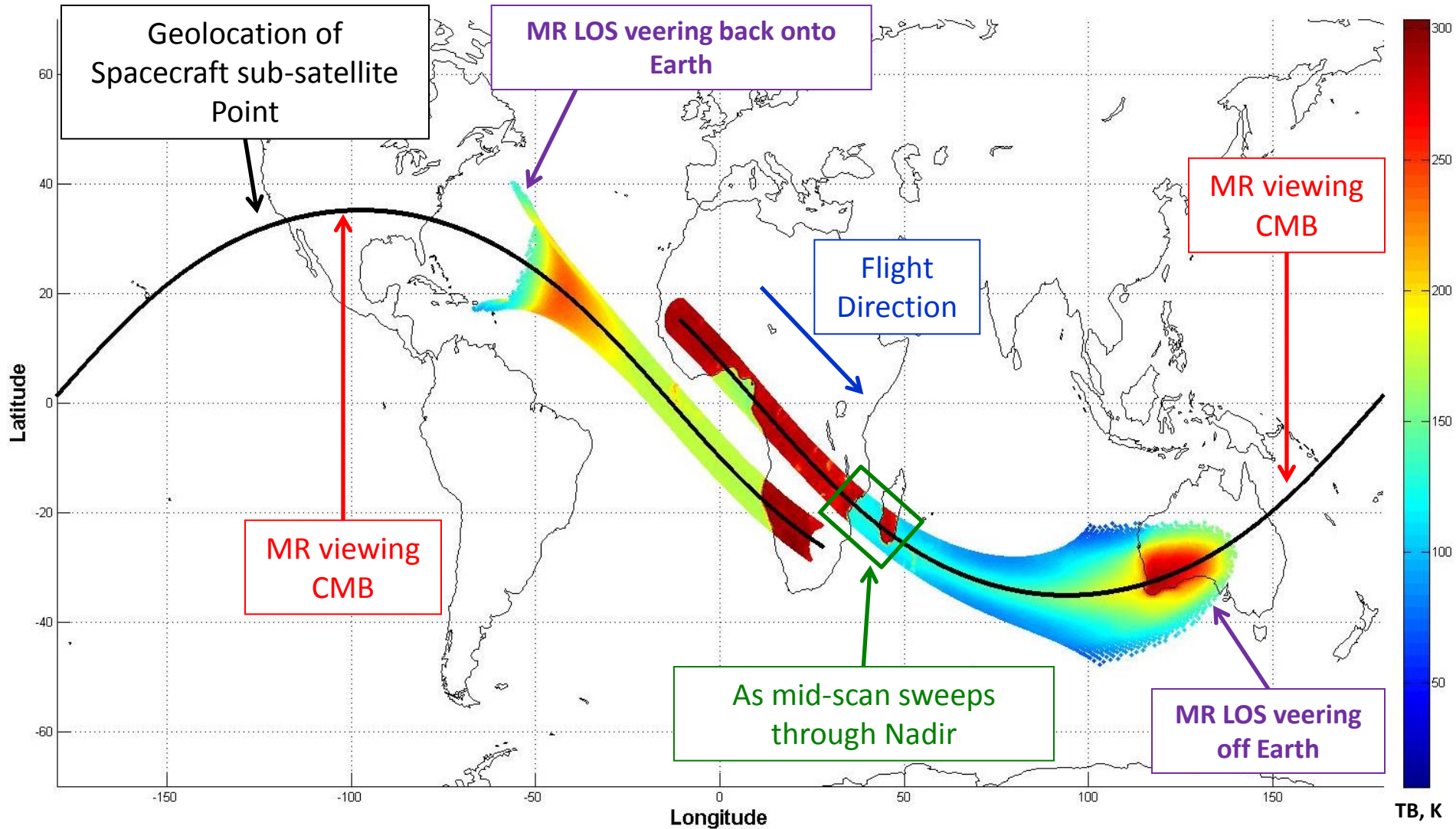
- Reconstruction of T_A
 - First presented in Proposal
 - Developed 2nd method
- Beamwidth & Boresight Point
 - Uses the Earth's Horizon
- Along-scan Bias
 - Very good agreement with RSS' results
- TMI Emissive Reflector
- Second Stokes using Nadir-Look

Discussed within this dissertation

Discussed in Dissertation & is placed in backup slides

Discussed within this Presentation

T_a for 10.65 GHz V-Pol During DSCM 1



DSCM Sets

DSCM Set	DSCM #	Date	Orbit #	Yaw (°)	Altitude (km)
1	1 – 6	Jan 7, 1998	641-646	180	349
		Jan 8, 1998	657-662		
2	7	Sept 2, 1998	4393-4394	0	350
3	8-10	July 22, 2014	95023-95028	0	400
4	11-16	Feb 26, 2015	98452- 98457	0	350
		Feb 27, 2015	98468- 98473		
5	17-20	Mar 25-26, 2015	98878-98883	90	341
			98893-98898		

Analysis

TMI Main Reflector Emissivity

TMI's Emissive Main Reflector

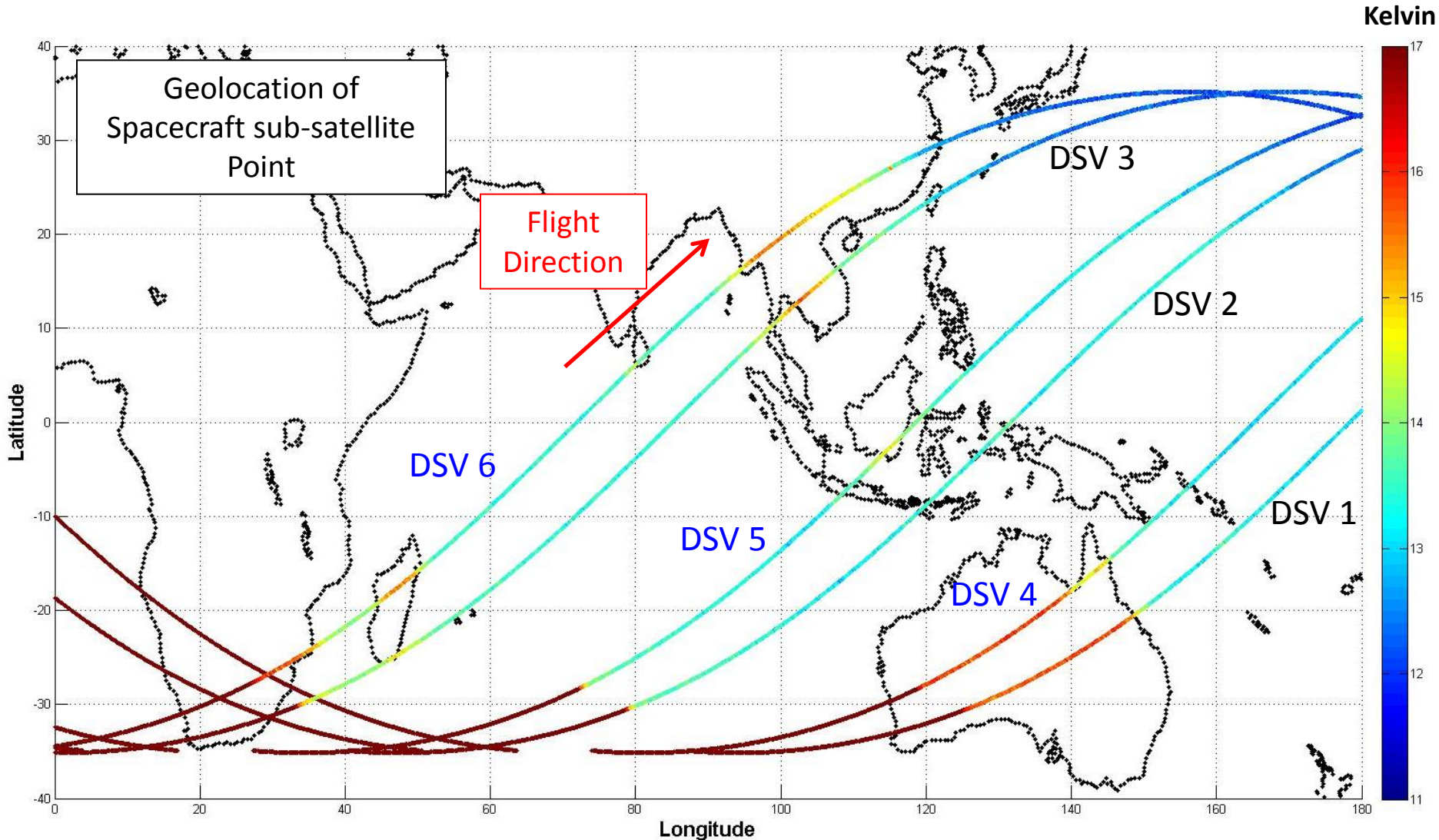
- Since the beginning of the mission, NASA observed a positive bias in TMI's T_B s
 - One theory was that RFI from TRMM's Precipitation Radar could be root cause (DSCM-7 in 1998 discarded this theory)
 - Since then it has been determined that TMI's MR is emissive as shown in RSS & CFRSL analyzes
 - Dependent on radiative transfer theory & intersatellite calibration

- An emissive reflector will reflect & emit energy

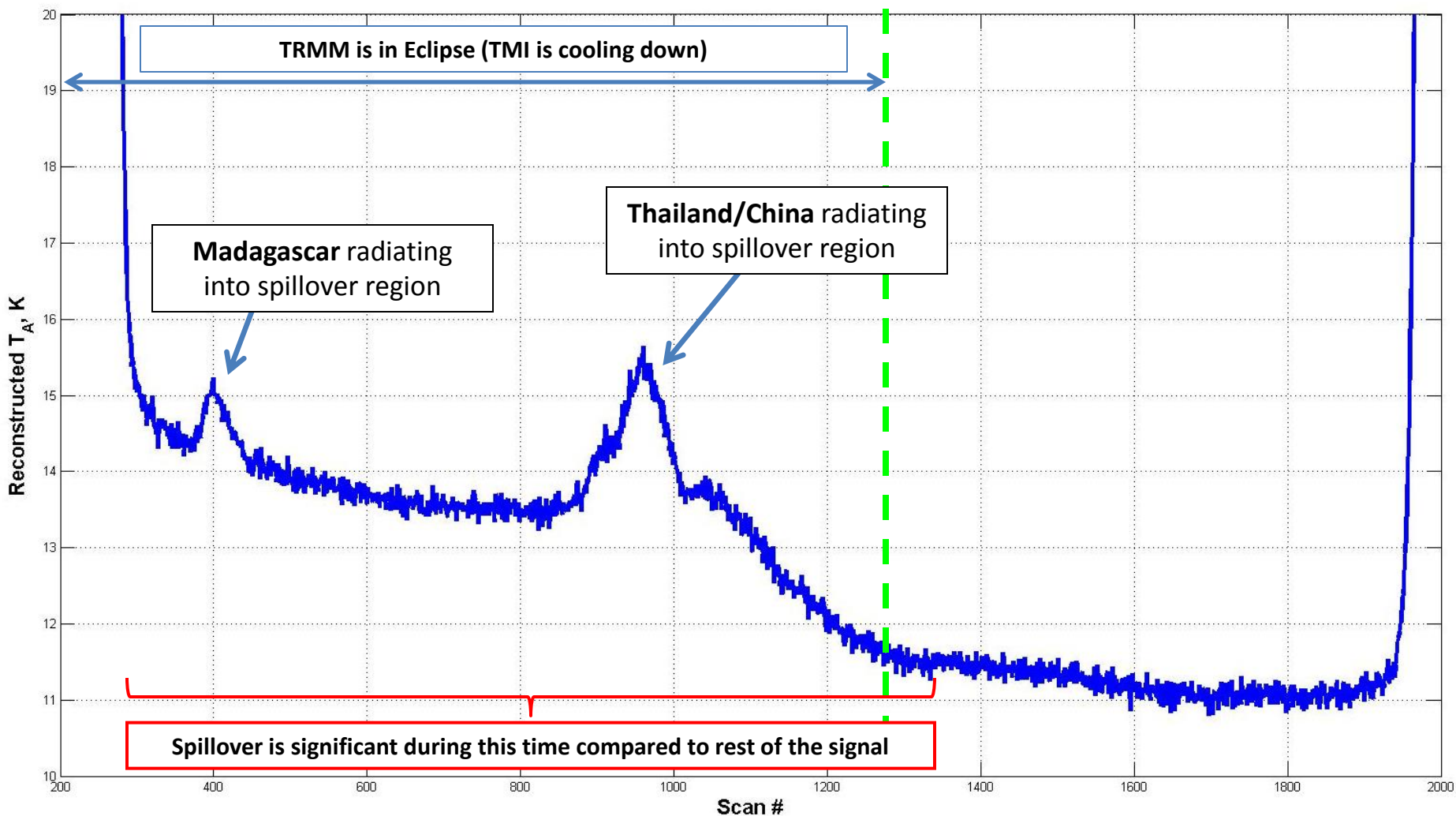
$$T'_{B,MR} = T_B \cdot (1 - \varepsilon) + T_{MR\text{ Physical}} \cdot \varepsilon \quad (\text{Eqn.1})$$

- T_B energy incident on the reflector, ε & $T_{MR\text{ Physical}}$ is the emissivity & physical temperature of the face of the reflector, respectively
- Goal: Determine the emissivity using the entire DSV time series

T_A (19 V-pol) Earth Contamination (Spillover) for DSV 1-6



Reconstruction of T_A for 10V

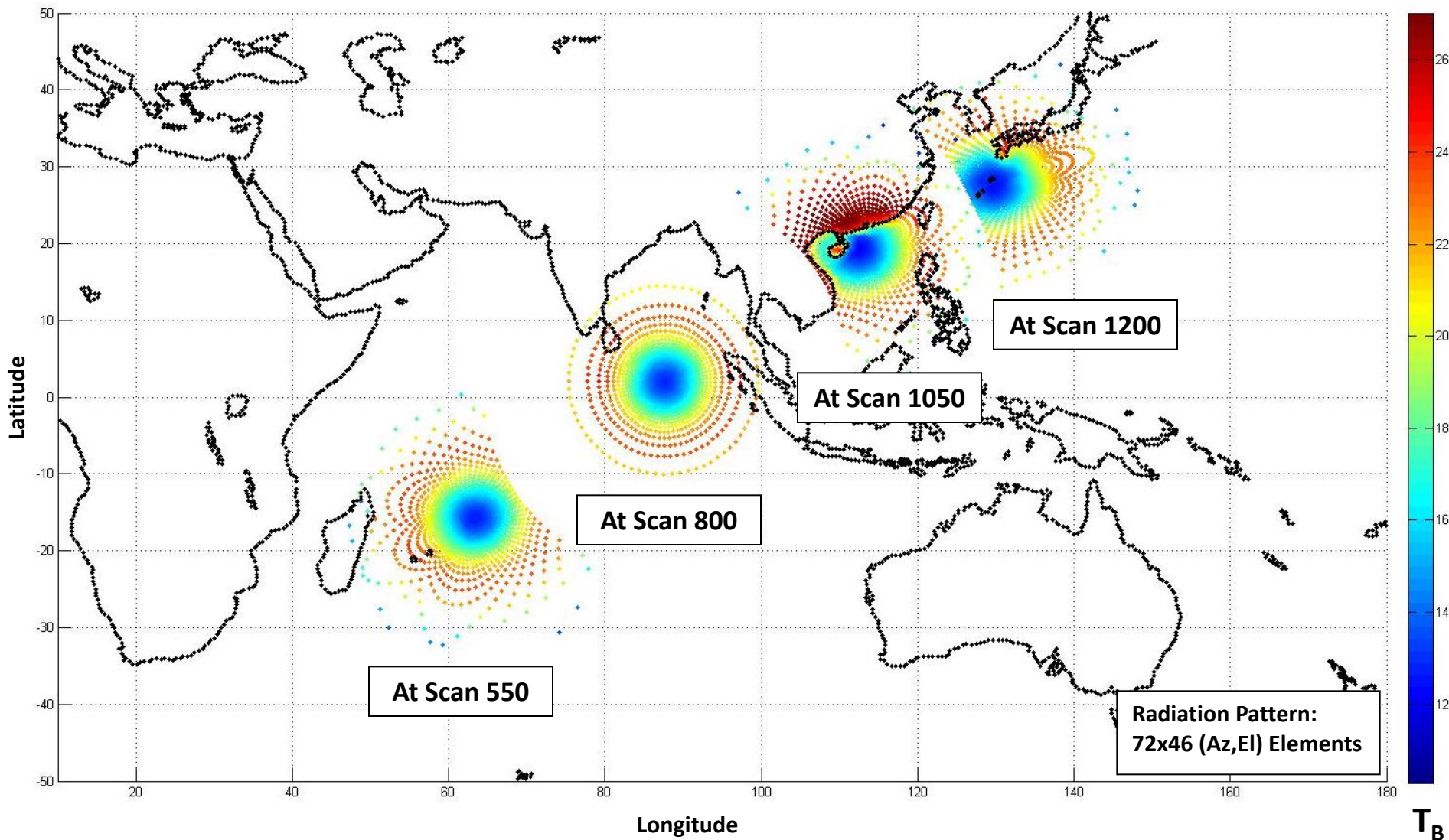


Removing Spillover

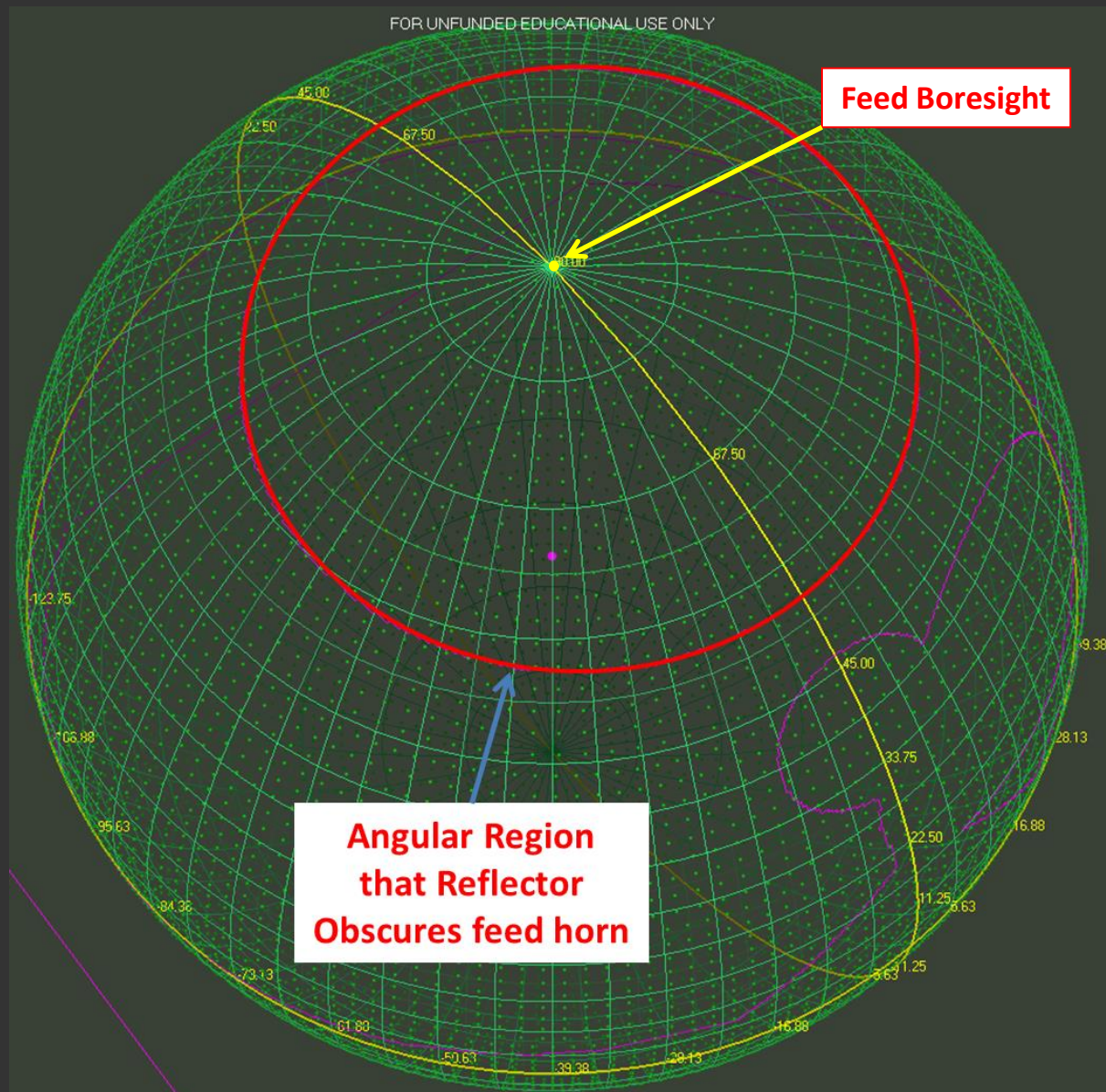
Removing Spillover Effect

- Overall we need to simulate the signal that the feed radiation pattern (primary pattern) is measuring
 - Need to characterize:
 - main reflector signal ($T'_{B,MR}$)
 - the spillover: illuminate parts of TMI & TRMM, Space, Earth (Land/Ocean)
1. Geolocate Radiation Pattern for removal of spillover (modified TMI geolocation code)
 - Obtain Feed Radiation Pattern (Primary) – the weighting function
 - Obscure Feed Pattern
 2. Simulate spillover portion that intersects Earth (discussed in Dissertation & Back-up slides)

Projection of Spillover with assigned TB Values (11 V-pol)

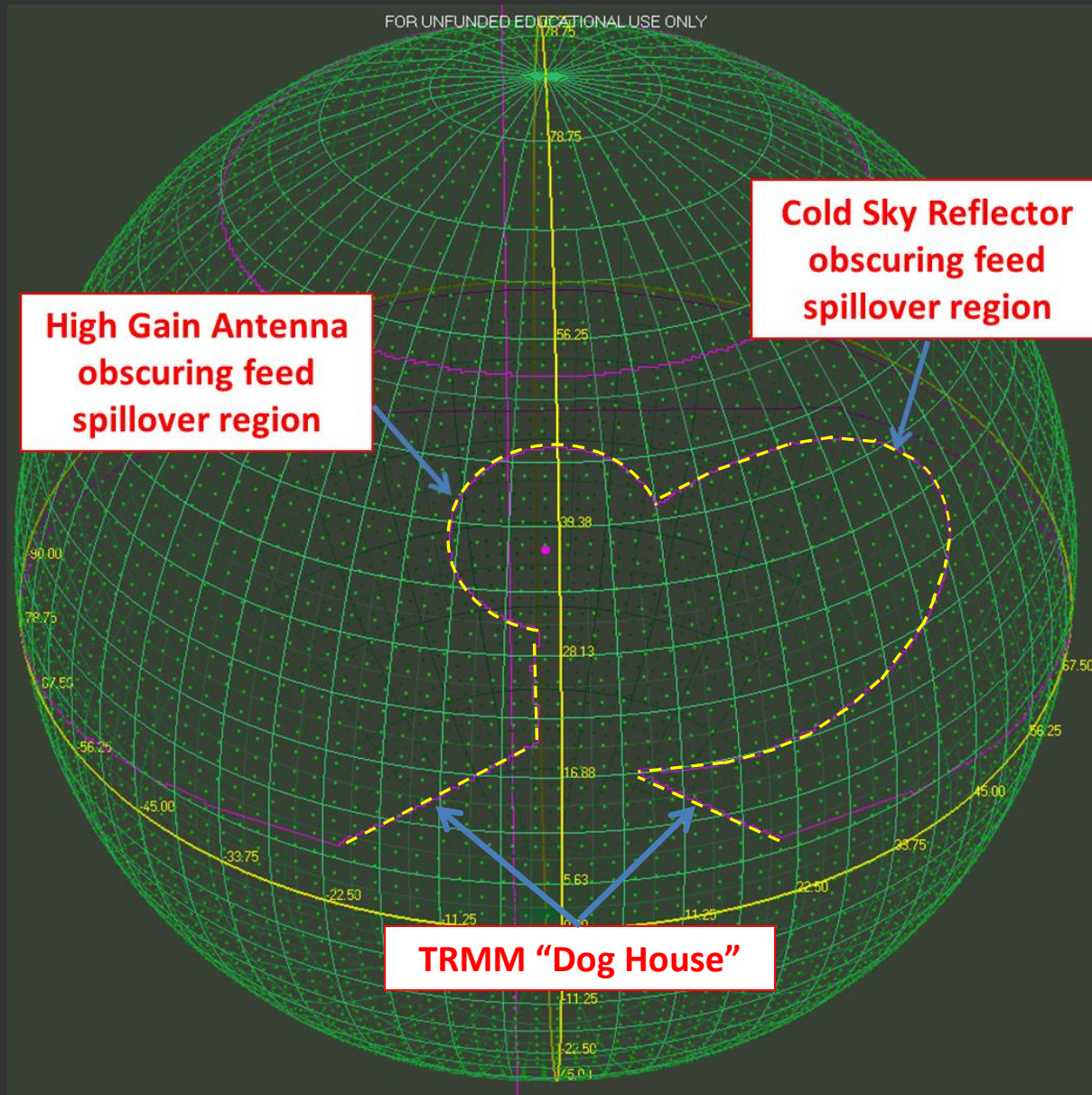


Radiation Mask – Main Reflector



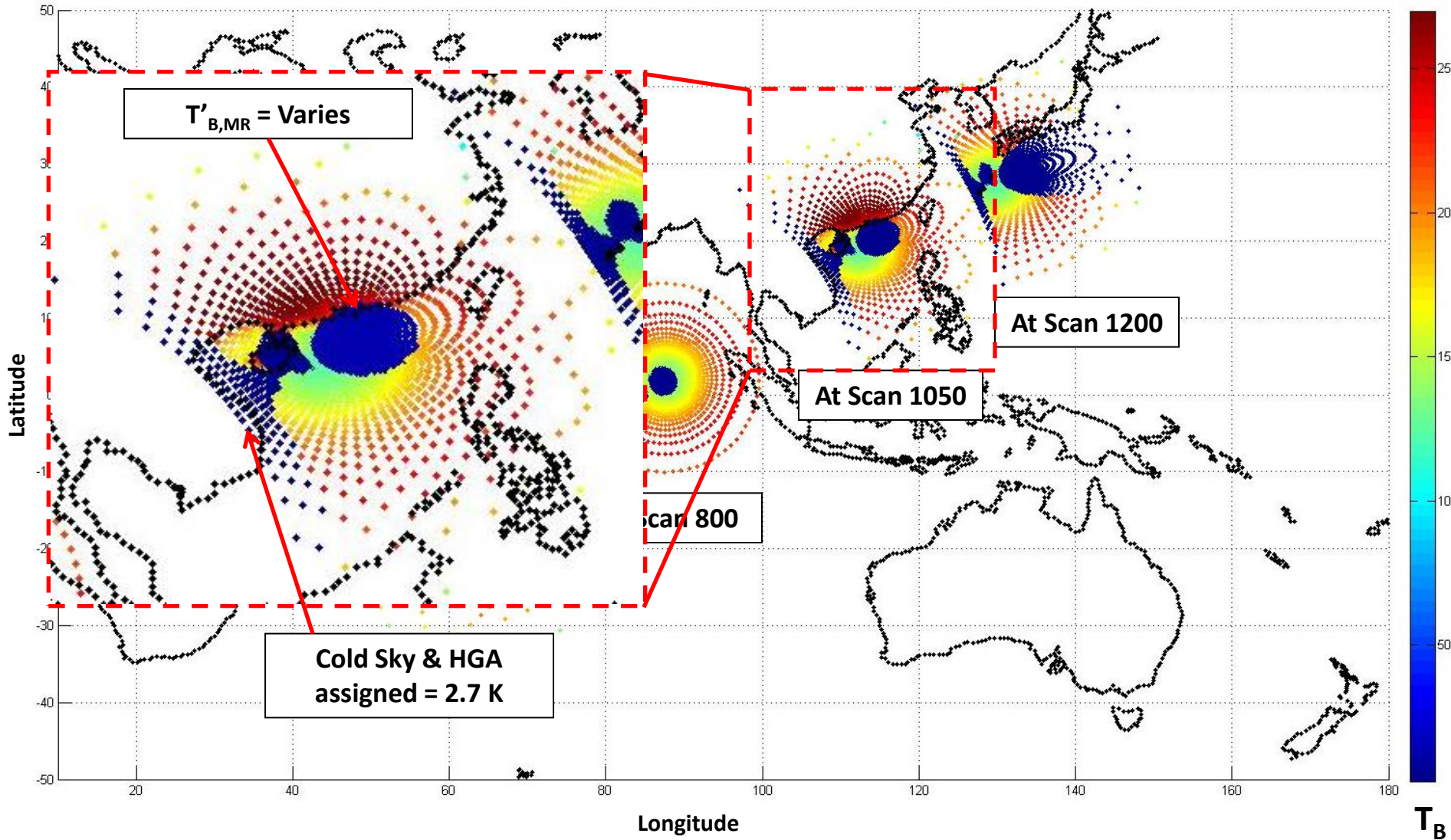
Using TRMM
CAD model &
AGI STK

Radiation Mask – HGA, CSR, Spacecraft



Using TRMM
CAD model &
AGI STK

Projection of Spillover with assigned TB Values with Obscuration



Separating Feed Horn T_A : Main Reflector & Spillover Regions



$$T'_A = \frac{\iint_{MR\ Angles} T'_{B,MR}(\Omega_{MR}) F_{MR}(\Omega_{MR}) d\Omega}{\iint_{2\pi\ sr} F_{MR}(\Omega_{MR}) d\Omega} + \frac{\iint_{Spillover\ Region} T_{B,SR}(\Omega_{SR}) F_{SR}(\Omega_{SR}) d\Omega}{\iint_{2\pi\ sr} F_{SR}(\Omega_{SR}) d\Omega} \quad (Eqn.2)$$

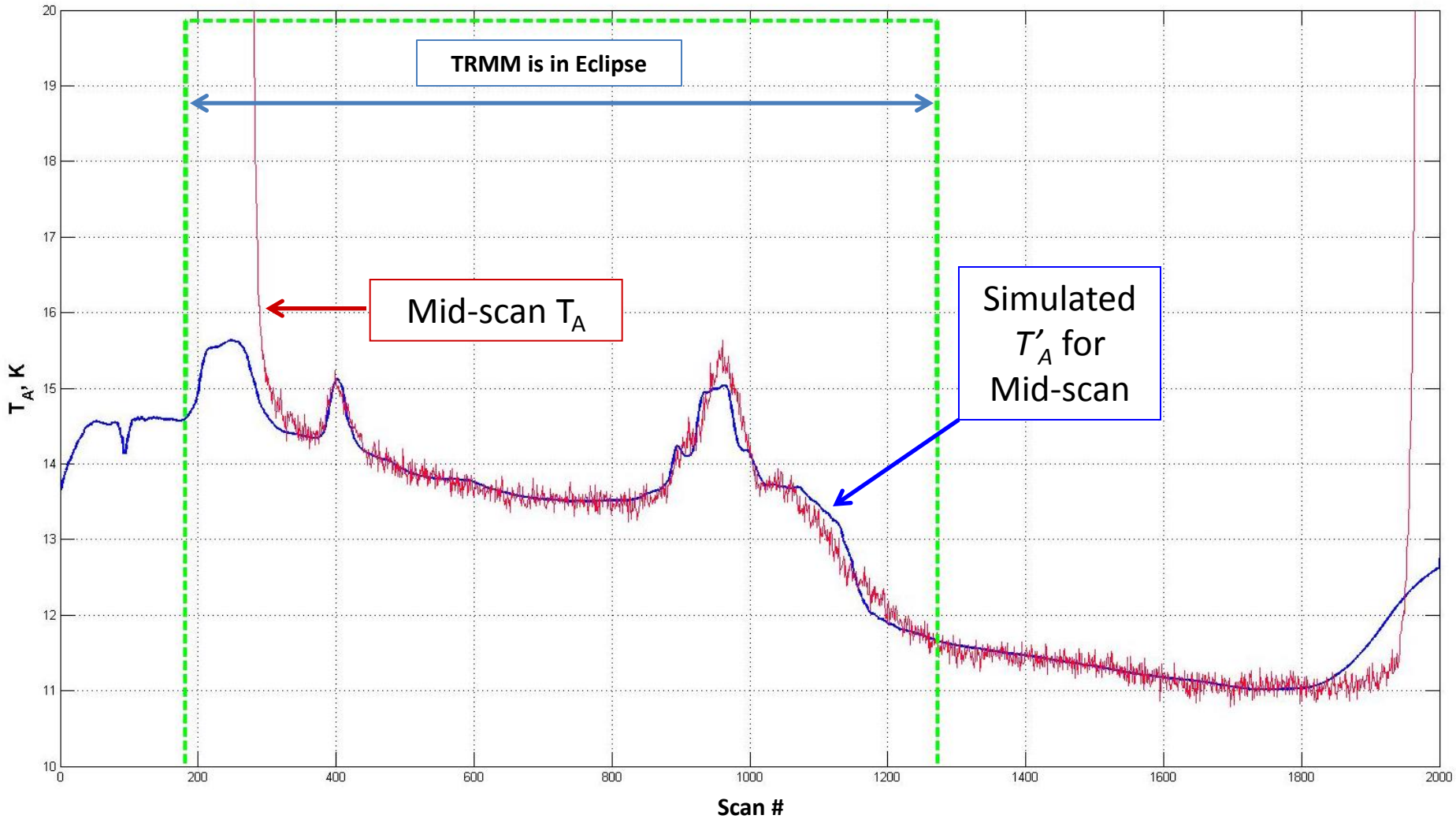
From T'_A
reconstruction
method

$T'_{B,MR}$ is
parametrically
varied until
right side of
eqn matches
 T'_A

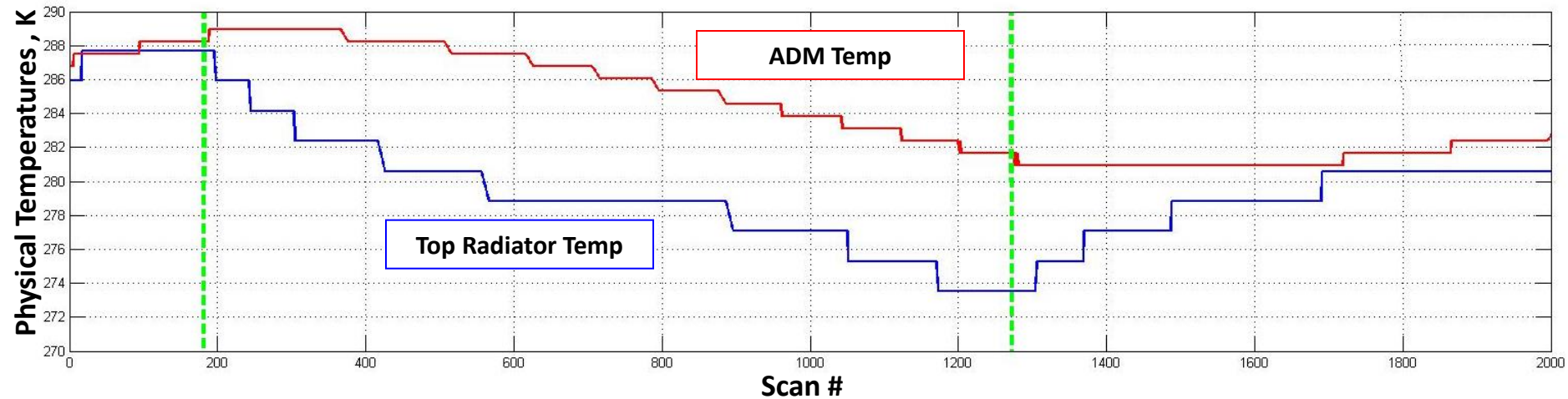
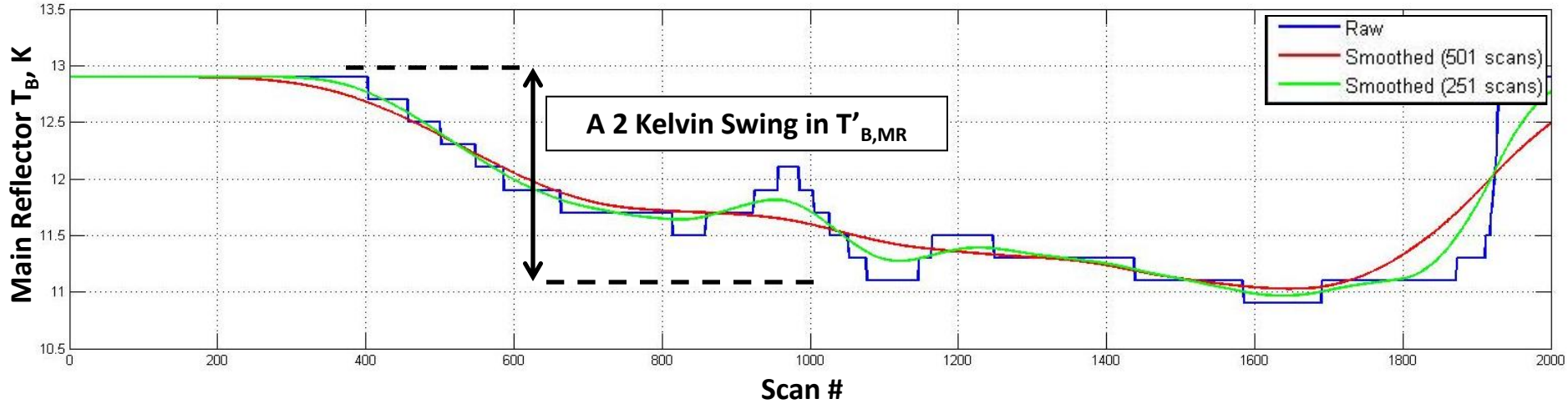
Simulated as
discussed in
dissertation

MR: Main Reflector
SR: Spillover Region
F: Feed Radiation pattern

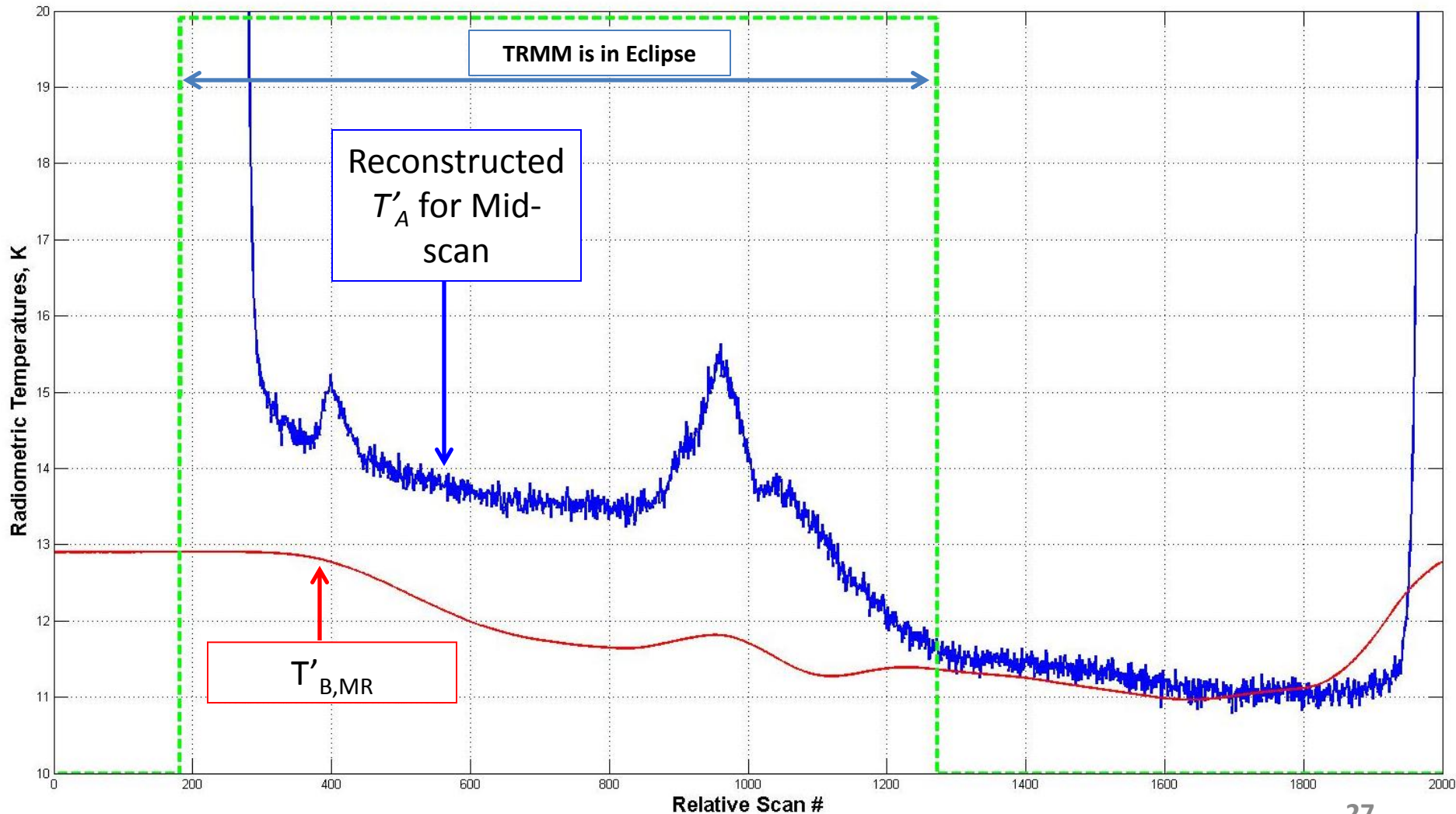
Matching Simulated T_A to Truth: 10V



DSCM 3: $T_{B,MR}$ & Physical Temperatures



Comparing 10 V-pol Signals DSV-3



Solving for TMI Emissivity

TMI Main Reflector

- An emissive MR during DSV:

$$T'_{B,MR} = \underline{T_B} \cdot (1 - \varepsilon) + \underline{T_{MR\ Physical}} \cdot \varepsilon, \quad \rightarrow \quad \varepsilon : \textit{emissivity of the main reflector}$$

↓
Depends on
frequency
(2.7-3.2 K)

↓
Independent
of frequency

↓
Depends on
frequency

- Unknowns: $T_{MR\ Physical}$ & ε (2 unknowns)
 - Only T_B & ε are unique to each channel

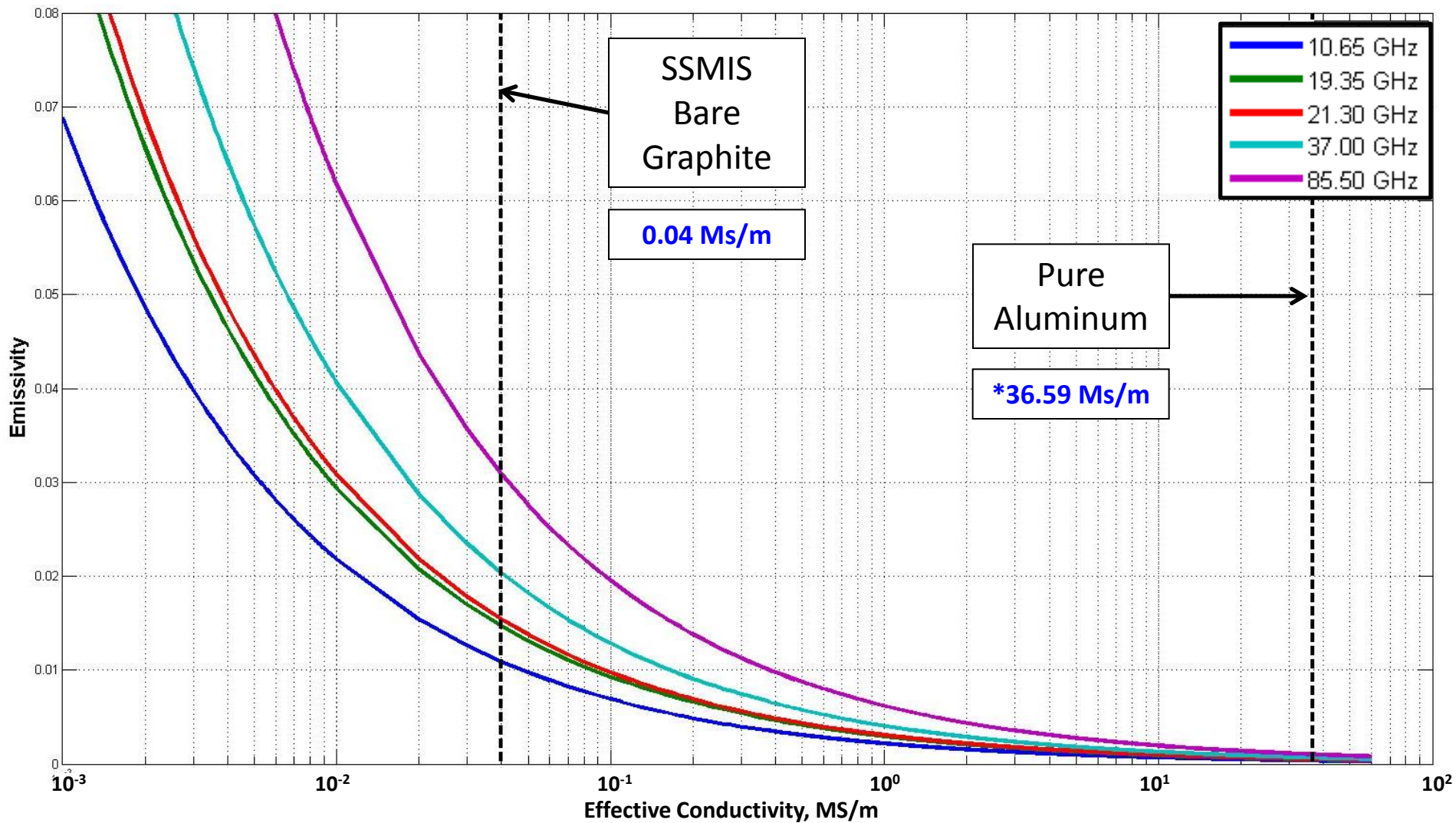
Research on SSMIS Reflector

- Special Sensor Microwave Imager/Sounder (SSMIS) is DOD microwave radiometer on the DMSP series
- Using previous work by JPL (Shannon Brown) on SSMIS Emissive Reflector*; where the emissivity for V & H-Pol are:

$$\epsilon_v \cong \sqrt{\frac{16\pi\nu\epsilon_0}{\sigma_{eff}}} \sec \theta_i \qquad \epsilon_h \cong \epsilon_v \cos^2 \theta_i \qquad (Eqns.3 \& 4)$$

- ν = frequency [Hz], ϵ_0 = free-space permittivity [F/m], σ_{eff} = effective conductivity [S/m], ϑ_i is incidence angle
- Assuming effective conductivity is constant then emissivity varies due to the operating frequency
- As MR views Deep Space, a non-polarized signal, incidence angle is neglected $\sec(\theta)=1$ & $\epsilon_v = \epsilon_h$

Emissivity Response to Frequency



Constraints & Method

- Constraints

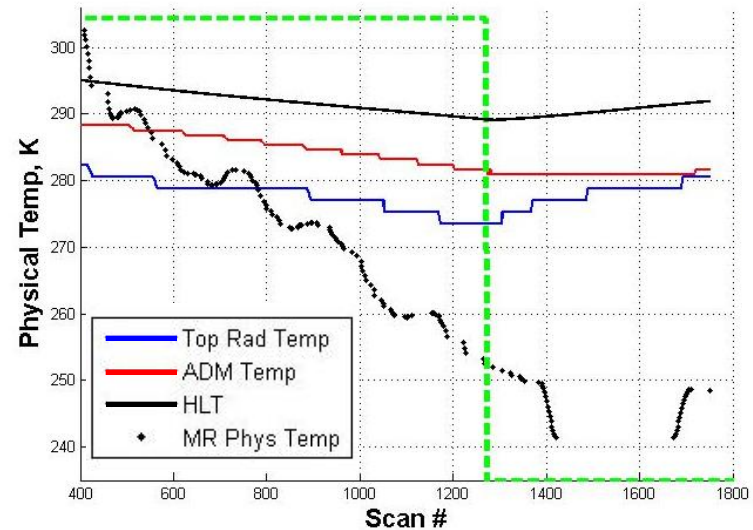
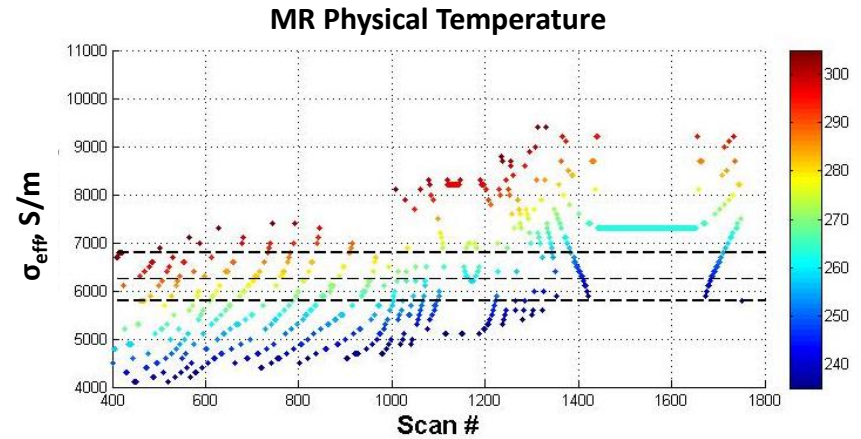
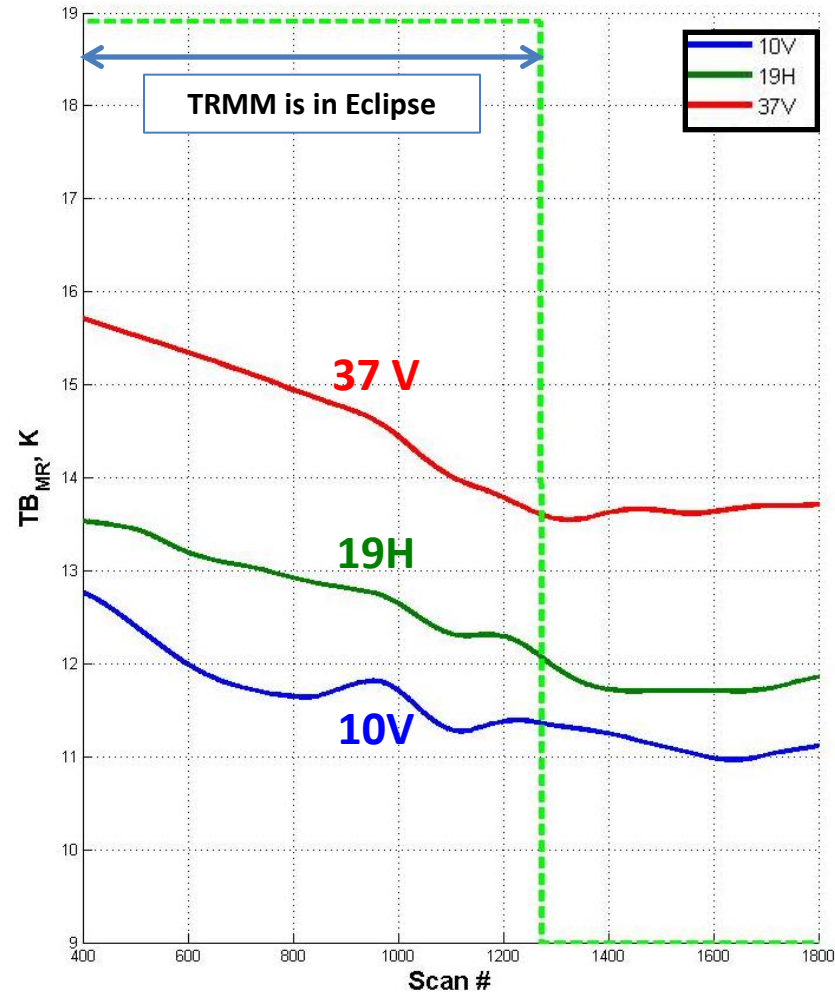
- There are two unknowns: $T_{MR,Phys}$ & σ_{eff}
- Using [GMI MR temperature](#) sensor as a proxy for TMI MR physical temperature limits:
 - Based on Solar Beta angle $\pm 45^\circ$ & Inertial hold maneuvers (240 – 300 K)
 - Temp Constraints: 235 - 305 K
- Conductivity was bounded by 1000 to 36e6 S/m

- Method

1. For each scan of a given channel
 - a) Simulate $T'_{B,MR}$ ($SimT'_{B,MR}$) for all combinations of $T_{MR,Phys}$ & σ_{eff}
 - b) Calculate the $|T'_{B,MR} - SimT'_{B,MR}| = \Delta T_{B,MR}$
2. Average of $\Delta T_{B,MR}$ for 10V, 19H, 37V channels , $\langle \Delta T_{B,MR} \rangle$
3. Obtain the minimum $\langle \Delta T_{B,MR} \rangle$ with respect to scan

Determining Conductivity

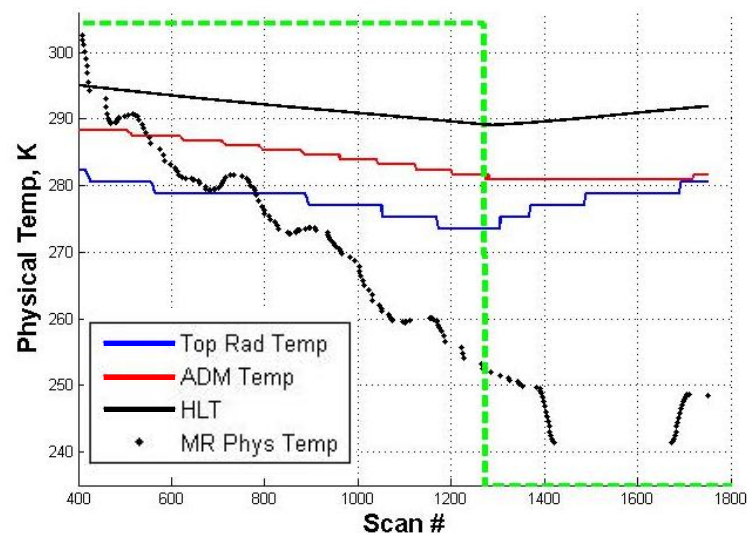
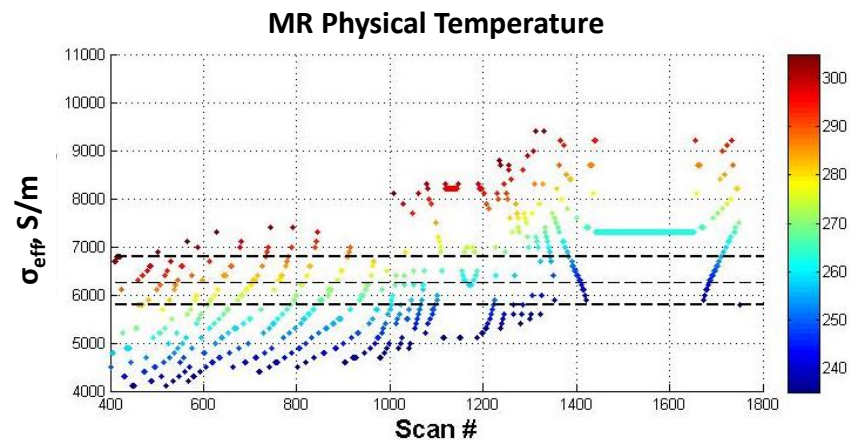
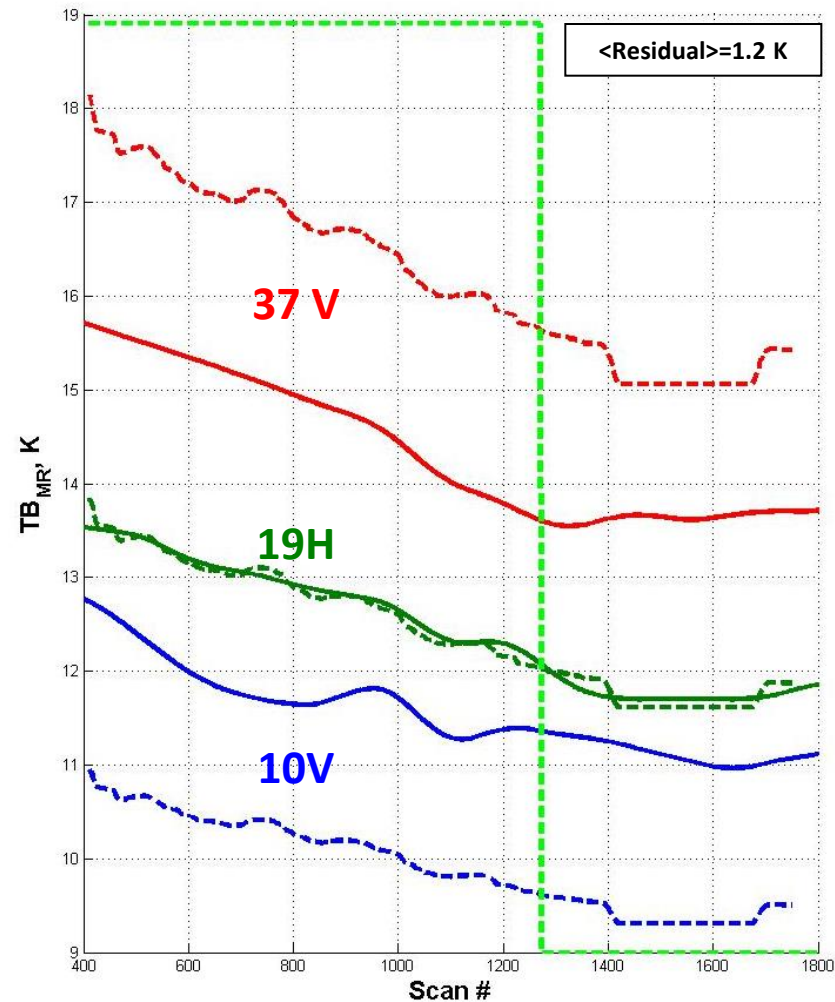
Scan Bias Correction off



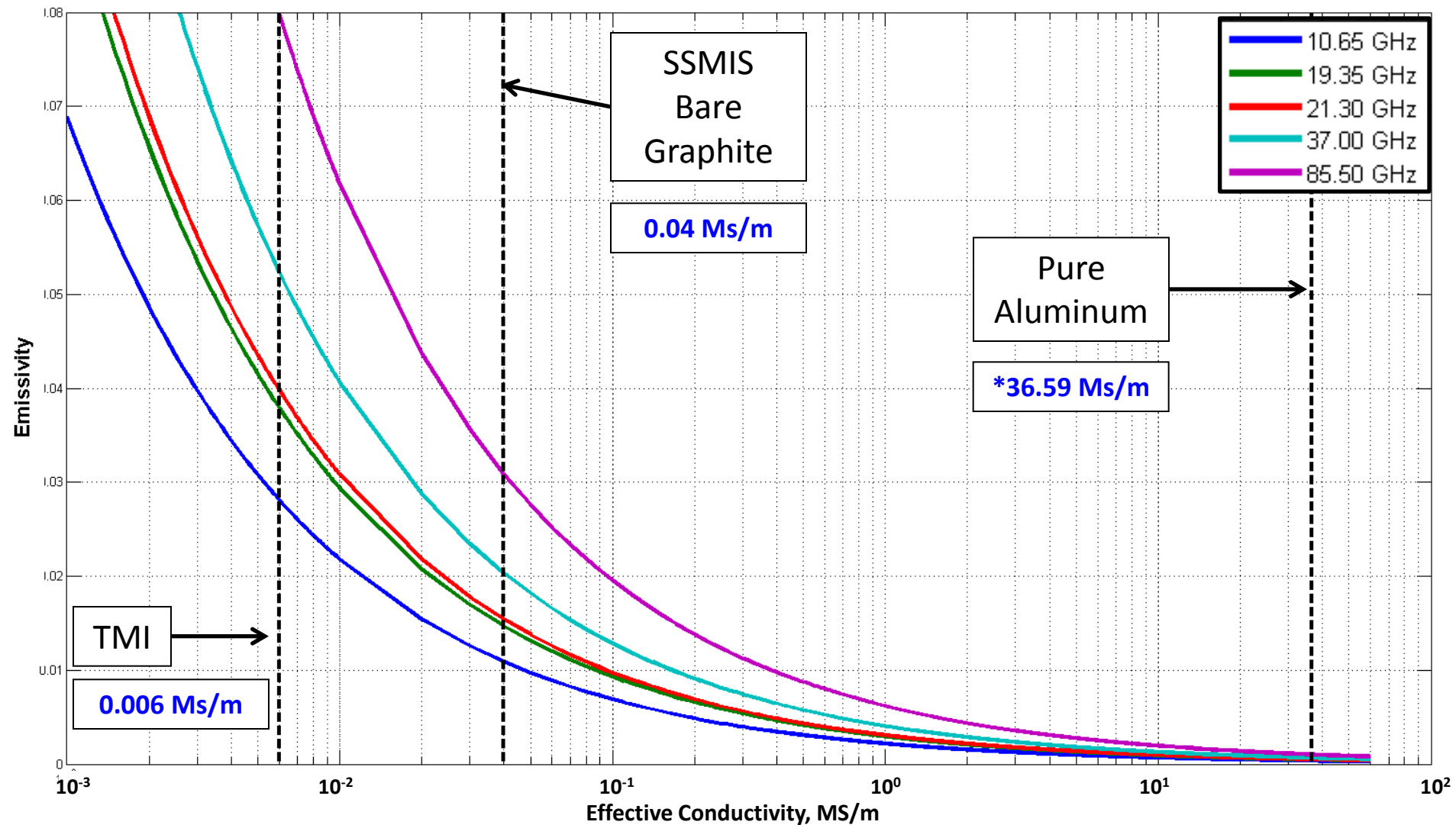
Determining Conductivity

— Lines: Is what I use determine σ_{eff}
 - - - Lines: Using σ_{eff} and $T_{\text{MR,Phys}}$ to recalculate TB,MR

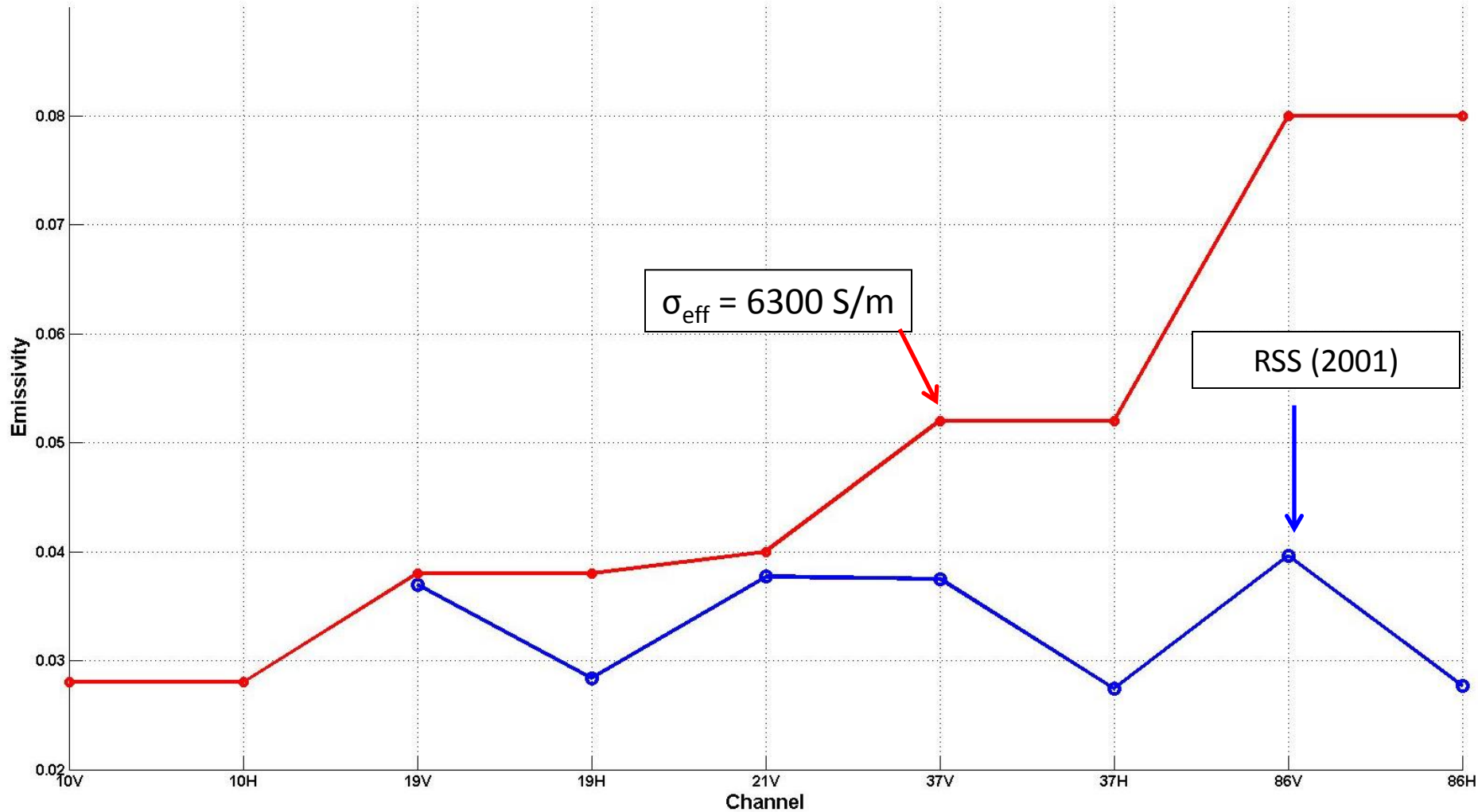
Scan Bias Correction off



Emissivity Response to Frequency



Estimated TMI Emissivity Values



$\sigma_{\text{eff}} = \text{Based on DSCM 1-6}$

Estimated TMI Emissivity Values



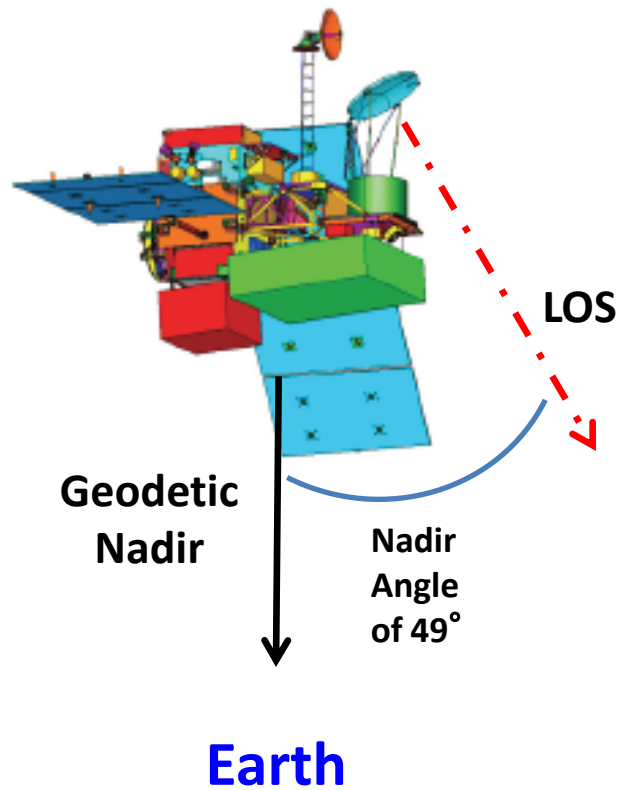
Channel	RSS (TGARS 2001)	CFRSL Viewing Space / Viewing Earth
10.65 V-pol	NA	0.028 / 0.031
10.65 H-pol	NA	0.028 / 0.025
19.35 V-pol	0.0370	0.038 / 0.042
19.35 H-pol	0.0284	0.038 / 0.034
21.30 V-pol	0.0377	0.040 / 0.044
37.00 V-pol	0.0375	0.052 / 0.058
37.00 H-pol	0.0274	0.052 / 0.048
85.50 V-pol	0.0396	0.080 / 0.088
85.50 H-pol	0.0277	0.080 / 0.072

Analysis

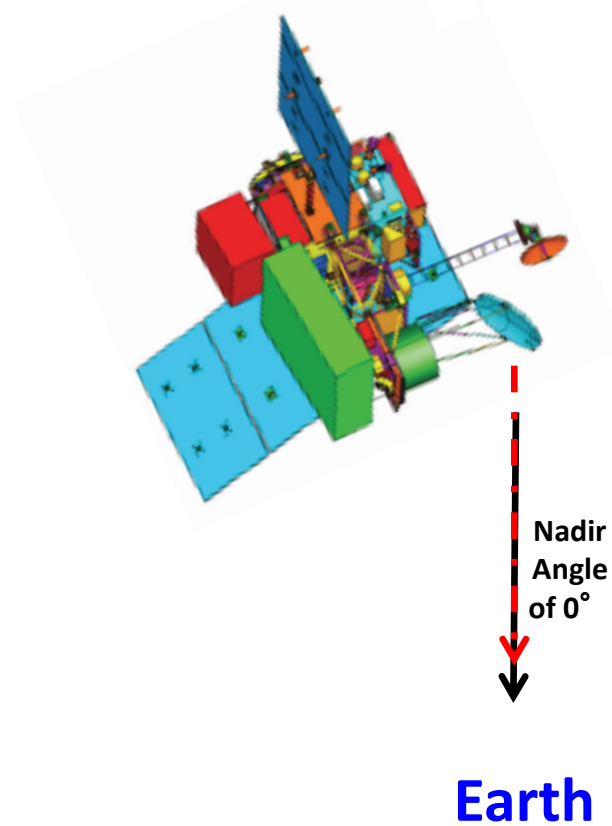
Second Stokes Analysis Using a Nadir Look

Nadir-Look

Normal Mode



Locked Pitch Angle at 49°



2nd Stokes Analysis (SS)

Image Source: Microwave Radar & Radiometric Remote Sensing (Ulaby)

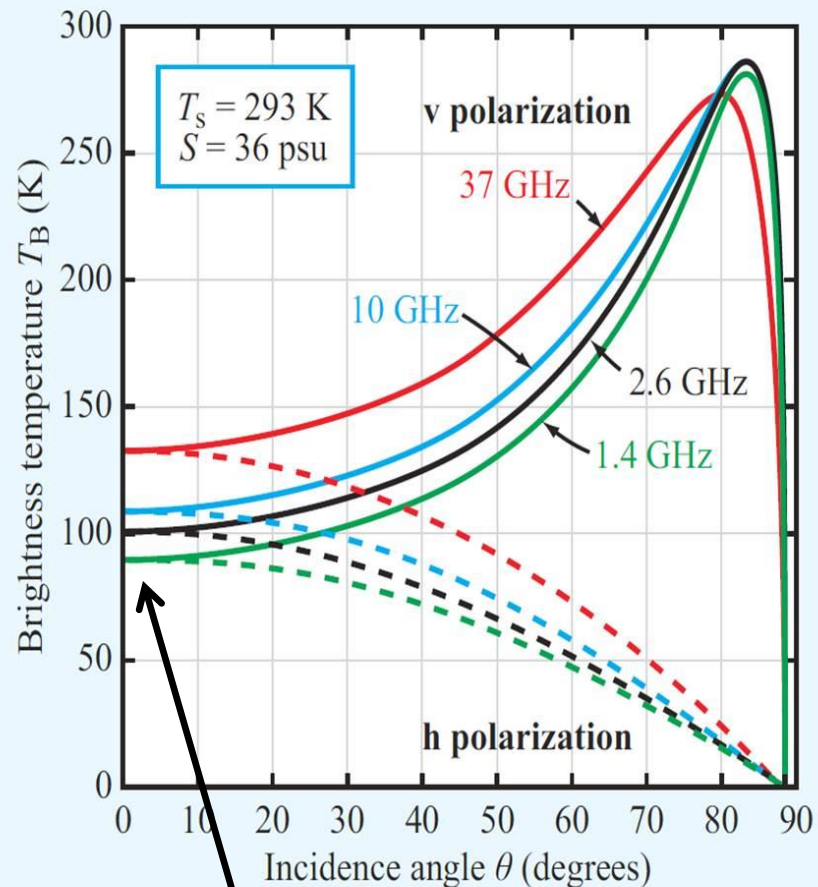
- Stokes Parameters:

$$I = \frac{\langle |E_v|^2 \rangle + \langle |E_h|^2 \rangle}{\eta} = S_v + S_h, \quad U = \frac{2 \cdot \text{Re} \langle E_v E_h^* \rangle}{\eta} = S_{+45} - S_{-45},$$

$$Q = \frac{\langle |E_v|^2 \rangle - \langle |E_h|^2 \rangle}{\eta} = S_v - S_h, \quad V = \frac{2 \cdot \text{Im} \langle E_v E_h^* \rangle}{\eta} = S_{lc} - S_{rc},$$

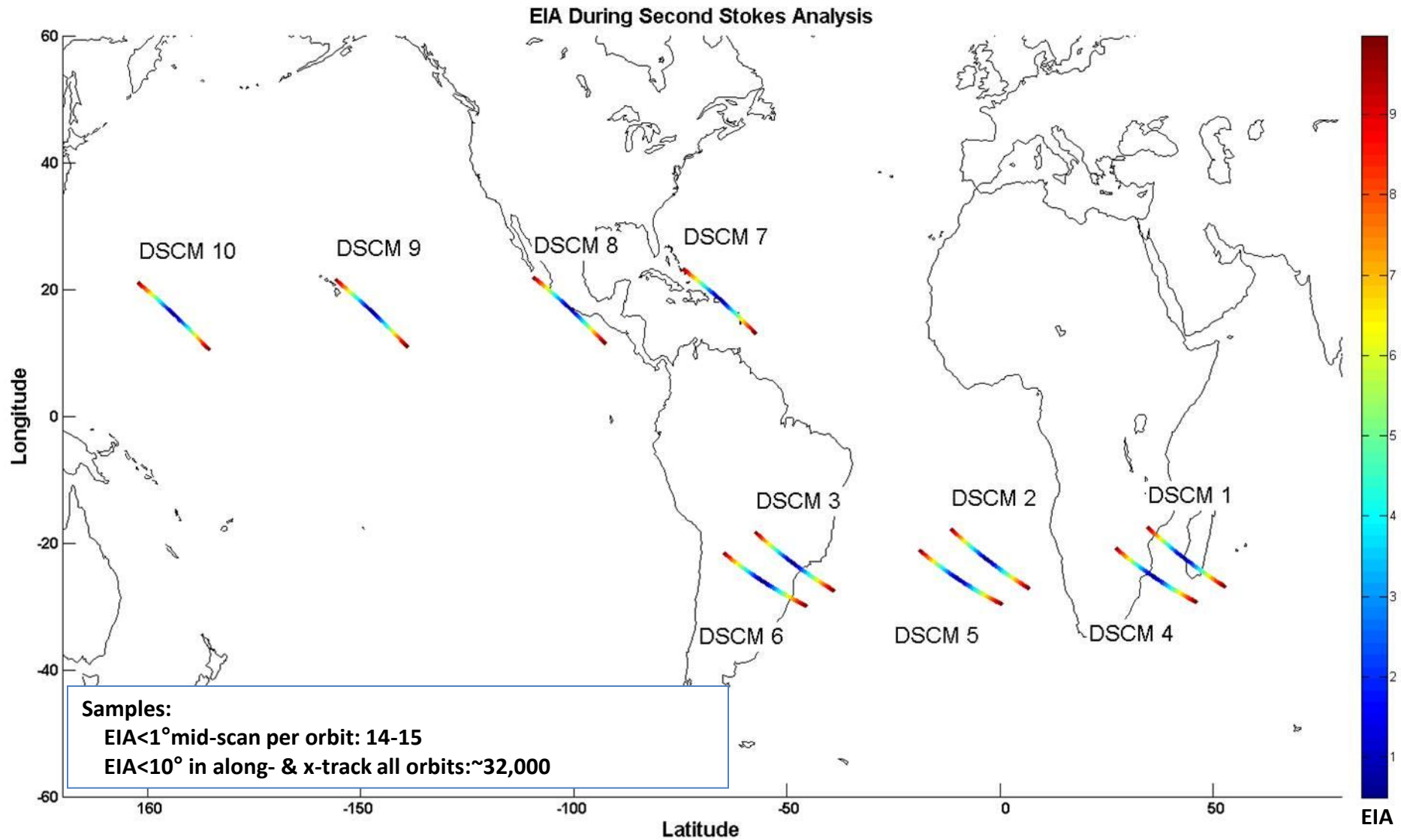
- During the “nadir” look

- The polarization of the same frequency should be equal
- This should be true over a land and ocean (assuming low oceans wind speeds)
- Cross pol should be negligible
- Hence, if $Q \neq 0$, there are calibration issues
- Insight into the relative calibration of channels at “warmer” TBs compared to cold space

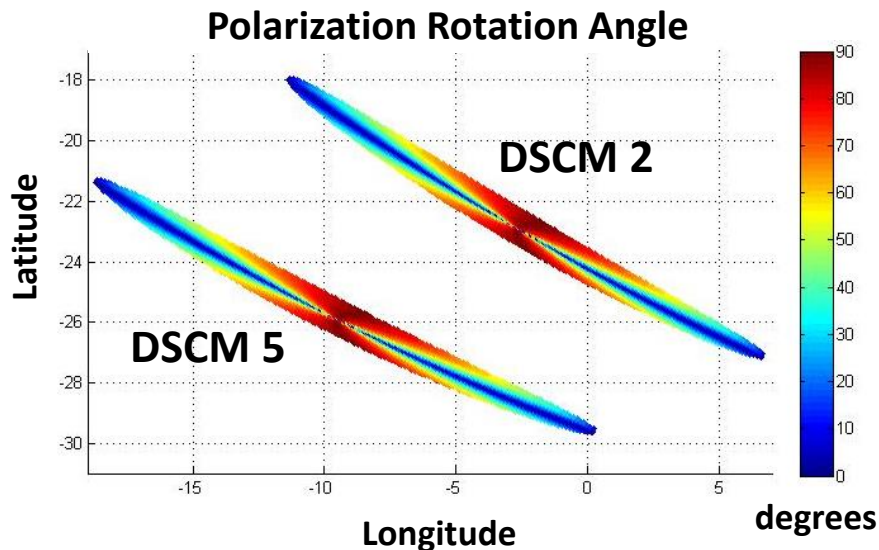
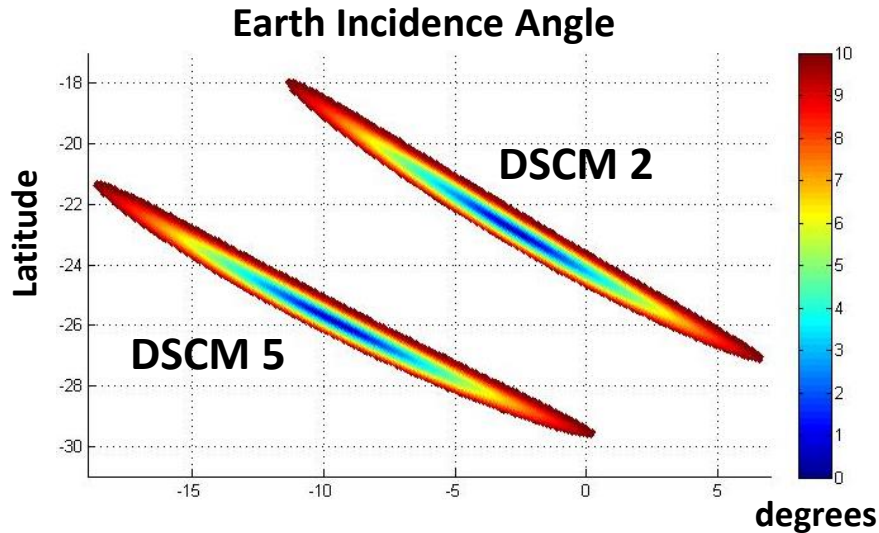


Nadir Look
V = H-Pol

Geolocation of EIA for Mid-scan Position



EIA & Polarization Rotation Effects

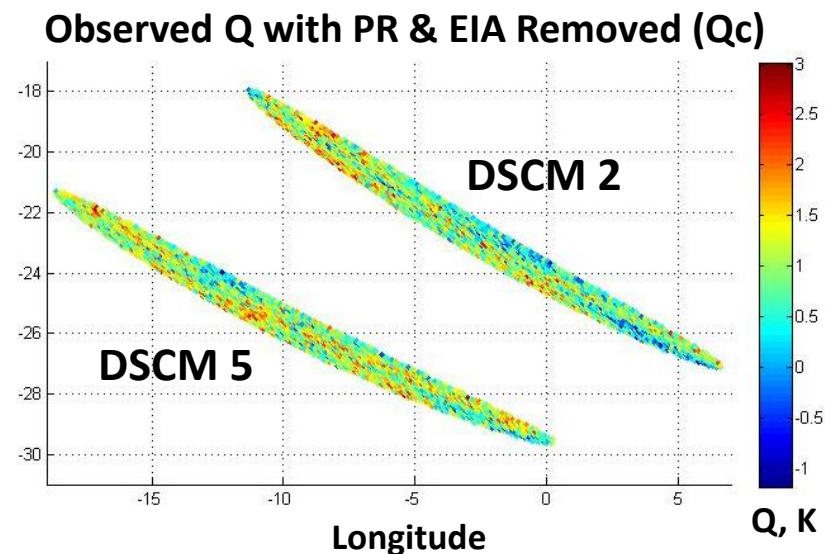
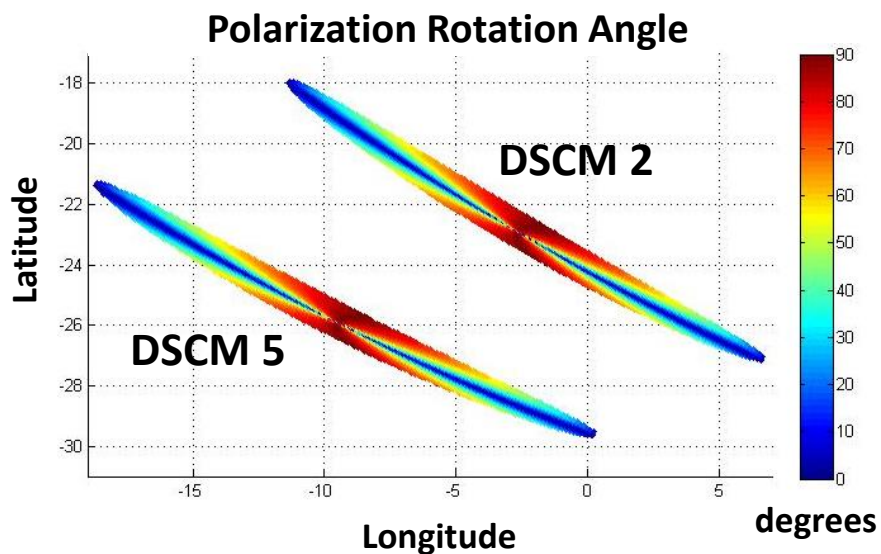
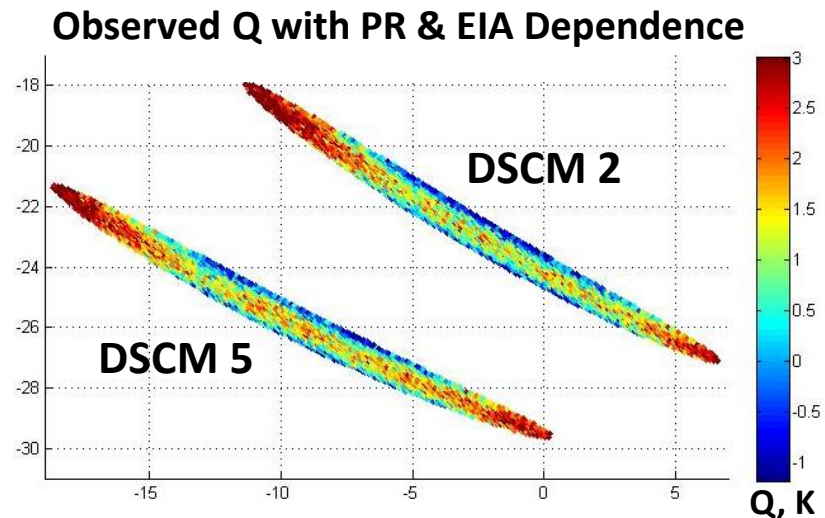
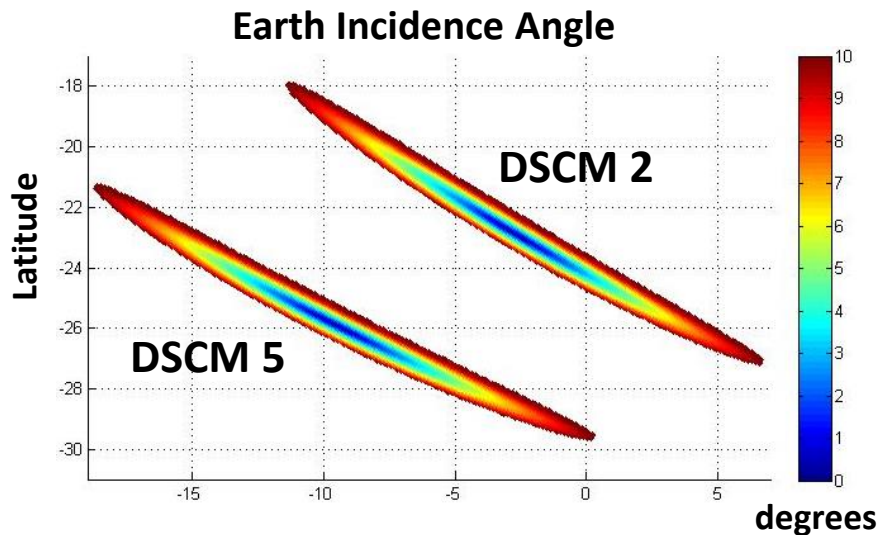


- EIA & PR dependence must be removed
 - Using RTM code provided by CSU
- The corrected Q (Q_C) with EIA & PR effects removed is:

$$Q_C = Q_{Obs} - Q_{Sim,PR}$$

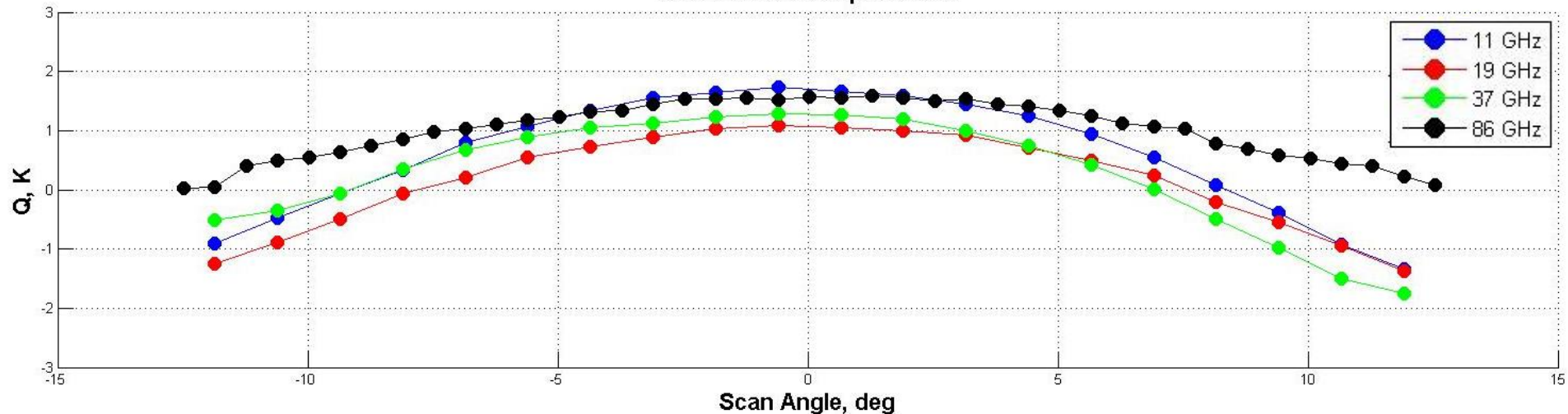
- Q_{Obs} is the observed Q with EIA & PR effects
- $Q_{Sim,PR}$ simulated Q with PR effects

Correcting for PR & EIA Effects: 11 GHz

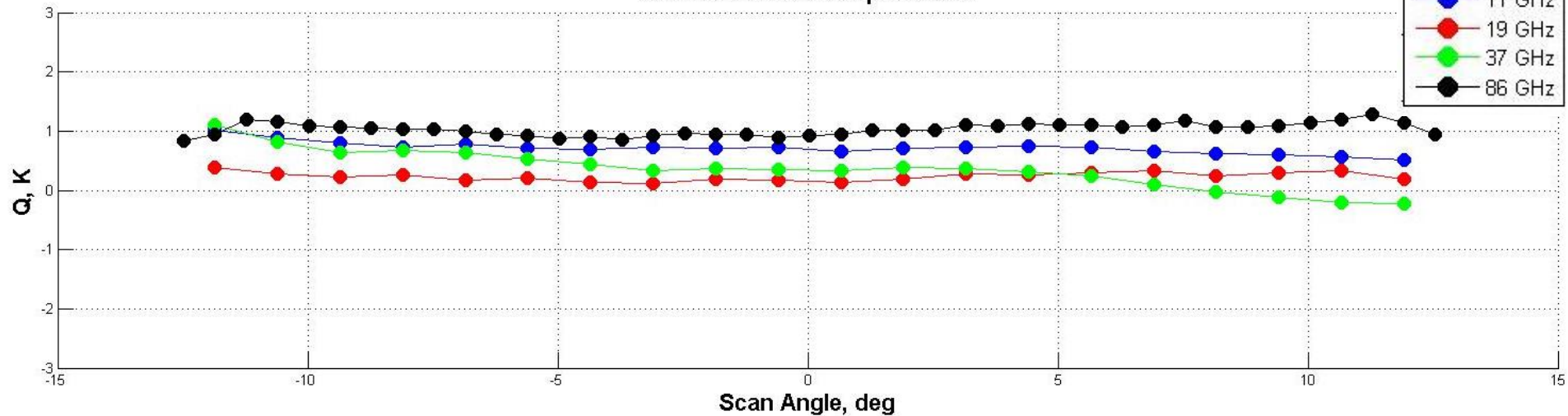


Before & After Correction: All Freqs

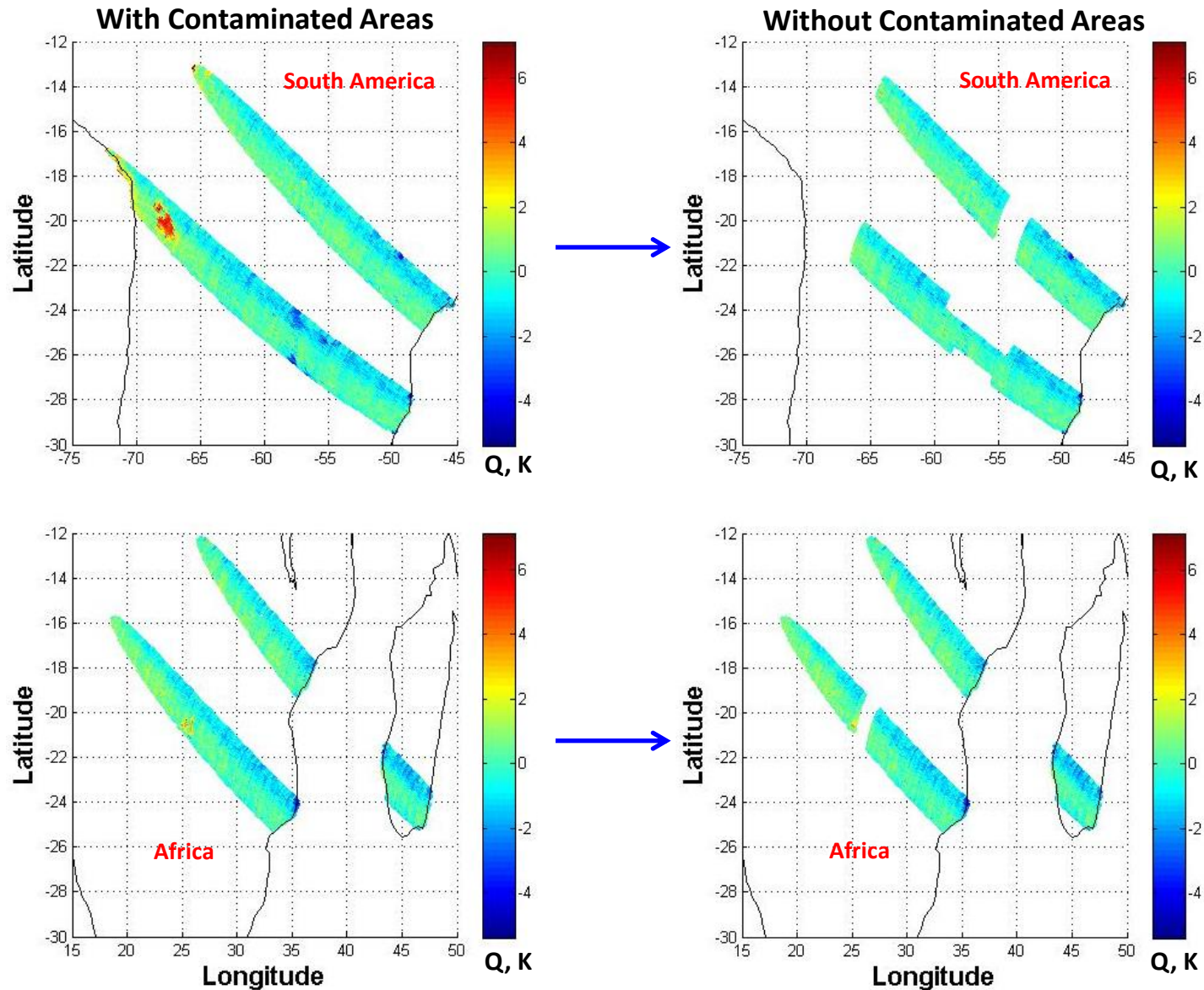
With PR & EIA Dependence



Without PR & EIA Dependence

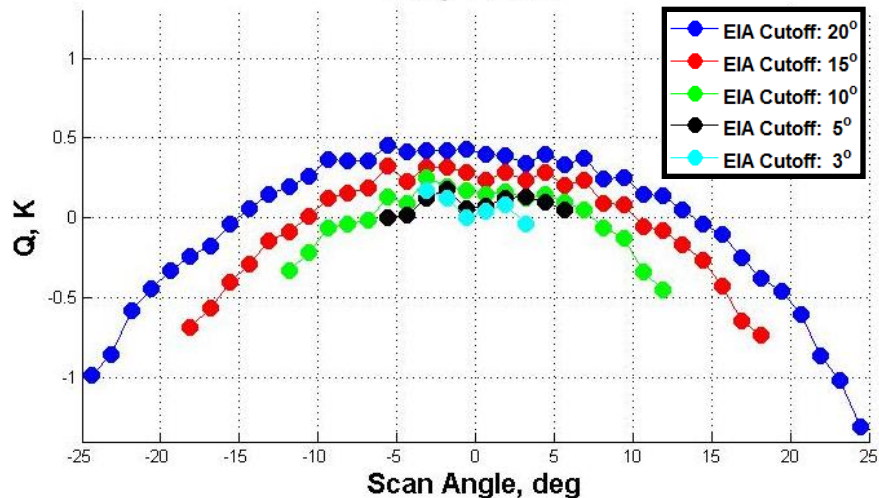


Q Over Land for 37 GHz (EIA Cutoff:20°)

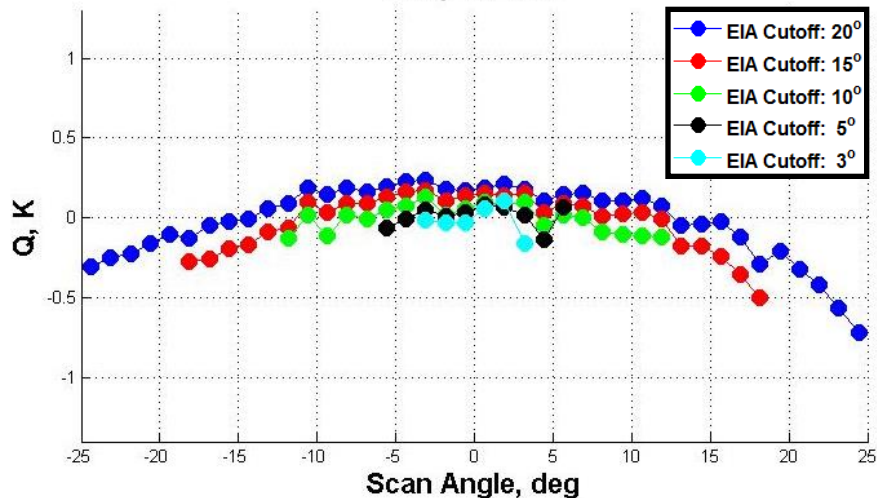


Determining the Proper EIA Cutoff

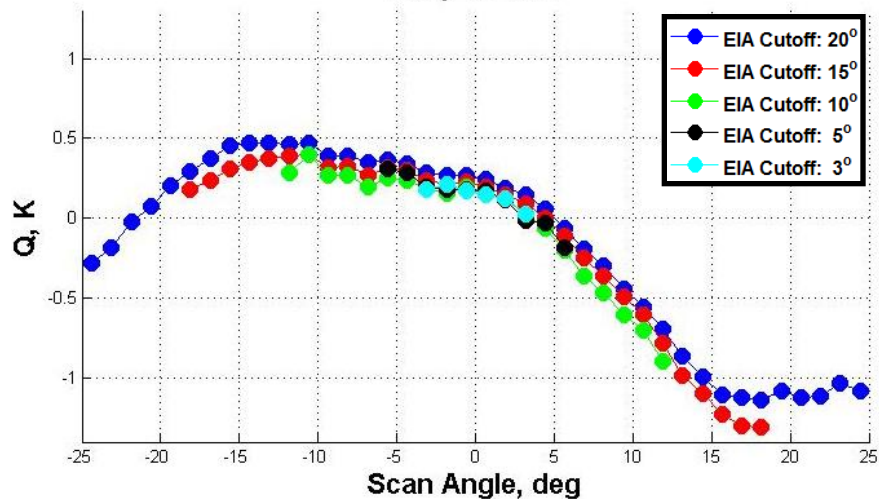
Freq: 11 GHz



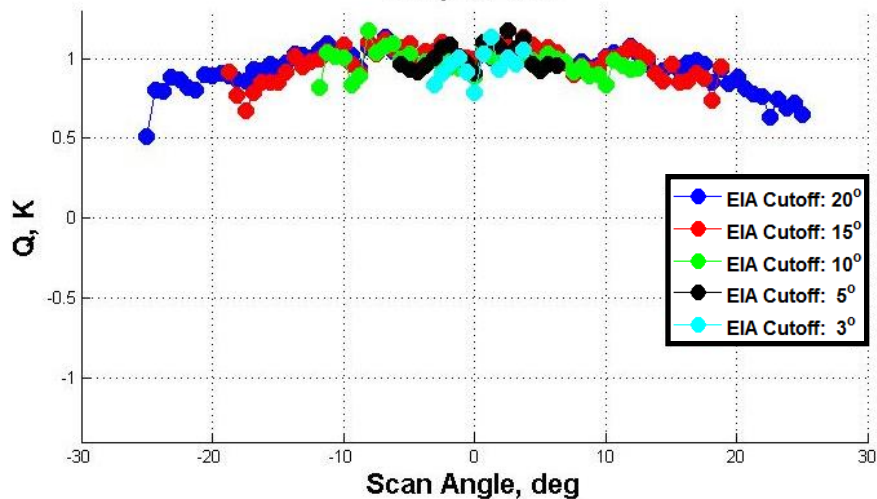
Freq: 19 GHz



Freq: 37 GHz



Freq: 86 GHz



Comparing Land & Ocean Q Values

Frequency	$\langle Q \rangle / \sigma$		$\langle Q_{\text{Ocean}} \rangle - \langle Q_{\text{Land}} \rangle$
	Ocean (EIA cutoff: 10°)	Land (EIA cutoff: 3°)	
10.65 GHz	0.78 / 0.67	0.06 / 0.83	0.72
19.35 GHz	0.27 / 0.82	-0.00 / 0.74	0.27
37.00 GHz	0.57 / 0.93	0.15 / 0.52	0.42
85.50 GHz	1.08 / 1.20	0.96 / 1.21	0.12

Speculation if differences are erroneous:

- Correction over ocean needs work
- Correction over land is required
- Non-linearity of TMI Receivers

Speculation if differences are correct:

- 10 GHz: Has Boresight misalignment
- 37 GHz: Along-scan Bias is present

Work & Timeline

Analysis	Performed Before	New	Notes
Beam Width	✓		JAXA used for AMSR-E
Boresight Pointing		✓	Using Earth's Horizon
Along-scan Bias	✓		RSS did not use full DSV
TMI MR Emissivity	✓		RSS did not use full DSV
SS Analysis		✓	

- This timeline dissertation (Based on Weekly Reports):
 - **Part Time:** 03-2010 to 05-27-2011 (just over 1 year)
 - Developing Matlab code to read binary 1A11 & geolocated LOS during inertial hold
 - Import ephemeris & attitude data into STK for visualization & confirmation
 - Started Reconstruction of T_A for 10 V-pol
 - **Other Projects:** June 2011 to March 2013 (1 year 9 months)
 - **Full Time:** 03-29-2013 to Present (~ 2 years)

Conclusion

- Develop & document methods for post-launch calibration of spaceborne microwave radiometers
 - Use pre-existing & new Calibration Attitude Maneuvers
- Used TRMM Deep Space Calibration maneuvers for developing this plan using Jan & Sept 1998 and July 2014
- All objectives for bullets-1 & -2 have been successfully achieved
- Calibrate TRMM Microwave Imager (TMI) for the upcoming Archived T_B data product
 - Has mostly been completed with remaining work to be completed as post-doc research during the summer 2015

Future Work – To Be Included in the Dissertation



- Beam Width Analysis:
 - Use range of scan positions for better determining TMI beam width
 - reduce the variance as well as more sample points for the 10.65 GHz channels to improve the mean (refer to [back-up](#) for examples)
- Beam Boresight:
 - Obtain boresight differences between X-band feed to multi-frequency feed channels
 - Use STK or TMI geolocation code to determine match the nadir angles for the convex & concave cases

Future Work – Post Dissertation



- Plans to write two Journal Papers:
 - TMI Calibration:
Authors: CFRSL, Wyle Systems
 - GMI Calibration:
Authors: CFRSL, Wyle Systems, Ball Aerospace, & RSS
- Use Feb & Mar 2015 Maneuvers:
 - March 2015 maneuvers, Yaw 90° , to better estimate this angle in the along-scan direction
- For Journal Papers
 - Investigate ERA-I for spillover
- Use multi-freq horn primary pattern from Boeing

What this Research Has Influenced

- GPM Has Used This Nadir-Look Maneuver
 - 2 Orbits in December 2014
 - Locked-pitch (LOS stays aligned with Nadir) over ocean & land (Amazon)
- Detection of RFI in TMI's Cold Sky View
 - Analysis (week of DSCM Set 3) on T_A reconstruction revealed that there is RFI from geostationary satellites in the CSR view
- TRMM 90° Yaw Inertial-Hold - To:
 - provide a different DSV compared to Yaw 0° /180° maneuvers
 - Along Scan bias & back lobe location
 - determine azimuthal Cold Sky Mirror boresight

Recommendations

- Soil Moisture Active Passive (SMAP)
 - L-Band Radar/Radiometer
 - Internally calibrated
 - Feed horn illuminates a 6 m parabolic mesh reflector
 - Reflector supported by a single boom
 - Not a hard surface reflector so compared to simulation or on ground testing the
 - beam boresight & beam width can change
 - Back lobes can change which is of importance because galactic background at L-Band is not homogenous

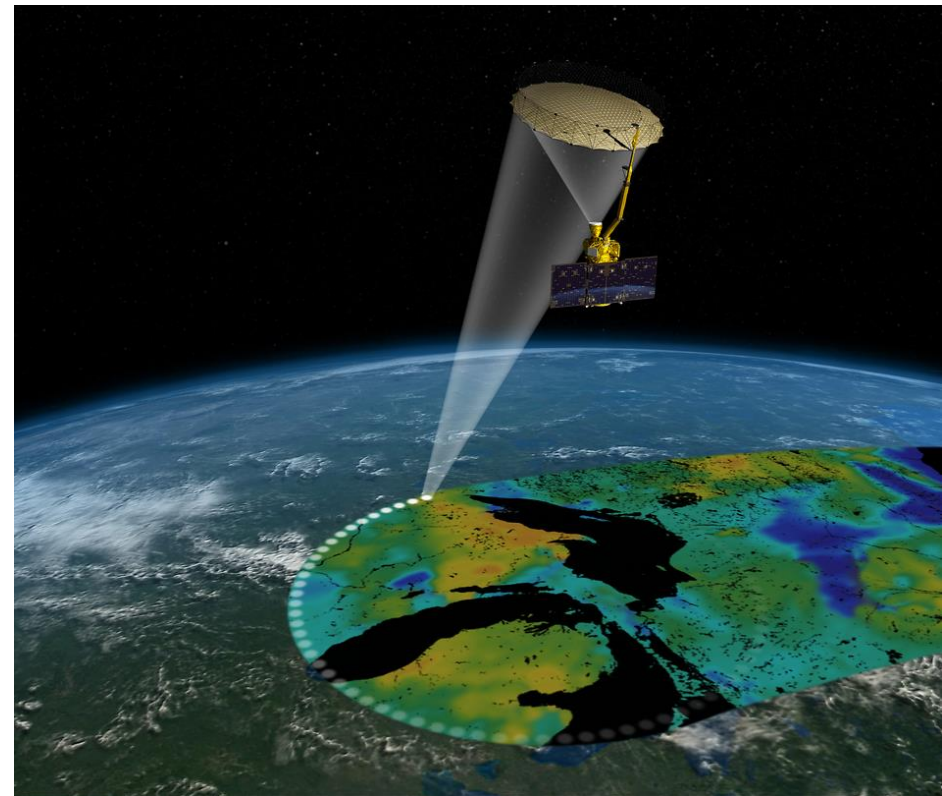


Image Credit: NASA/JPL-Caltech
<http://www.nasa.gov/jpl/smap/pia19133/>

Recommendations Cont'd

- Synthetic Aperture Radiometers:
 - Soil Moisture Ocean Salinity (SMOS) or Hurricane Imaging Radiometer (HIRAD)
 - Uses an arrangement of feeds or stick/patch antennas to increase beam resolution
 - IFOVs are obtained by using aperture synthesis
 - Benefit from all analysis mentioned within this dissertation
- Compact Ocean Vector Wind Radiometer (COVWR)
 - Low cost, low mass, low-power internally calibrated radiometer
 - Conical scanner but feed does not rotate with reflector
 - Fully-polarimetric as scan position changes
 - Big advantage would be SS & DSV with spillover & Back lobe illuminating the Earth

Conference Publications



- [1] **S. Farrar**, L. Jones, T. Kasparis, “Comparisons of Ocean Precipitation Measurements between SeaWinds and TRMM 3B42 Data Product”, paper presented at IEEE International Symposium on Antennas & Propagation and USNC/URSI National Radio Science Meeting, June 1-5, 2009, Charleston, S.C.
- [2] **S. Farrar**, L. Jones, S. Masuelli, J. Gallo, “Microwave Radiometer (MWR) Oceanic Integrated Rain Rate Algorithm for Aquarius/SAC-D” , poster presented at the 11th Specialist Meeting on Microwave Radiometry and Remote Sensing of the Environment, March 1-4, 2010, Washington, D.C.
- [3] R. Amarin, S.El-Nimri, S.Biswas, **S. Farrar**, J. Johnson, L. Jones, “Enhancing Oceanic Retrievals using Microwave Radiometry” , presented at the 2010 IGARSS, July 25-30, 2010, Honolulu, HI
- [4] **S. Farrar**, L. Jones, “Preliminary Analysis of the Aquarius/SAC-D Microwave Radiometer (MWR) Antenna Temperature: Possible Antenna Pattern Issue” , presented at the 2012 IEEE SoutheastCon, Mar 15-18, 2012, Orlando, FL
- [5] **S. Farrar**, M. Labanda, M. Jacob, S. Masuelli, S. Biswas, H. Raimondo, L. Jones, “An Empirical Correction for the MWR Brightness Temperature” , IGARSS 2012, July 22-27, 2012, Munich, Germany
- [6] T. Miller, M. James, J. Roberts, S. Biswas, E. Uhlhorn, R. Atlas, P. Black, L. Jones, J. Johnson, **S. Farrar**, S. Sahawneh, C.S. Ruf, M. Morris, “Observations of C-Band Brightness Temperature from the Hurricane Imaging Radiometer (HIRAD) on-board the NASA WB-57 during GRIP in Hurricanes Earl And Karl (2010),” *Fall Meeting, American Geophysical Union*, San Francisco, CA, 3-7 Dec., 2012
- [7] Timothy L. Miller, M. W. James, J. B. Roberts, S. Biswas, D. Cecil, W. L. Jones, J. Johnson, **S. Farrar**, C. S. Ruf, E. W. Uhlhorn, R. Atlas, and Peter G. Black, “Observations of C-band Brightness Temperatures and Ocean Surface Wind Speed and rain Rate from the Hurricane Imaging Radiometer (HIRAD) during GRIP and HS3,” AMS 17th Conf on Integ. Observing and Assimilation Sys, Austin, TX, 6-10 Jan, 2013.

Conference Publications



- [8] *S. Sahawneh, **S. Farrar**, J. Johnson, L. Jones*, “Hurricane Wind Speed and Rain Rate Measurements using the Airborne Hurricane Imaging Radiometer (HIRAD)” , presented at the 2013 IEEE SoutheastCon, Apr 4-7, 2013
- [9] *T. Miller, M. James, J. Roberts, S. Biswas, D. Cecil, W. Jones, J. Johnson, **S. Farrar**, et al*, “The Hurricane Imaging Radiometer: Present and Future,” , IGARSS 2013, July 21-26, 2013, Melbourne, Australia
- [10] ***S. Farrar**, L. Jones*, “Estimation of TRMM Microwave Imager Antenna Temperature During Deep Space Calibration Maneuvers”, 13th Specialist Meeting on Microwave Radiometry and Remote Sensing of the Environment, March 24-27, 2014, Pasadena, CA.
- [11] ***S. Farrar**, L. Jones*, “GPM Microwave Imager On-Orbit Radiometric Calibration Using a Satellite Deep Space Calibration Maneuver” , IGARSS 2014, July 13-18, 2014, Quebec, Canada
- [12] *M. Morris, C. Ruf, S. Biswas, **S. Farrar***, “A Coupled-Pixel Retrieval Algorithm for High Resolution Imagers” , 95th AMS Annual Meeting, Phoenix, AZ, Jan 4-8, 2015

Journal Publications

- [1] *S. Biswas, **S. Farrar**, K. Gopalan, A. Santos-Garcia, L. Jones, S. Bilanow*, “Inter-Calibration of Microwave Radiometer Brightness Temperatures for the Global Precipitation Measurement Mission”, *IEEE Trans. GeoSci. & Rem Sens*, Vol. 51, No. 3, March 2013
- [2] *M. Labanda, M. Jacobs, **S. Farrar**, L. Jones*, “MWR Smear Effect: A Counts-level Empirical Correction and Possible Causes”, *JSTARS - Journal of Selected Topics in Applied Earth Observations and Remote Sensing*, vol. 8. **Under Review**

NASA Project Presentation - XCAL



Orlando, FL – June 2010

- [1] **S. Farrar**, *S. Biswas, W.L. Jones*, “TMI With Respect to WindSat Over the Amazon” , XCAL Science Team Meeting, June 29-30, 2010 Orlando, FL

Ashville, NC – October 2010

- [2] **S. Farrar**, *W.L. Jones, S. Bilanow, K. Gopalan, C. Lyu, J. Shiue*, “TMI Deep Space Calibration (DSC) Re-Analysis” , XCAL Science Team Meeting 21-22 October 2010 Ashville, NC
- [3] **S. Farrar**, *S. Biswas, L. Jones, K. Gopalan*, “WindSat / AMSR-E Biases” , XCAL Science Team Meeting October 21-22, 2010, Ashville, NC

College Park, MD – March 2010

- [4] **S. Farrar**, *L. Jones, S. Bilanow, K. Gopalan*, “AMSR-E Revisited” , XCAL Science Team Meeting March 1-2, 2011 College Park , MD
- [5] *S. Bilanow, K. Gopalan, S. Farrar, W.L. Jones*, “Notes on Earth incidence Angle (EIA) Uncertainty Contribution to Tb Uncertainty” , XCAL Science Team Meeting March 1-2, 2011 College Park, MD
- [6] **S. Farrar**, *L. Jones, S. Bilanow, K. Gopalan*, “TMI Deep Space Calibration (DSC) Gain and Offset Relationship Update Status” , XCAL Science Team Meeting March 1-2, 2011 College Park , MD
- [7] **S. Farrar**, *L. Jones, S. Bilanow, K. Gopalan*, “Uncertainty Estimate for UCF XCAL Biases” , XCAL Science Team Meeting March 1-2, 2011 College Park , MD

Fort Collins, CO – July 2011

- [8] *S. Bilanow, K. Gopalan, S. Farrar, W.L. Jones*, “Notes on GMI Alignment” , XCAL Science Team Meeting July 13-14, 2011 Fort Collins, CO
- [9] **Spencer Farrar**, “TMI TB Striping Analysis” , XCAL Science Team Meeting July 13-14, 2011 Fort Collins, CO
- [10] **S. Farrar**, “TMI Gyro-Hold Status Update Using STK” , XCAL Science Team Meeting July 13-14, 2011 Fort Collins, CO

Denver, CO – November 2011

- [11] **S. Farrar**, *S. Aslebagh, W.L. Jones, S. Bilanow*, “The Effects of TMI 1B11 V7 Solar Beta/Time Varying Bias Correction on 2A12 Rain Rates” , XCAL Science Team Meeting November 5-6, 2011 Denver, CO
- [12] **S. Farrar**, *A. Santos-Garcia, W.L. Jones, S. Bilanow*, “TMI/SSMI Biases (F13, F14, & F15)” , XCAL Science Team Meeting November 5-6, 2011 Denver, CO

Ann Arbor, MI – July 2012

- [13] *W.L. Jones, A. Santos-Garcia, S. Aslebagh, S. Farrar, Y. Hejazin*, “Microwave Radiometer (MWR) on Aquarius X-Cal Update” , XCAL Science Team Meeting July 11-12, 2012 Ann Arbor MI
- [14] **S. Farrar**, *A. Santos-Garcia, W.L. Jones*, “Further Analysis on TMI/SSMI Biases (F13 through F15)” , XCAL Science Team Meeting July 11-12, 2012 Ann Arbor MI
- [15] **S. Farrar**, *W.L. Jones*, “SSMIS-TMI XCAL Cold End Analysis (F16 through F18)” , XCAL Science Team Meeting July 11-12, 2012 Ann Arbor MI

NASA Project Presentation - XCAL Cont'd



Orlando, FL – February 2013

- [16] **S. Farrar**, *W.L. Jones*, “AMSR2-TMI XCAL Cold End Analysis”, XCAL Science Team Meeting, February 21-22, 2013 Orlando, FL
- [17] **S. Farrar**, *W.L. Jones*, “Steps Towards Conventions Within XCAL”, XCAL Science Team Meeting, February 21-22, 2013 Orlando, FL

Toulouse, France – May 2013

- [18] *W.L. Jones, H. Ebrahimi, S. Farrar*, “TMI to MADRAS X-CAL Colde End Analysis”, XCAL Science Team Meeting, May 23-24, 2013 Toulouse, France
- [19] **S. Farrar**, *A. Santos-Garcia, W.L. Jones*, “Further Analysis on TMI/SSMI Biases (F13 through F15)”, XCAL Science Team Meeting, May 23-24, 2013 February 2013 Toulouse, France

Fort Collins, CO – August 2014

- [20] **S. Farrar**, *W.L. Jones*, “TMI-AMSR2 XCAL Cold & Warm End Analysis”, XCAL Science Team Meeting, August 22-23, 2014 Fort Collins, CO
- [21] **S. Farrar**, *M. Salemin, W.L. Jones*, “SSMI-TMI Cold & Warm End Analysis (F13 through F15)”, XCAL Science Team Meeting, August 22-23, 2014 Fort Collins, CO
- [22] **S. Farrar**, *R. Chen, W.L. Jones*, “SSMIS-TMI Cold & Warm End Analysis (F16 through F18)”, XCAL Science Team Meeting, August 22-23, 2014 Fort Collins, CO

College Park, MD – July 2014

- [23] **S. Farrar**, *H. Ebrahimi, W.L. Jones*, “GMI Anomalies”, XCAL Science Team Meeting, July 10-11, 2014 College Park, MD

Orlando, FL – February 2015

- [24] **S. Farrar**, *W.L. Jones*, “TMI Cold Sky Anomaly”, XCAL Science Team Meeting, February 28-29, 2015 Orlando, FL
- [25] **S. Farrar**, *W.L. Jones*, “GMI Second Stokes Analysis Using a Nadir-Look Maneuver”, XCAL Science Team Meeting, February 28-29, 2015 Orlando, FL

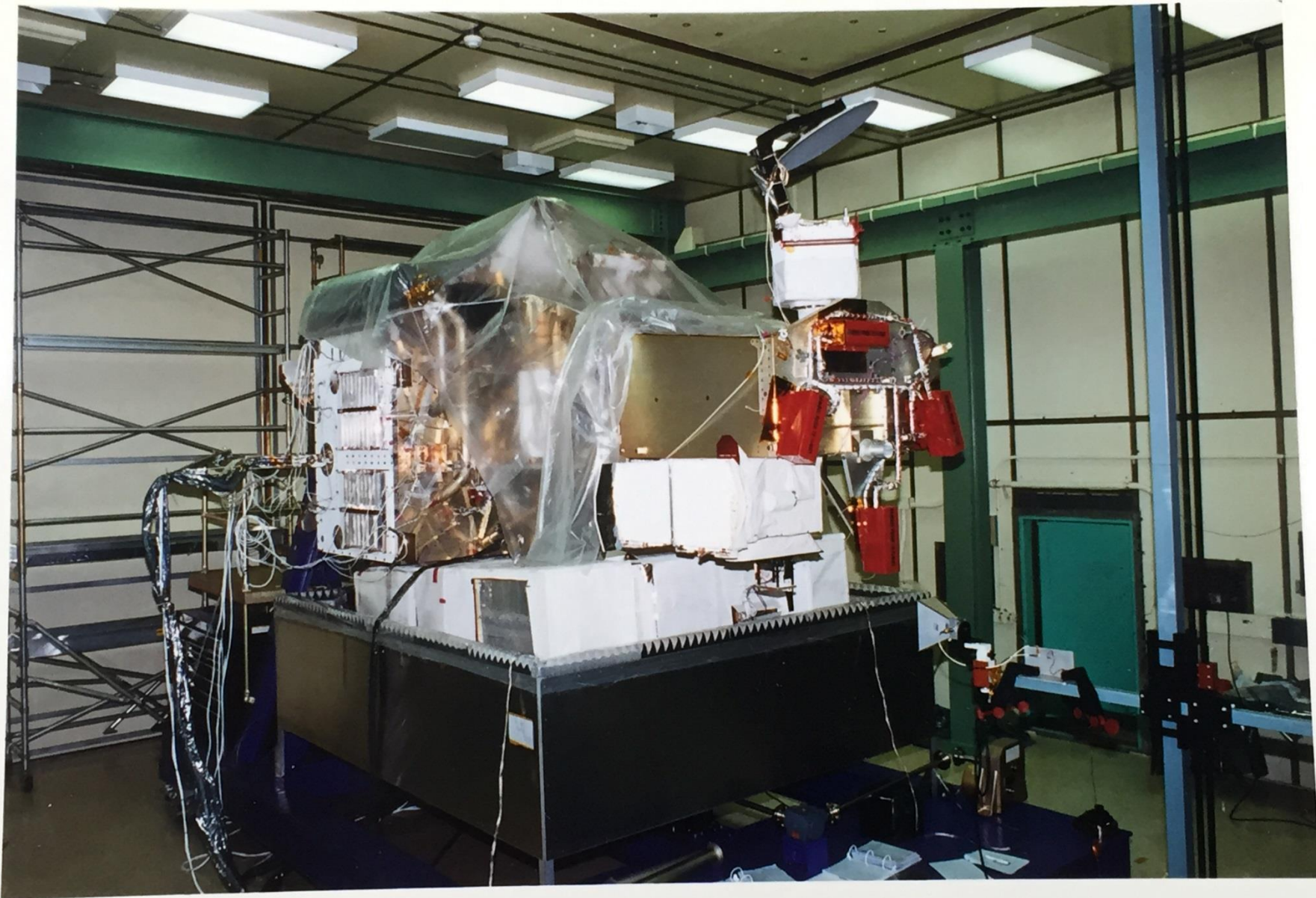
Other NASA Project Presentations



- [1] *L. Jones, K. Ahmad, **S. Farrar**, T. Kasparis*, “Ocean Precipitation Measurements using SeaWinds” , poster presented at the NASA Ocean Vector Winds Science Team Meeting, Nov 19-21, 2008, Seattle, WA
- [2] *L. Jones, S. AlSweiss, **S. Farrar**, S. Masuelli, and H. Raimondo*, “Microwave Radiometer (MWR) Contributions to Aquarius Science: Ocean Vector Winds & Ocean Precipitation Retrievals”, poster presented at the 4th AQUARIUS/SAC-D Int. Science Workshop, Dec 3-6, 2008, Argentina
- [3] ***S. Farrar**, L. Jones, R. Menzerotolo, S. Masuelli, M.M. Jacob, C. Tauror, H. Raimondo*, “Microwave Radiometer (MWR) Oceanic Integrated Rain Rate Algorithm for Aquarius/SAC-D” , poster presented at the 2010 Aquarius/SAC-D Science Team Meeting, July 19-21, 2010, Seattle, WA
- [4] *L. Jones, S. Bilanow, **S. Farrar**, S. Aslebagh*, “The Effects of TMI 1B11 V7 Solar Beta/Time Varying Bias Correction on 2A12 Rain Rates”, poster presented at the 2011 PMM Science Team Meeting, Nov 7-11, 2011, Denver, CO
- [5] *L. Jones and **S. Farrar***, “MWR Tb Anomaly: Antenna Pattern Effects”, AQ Cal/Val meeting, Nov. 15-17, 2011, Pasadena, CA
- [6] ***S. Farrar** and L. Jones, M. Labanda, March Jacobs and Sergio Masuelli*, “MWR Tb Anomaly: Smear Effect”, Aquarius Cal/Val meeting, March 27-28, 2012, Santa Rosa, CA.
- [7] *M. Labanda, M. Jacob, S. Masuelli, **S. Farrar**, H. Raimondo, W.L. Jones*, “MWR Smear Effect: Analysis and Its Possible Correction” , 7th Aquarius/SAC-D Science Meeting Preliminary Agenda 11-13 April 2012 Buenos Aires, Argentina
- [8] *L. Jones, S. Datta, **S. Farrar**, A. Santos-Garcia, and H. Ebahimi* “Inter-Satellite Microwave Radiometric Calibration for the GPM Constellation,” NASA PMM Internat. Science Team meeting, Annapolis, MD, March 20, 2013

Acknowledgements

- Yimin Ji (PPS)
 - Providing 1A11 & Base files and related material
- James Shiue (SGT Inc)
 - Providing insight of the instrument from our discussions & obtaining documents & data of TMI
- Steve Bilanow (PPS)
 - Helping resolve geolocation errors, questions, understanding of the inertial-hold, and help with reading the 1A11 data product
- Second Stokes Analysis
 - Rachael Kroodsma (PPS) for providing converted RSS Surface Emissivity Matlab Code
 - Wes Berg (CSU) for providing Fortran Code that contains XCAL atmospheric & RSS' new surface emissivity model to account for wind direction
- Shannon Brown (JPL)
 - Providing insight on his effective conductivity work with reflectors
- RSS for providing their Surface Emissivity Model (Fortran) to the XCAL group
- Tom Wilheit
 - For being an influential proponent for CAMS for the TMI & GMI instruments



Courtesy of Steve Bilanow (PPS)

Thank You!

Back Up Slides

Backup Slides Setup

- **Analyzes that Were Removed Due to Time Constraints**
 - TMI Main Beam Width ([Link](#))
 - TMI Main Beam Boresight ([Link](#))
 - Along-scan Bias ([Link](#))
- **Actual Backups**
 - Intro ([Link](#))
 - Beam Width ([Link](#))
 - Beam Pointing ([Link](#))
 - Along-scan Bias ([Link](#))
 - Second Stokes ([Link](#))
 - Emissivity ([Link](#))
 - Backups From Proposal ([Link](#))

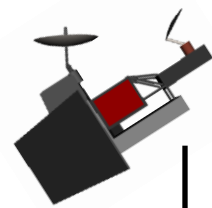
Analyses that Were Removed Due to Time Constraints

Analysis

TMI Main Reflector Beamwidth

Illustration of Nadir Angle

TRMM
Spacecraft



Geodetic
Nadir

Nadir Angle

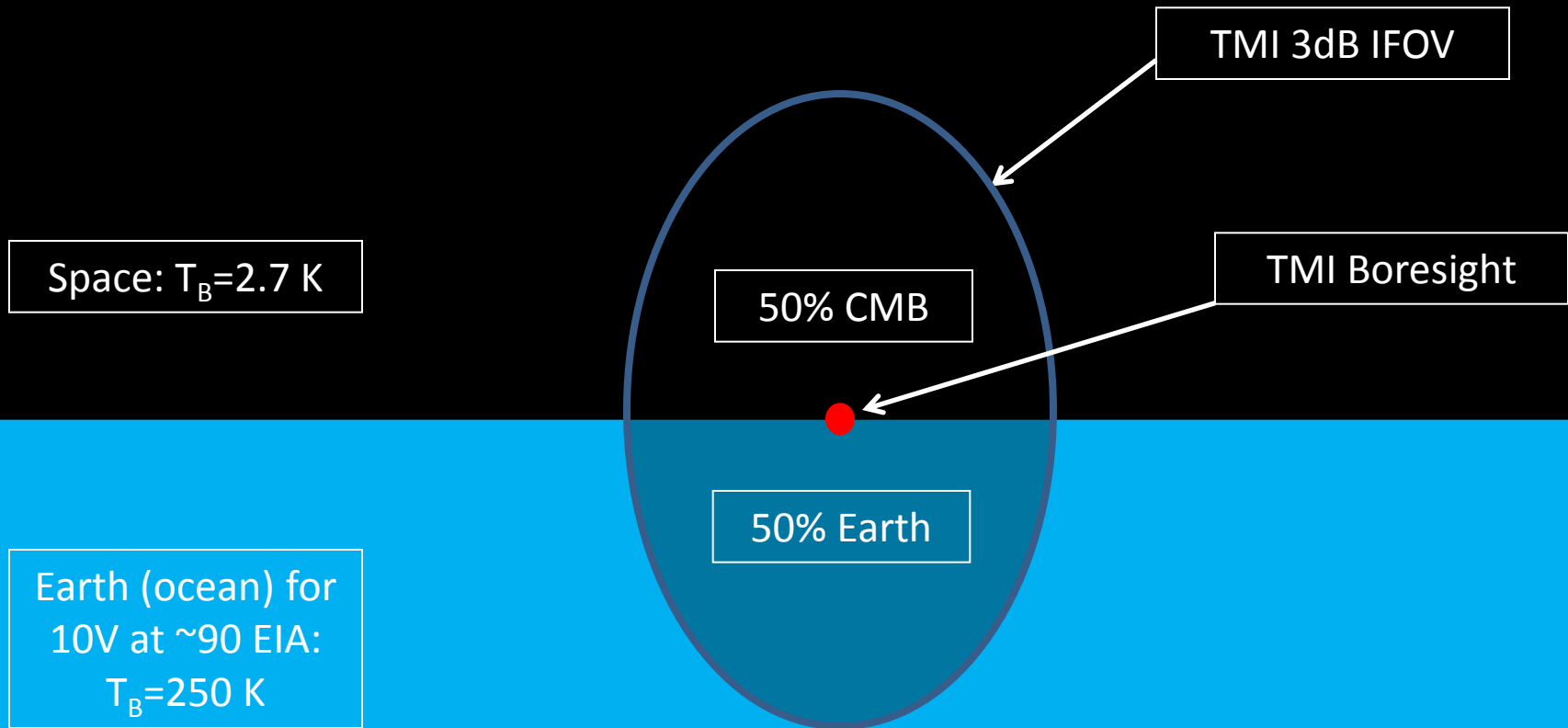
-3dB Beamwidth

Earth's Horizon

Earth

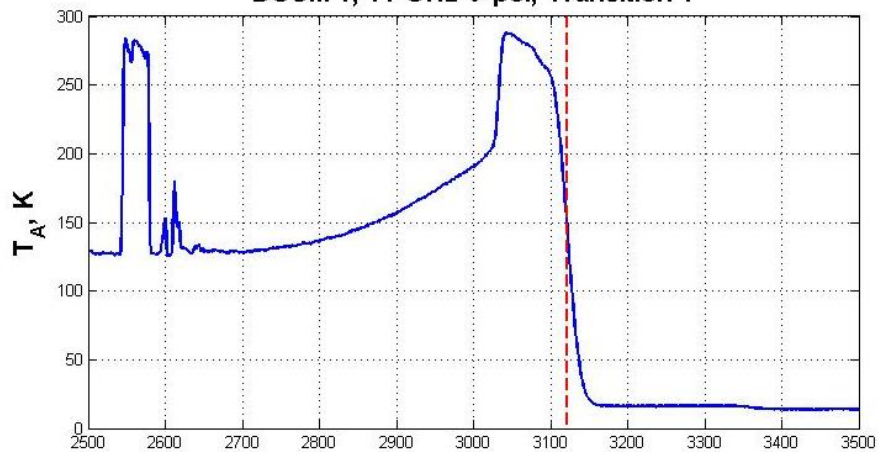
MR Boresight

TMI's IFOV While Leaving Earth

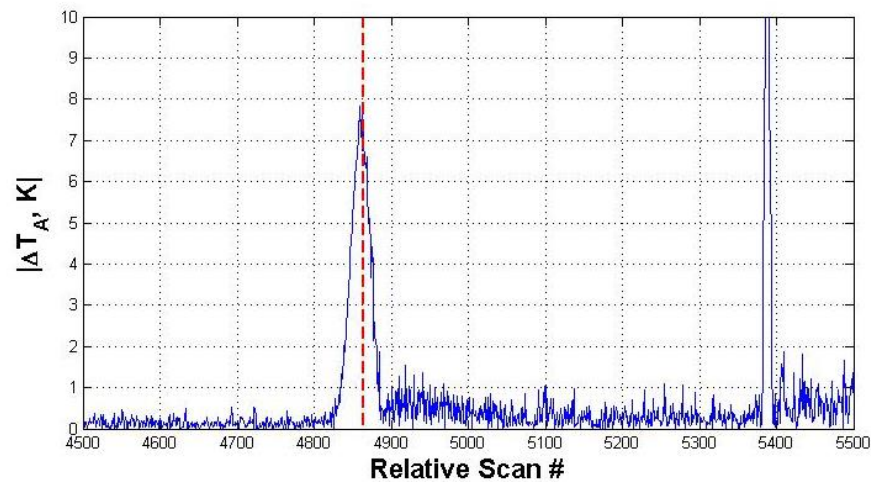
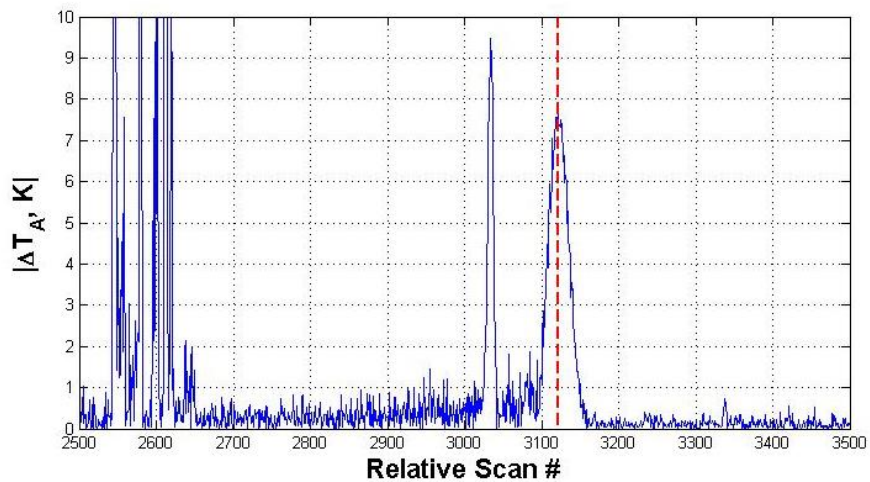
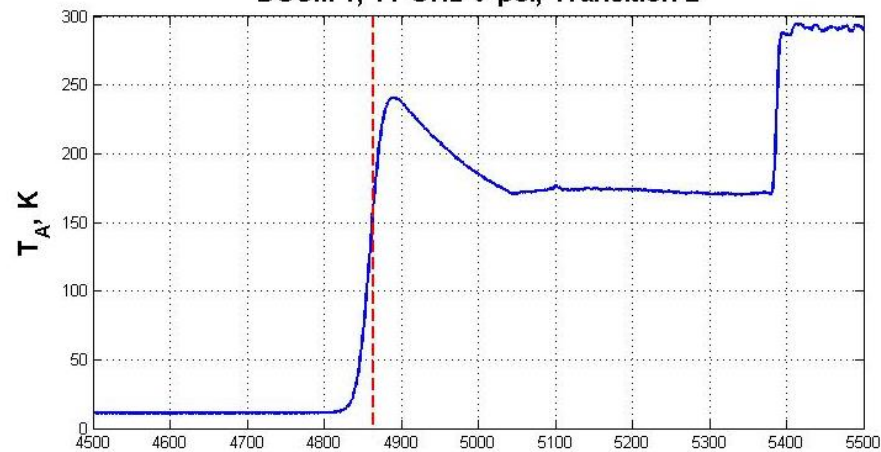


Example of $|\Delta T_A|$

DSCM 1, 11 GHz V-pol, Transition 1

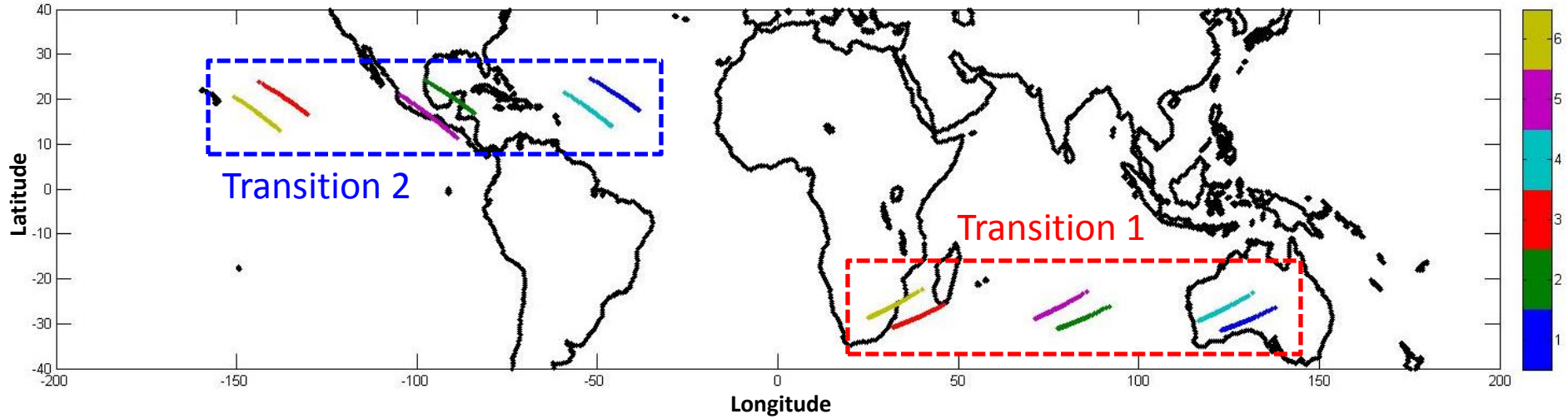


DSCM 1, 11 GHz V-pol, Transition 2

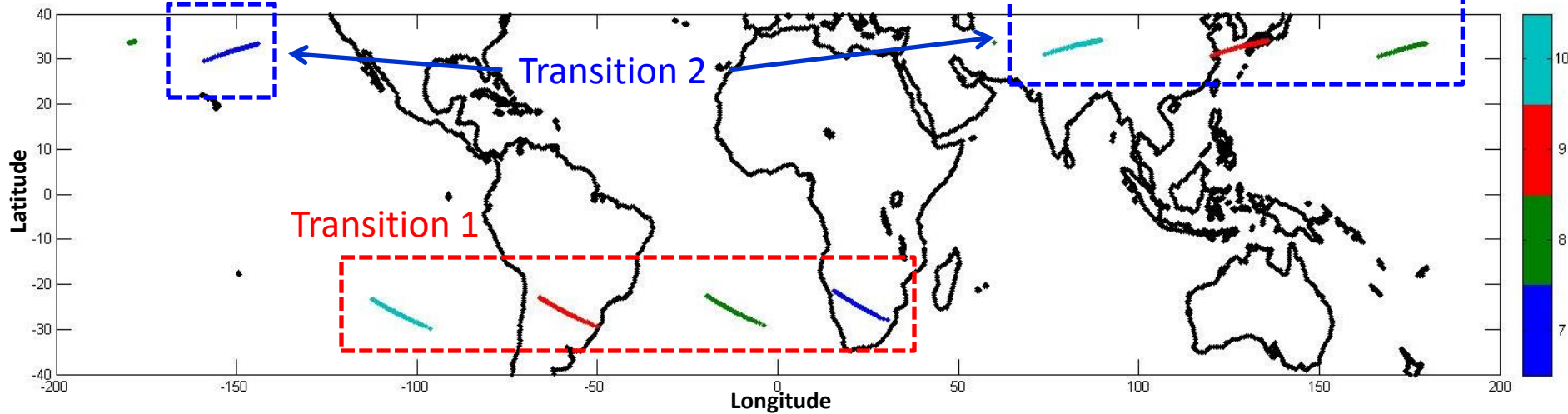


DSV Transitions Geolocated

DSCMs 1 - 6

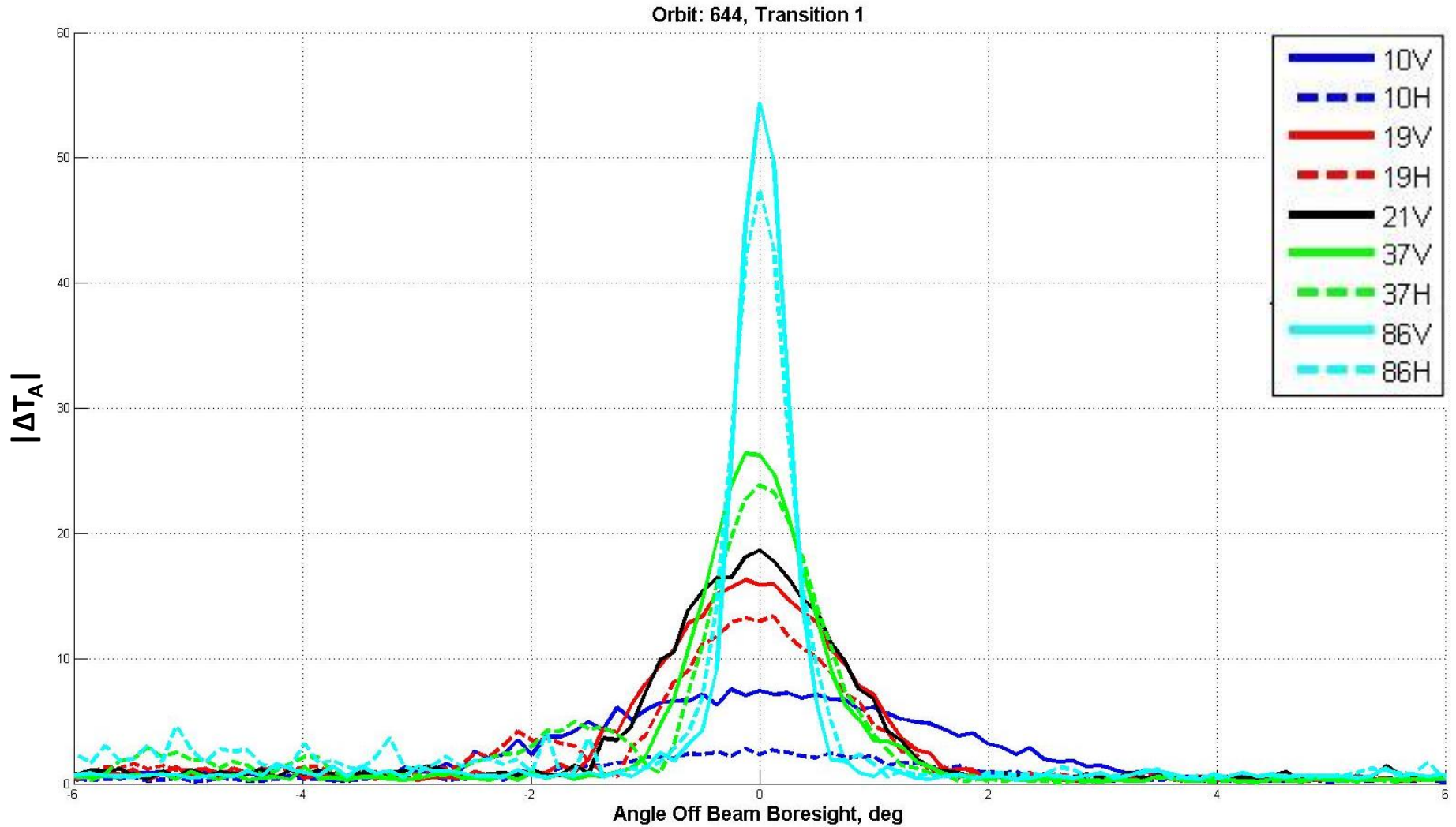


DSCMs 7 - 10



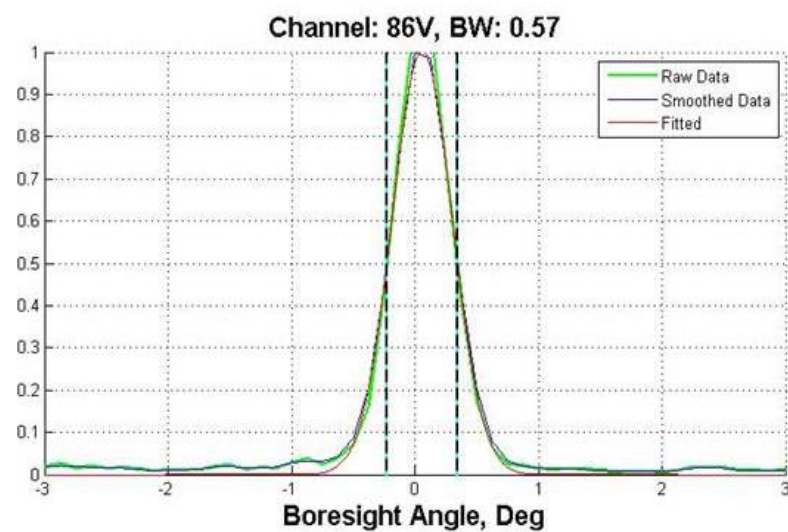
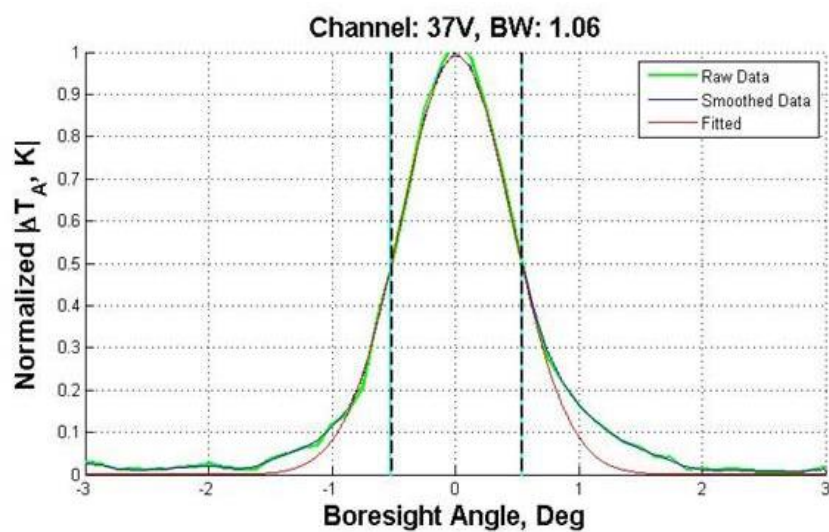
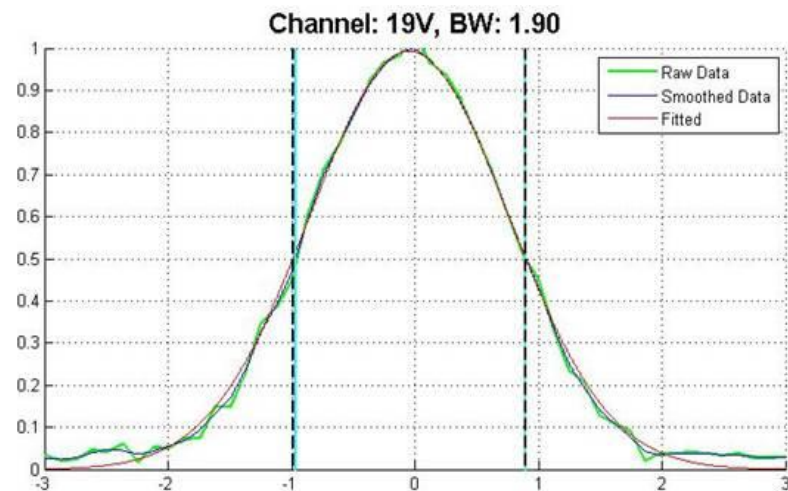
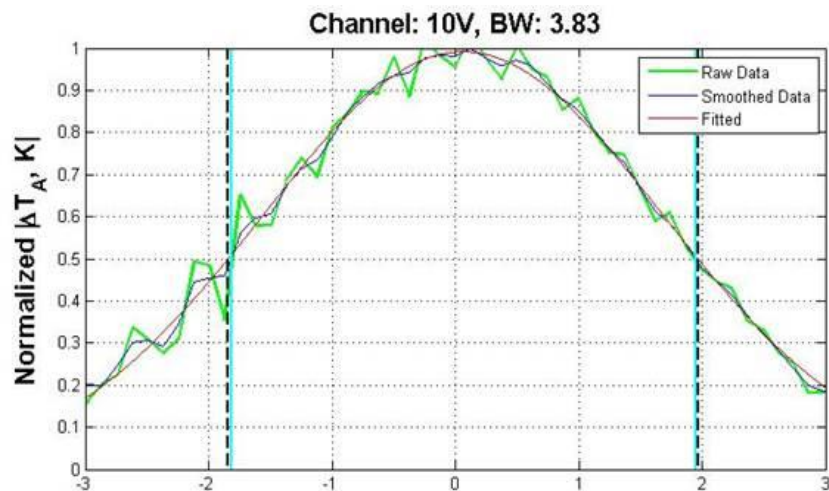
Note: Only half of transition is shown since other have views space

Amplitude of ΔT_A



Beamwidths

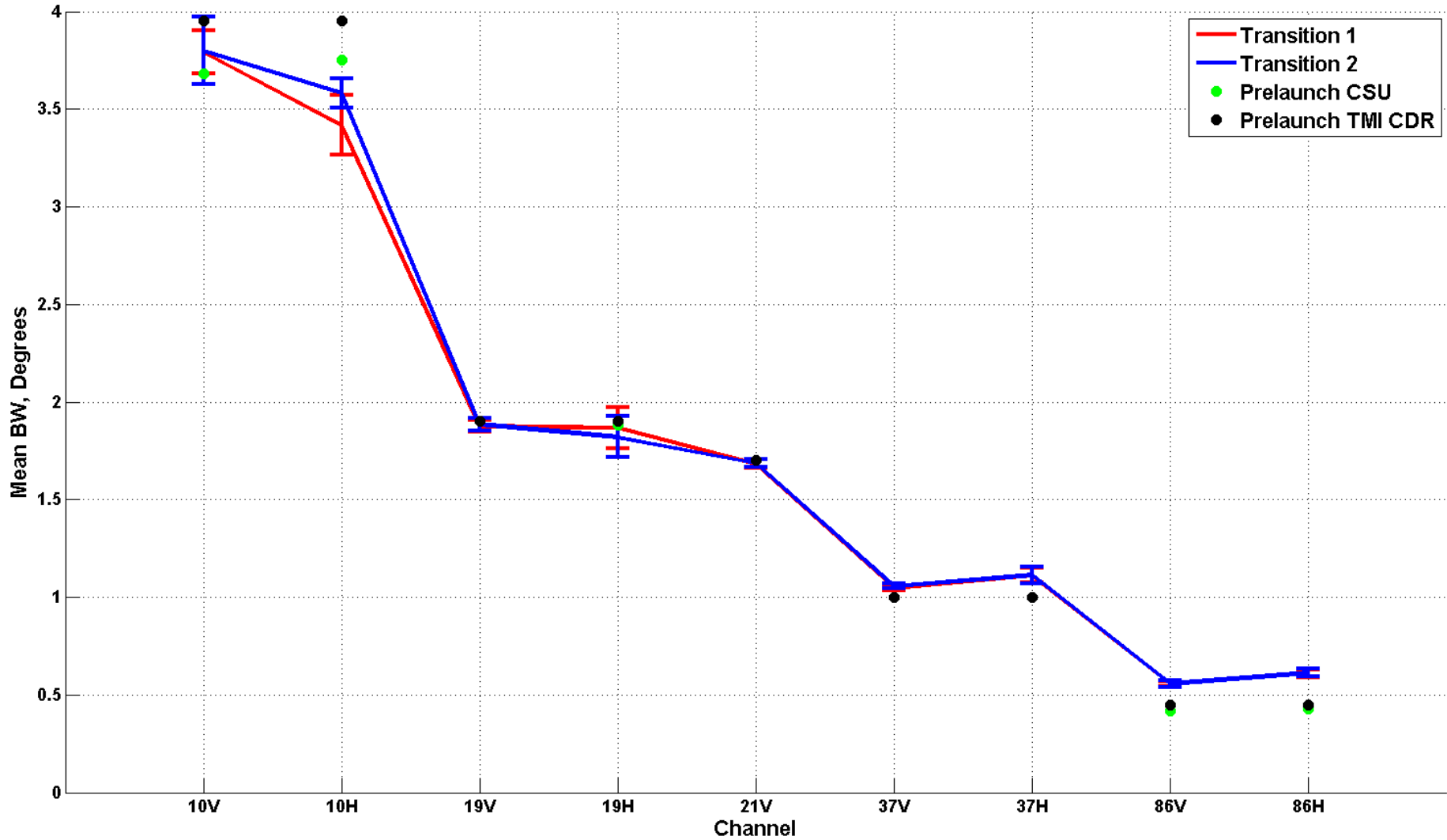
DSCM-4, Transition 1



(c)

(d)

Beamwidth For All Channels



Conclusion & Future Work

- This analysis uses the edge of the earth, a sharp transition in TB (Ex: $\sim\Delta 240$ K @ 10V-pol) for calculating TMI BW in the elevation plane
- H-Pol channels have the largest variation
- Disagreement between mean BW are largest for 10.65 GHz channels for Transition 1 to CSU & CDR beam widths
 - 10V: CSU ($\Delta=0.12^\circ$), CDR ($\Delta=0.15^\circ$)
 - 10H: CSU ($\Delta=0.35^\circ$), CDR ($\Delta=0.60^\circ$)
- Future Work To Be included in the Dissertation
 - Include multiple scan positions so to reduce the variance as well as more sample points for the 10.65 GHz channels to improve the mean (refer to [back-up](#) for examples)

Analysis

TMI Main Beam Boresight

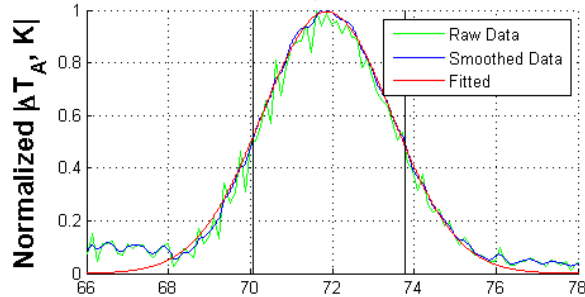
Main Reflector Boresight

- Method:
 - Follows similar method as Beamwidth analysis except:
 - interested in when the boresight (peak of the secondary radiation pattern) passes the Earth's horizon
 - angle between boresight & geodetic nadir (nadir angle) is used for comparisons
- It is understood that TMI's MR boresight for 11 GHz channels are misaligned compared to the multi-frequency feed
 - But by how much is in question?

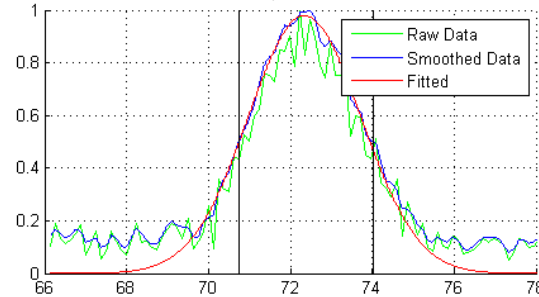
Channels	Offsets from Shiu Memo (deg)		Offsets from TMI Subsystem Test Doc (deg)	
	Along-Track	X-Track	Along-Track	X-Track
10.65 V	0.555	-0.185	0.487	0.09
10.65 H	0.185	0.555	0.568	0.134

Boresights w.r.t. Nadir Angle

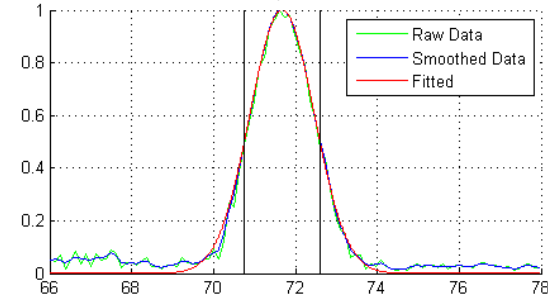
Channel: 10V, Bm Cntr: 71.87



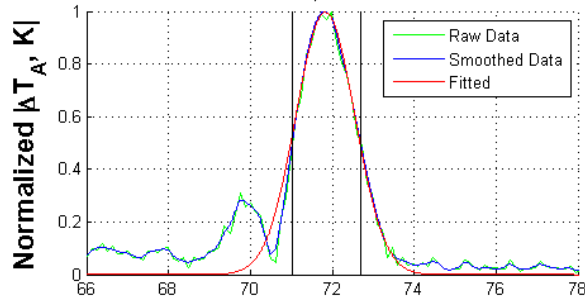
Channel: 10H, Bm Cntr: 72.35



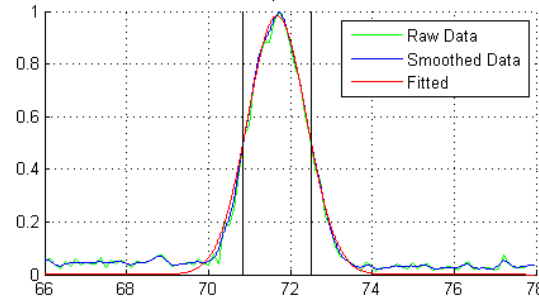
Channel: 19V, Bm Cntr: 71.68



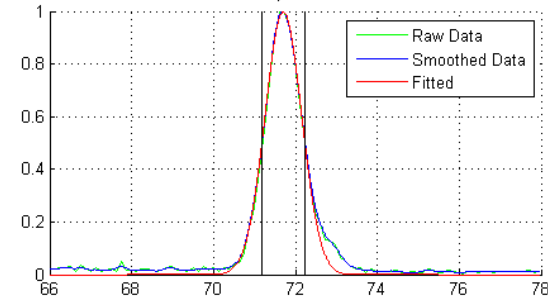
Channel: 19H, Bm Cntr: 71.83



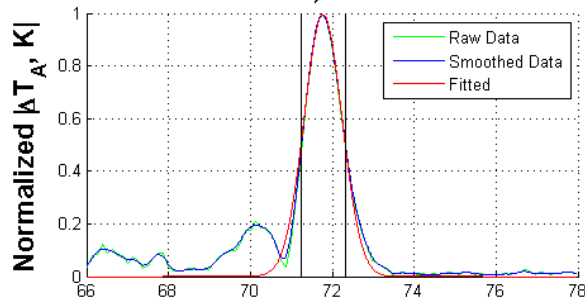
Channel: 21V, Bm Cntr: 71.68



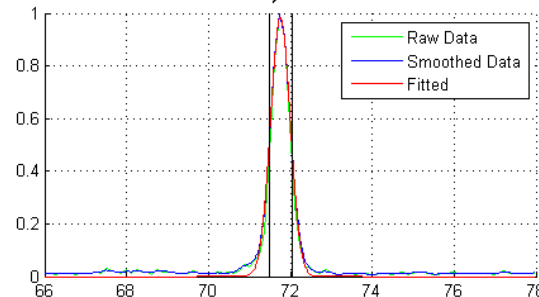
Channel: 37V, Bm Cntr: 71.71



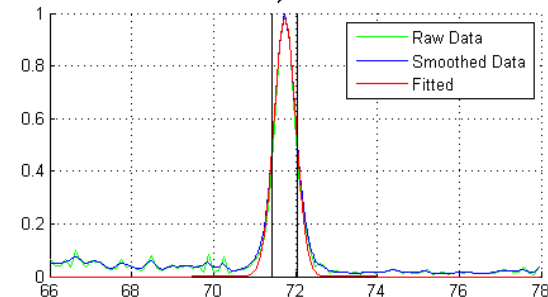
Channel: 37H, Bm Cntr: 71.78



Channel: 86V, Bm Cntr: 71.76



Channel: 86H, Bm Cntr: 71.74



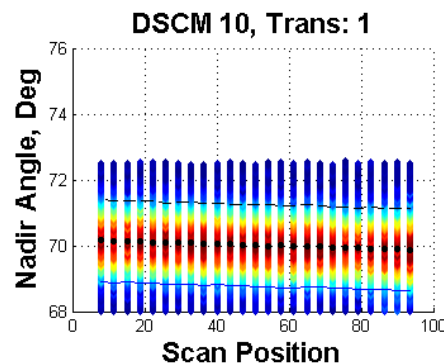
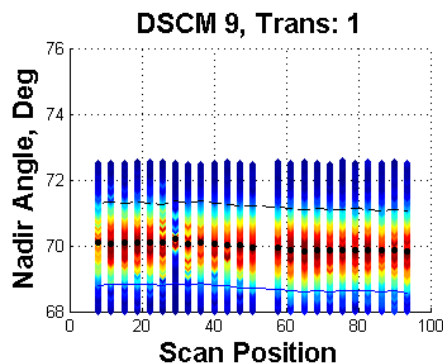
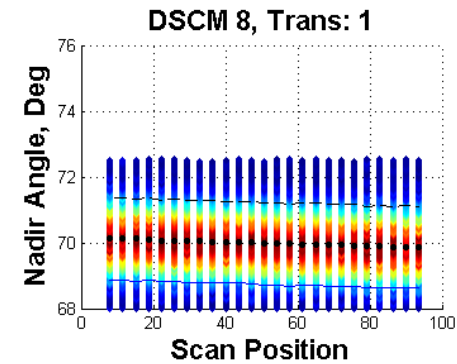
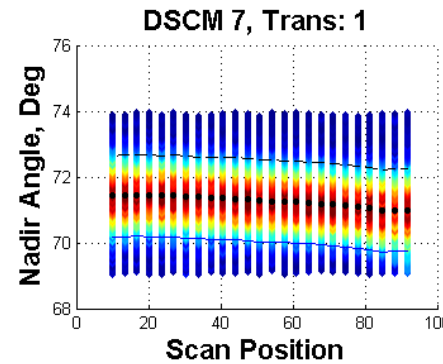
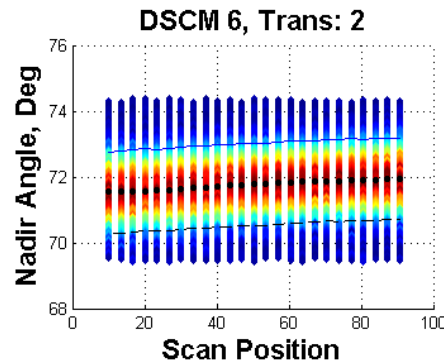
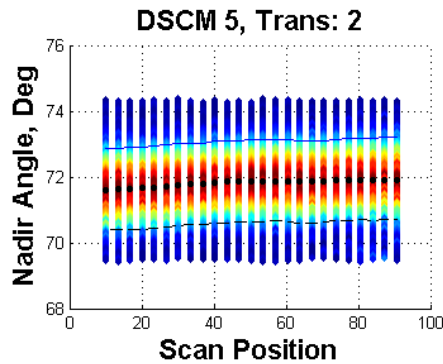
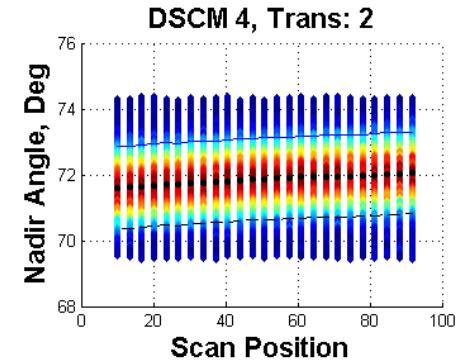
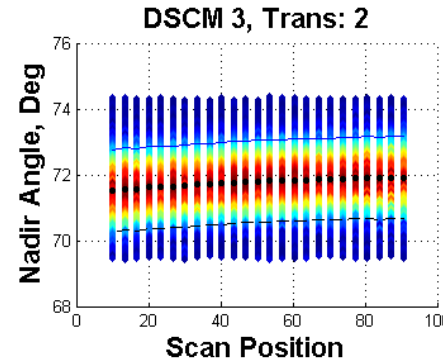
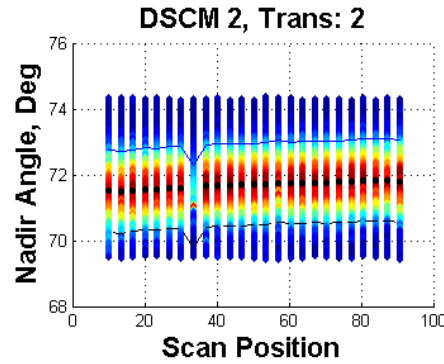
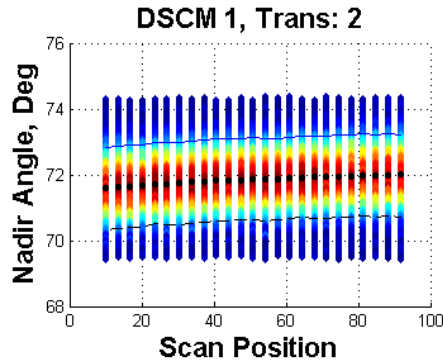
Geodetic Nadir Angle, deg

Geodetic Nadir Angle, deg

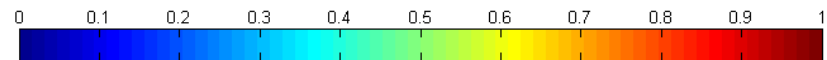
Geodetic Nadir Angle, deg

Nadir Dependence on Scan Position

19 V-pol

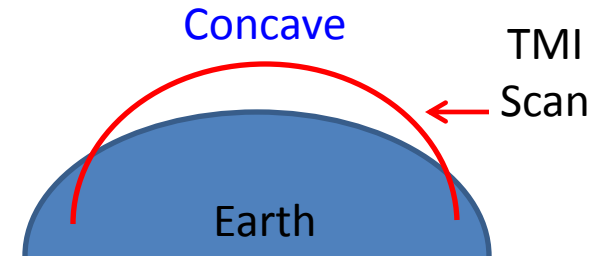
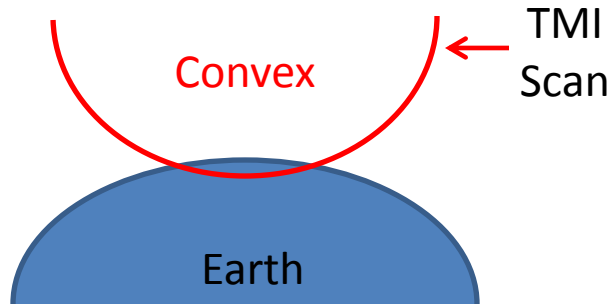


Amplitude of $|\Delta T_A|$ 19 V-pol

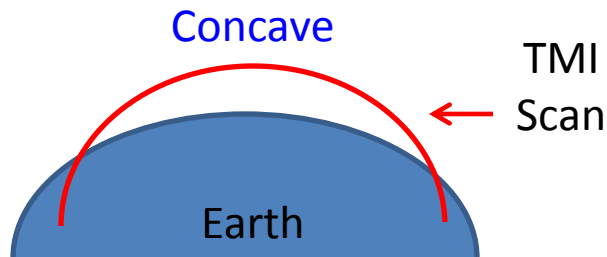


TMI Scan: Concave & Convex Transitions

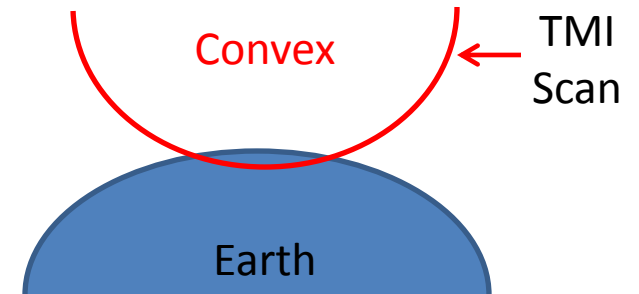
Yaw: 180



Yaw: 0

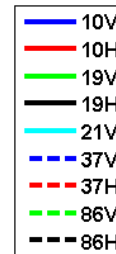
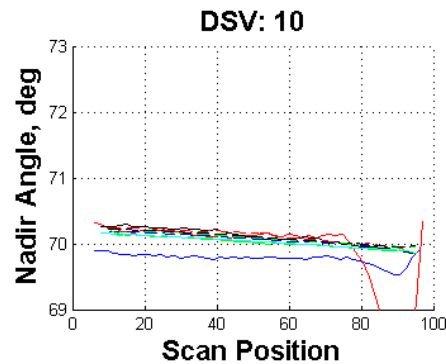
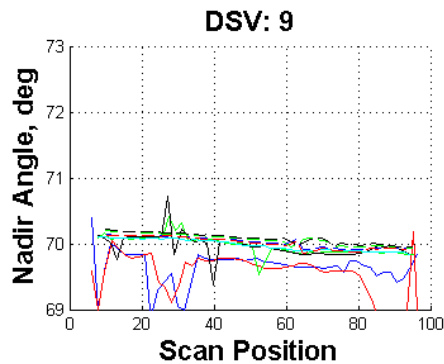
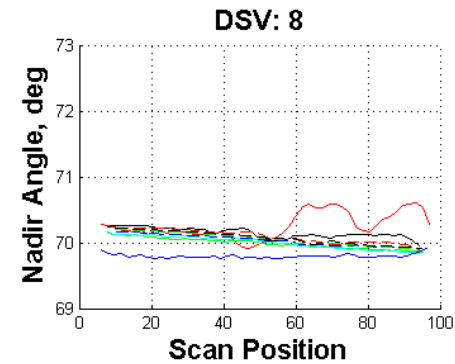
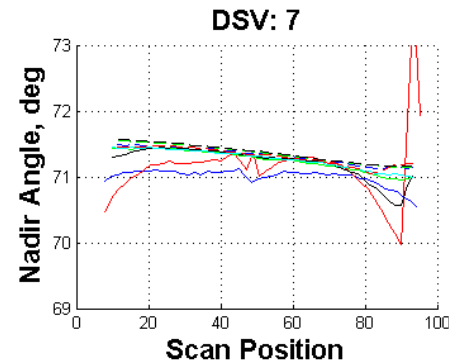
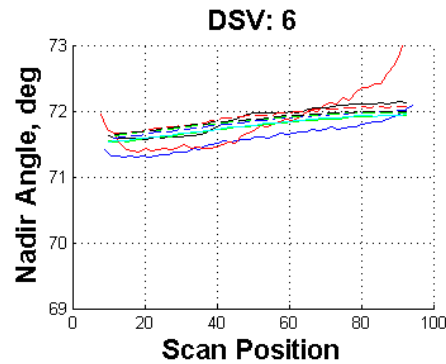
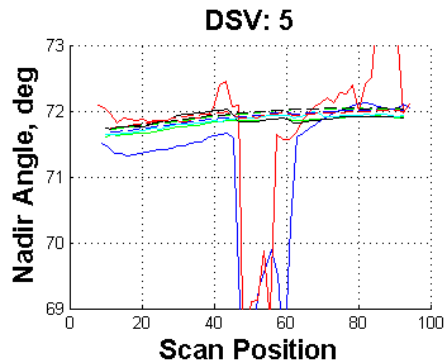
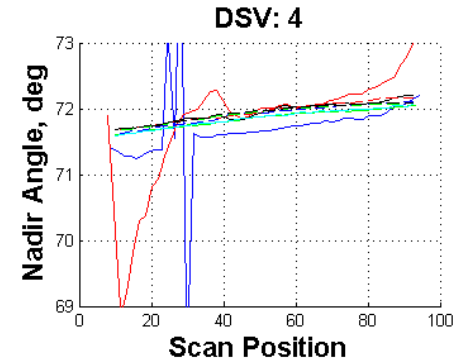
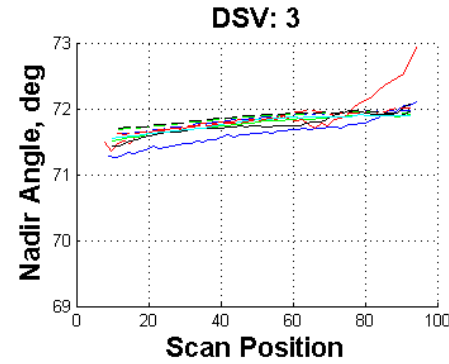
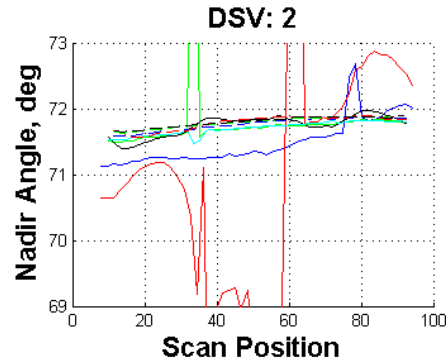
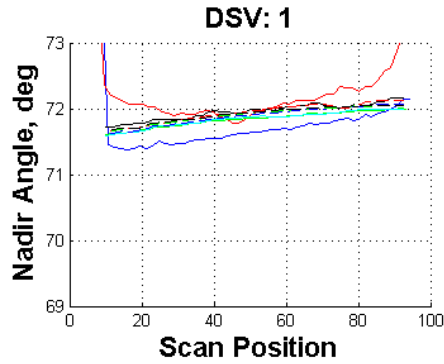


Transition 1



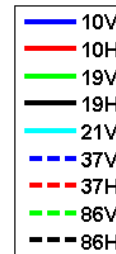
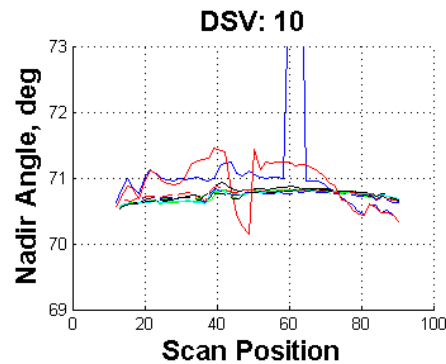
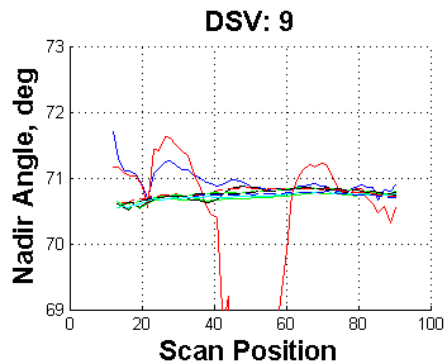
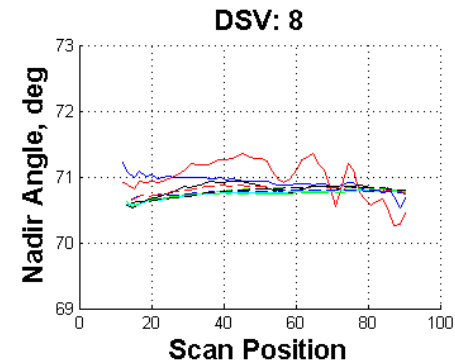
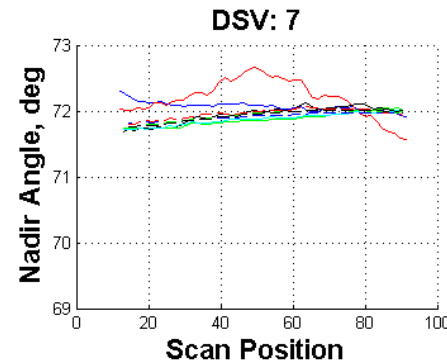
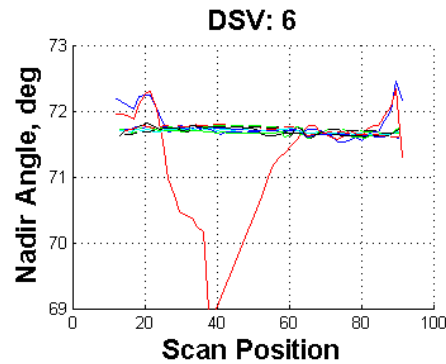
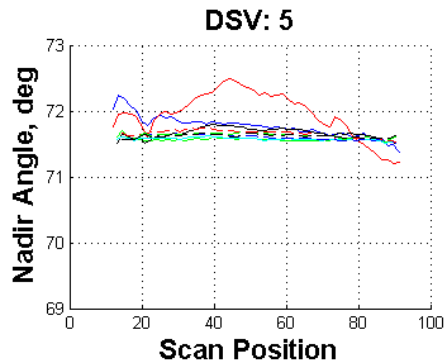
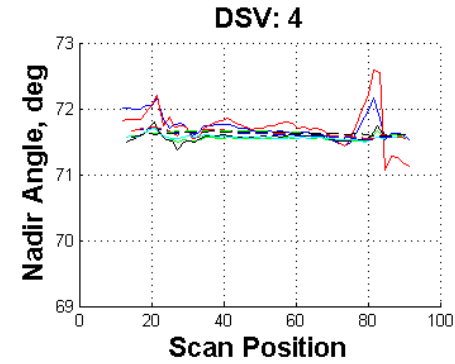
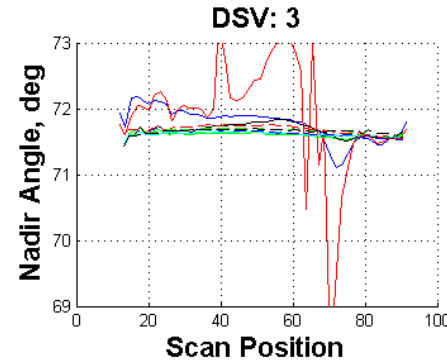
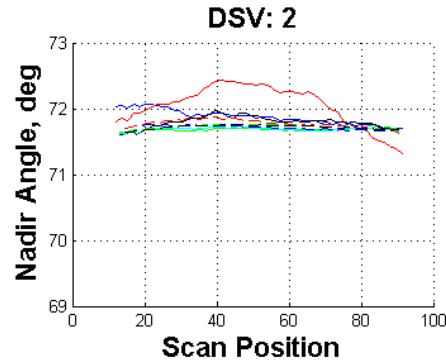
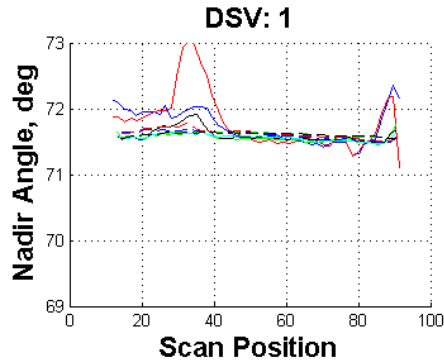
Transition 2

Concave Transitions



Difference between
10V & multi-freq
channels $\sim 0.3^\circ$

Convex Transitions



Difference in nadir angle is much different for convex case

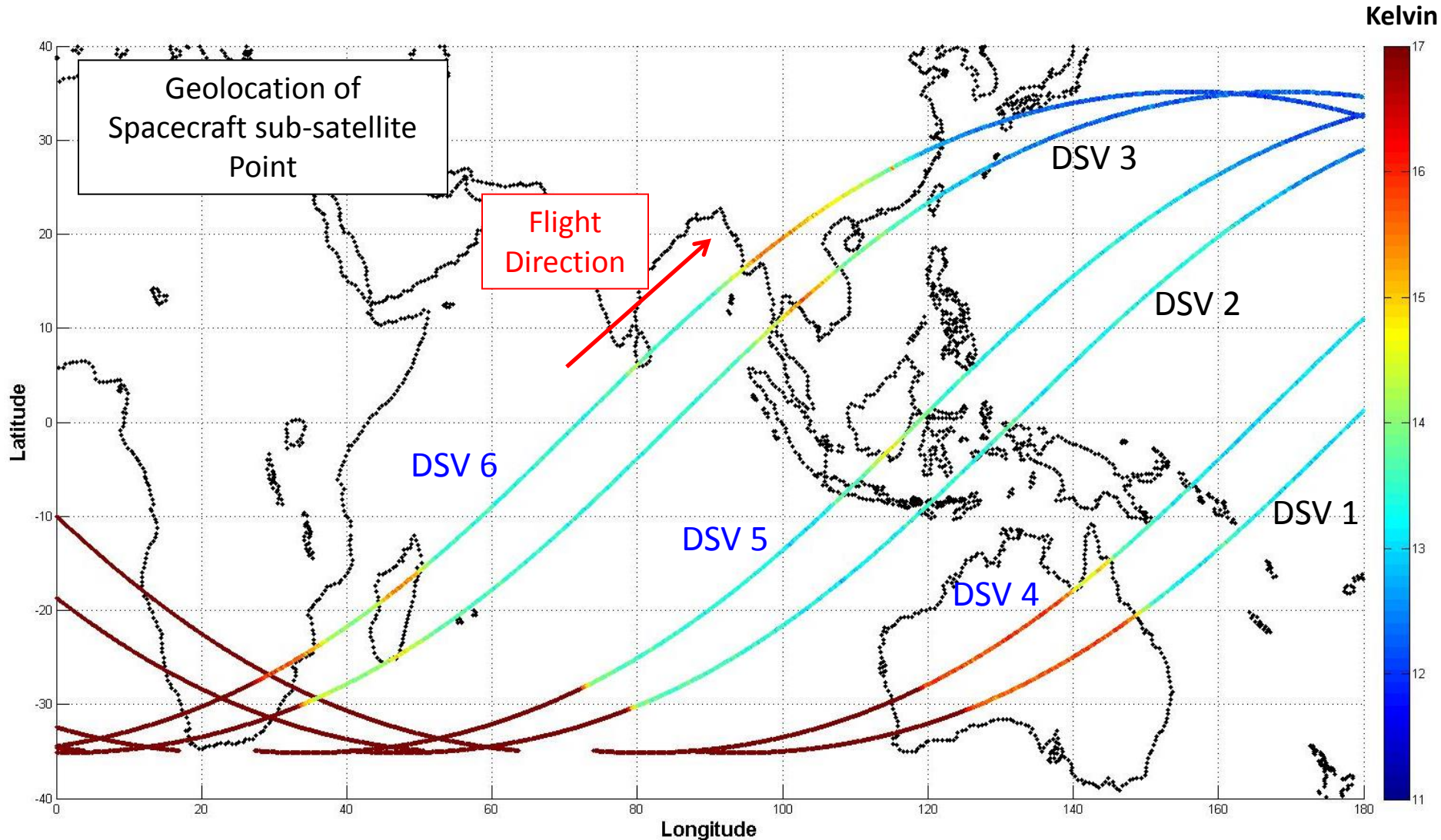
Conclusion & Future Work

- There are differences in the Nadir Angles for 10 V- & H-pol
 - Largest in 10 V for Concave but disappears for the convex case
 - There should be an offset in the along-scan direction which justifies why we don't see a difference in angle for convex cases
- Future Work To Be included in the Dissertation
 - Use STK or TMI geolocation code to determine match the nadir angles for the convex & concave cases
- Future Work: Post Dissertation
 - Use March 2015 maneuvers, Yaw 90° , to better estimate this angle in the along-scan direction

Analysis

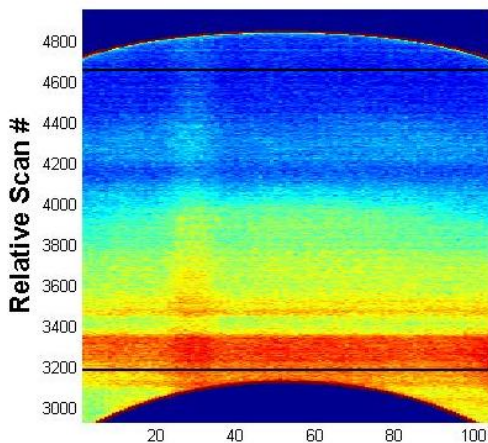
Along-scan Bias

T_A (19 V-pol) Earth Contamination (Spillover) for DSV 1-6



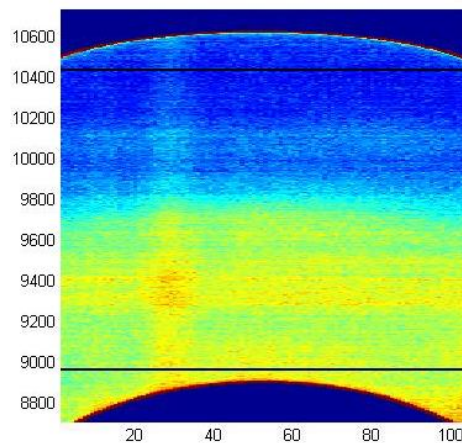
Deep Space Views for 19 V-Pol TA

Reconstructed T_A DSV 1



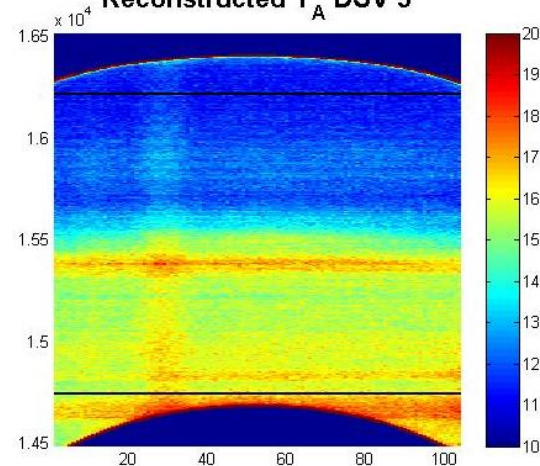
Scan Position

Reconstructed T_A DSV 2



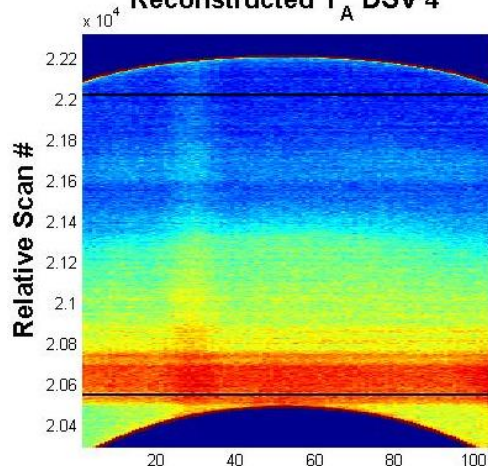
Scan Position

Reconstructed T_A DSV 3



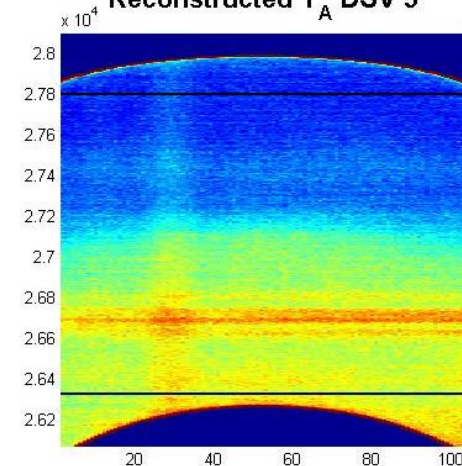
Scan Position

Reconstructed T_A DSV 4



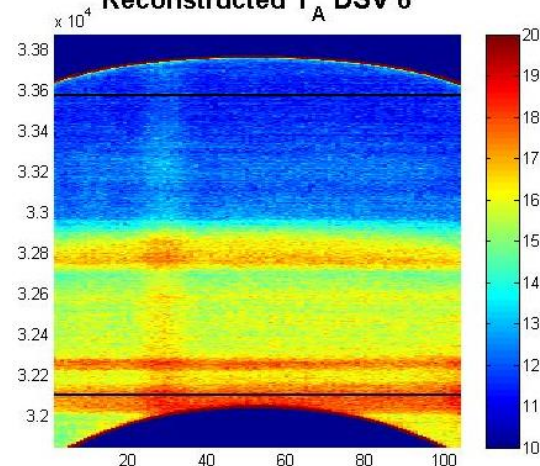
Scan Position

Reconstructed T_A DSV 5



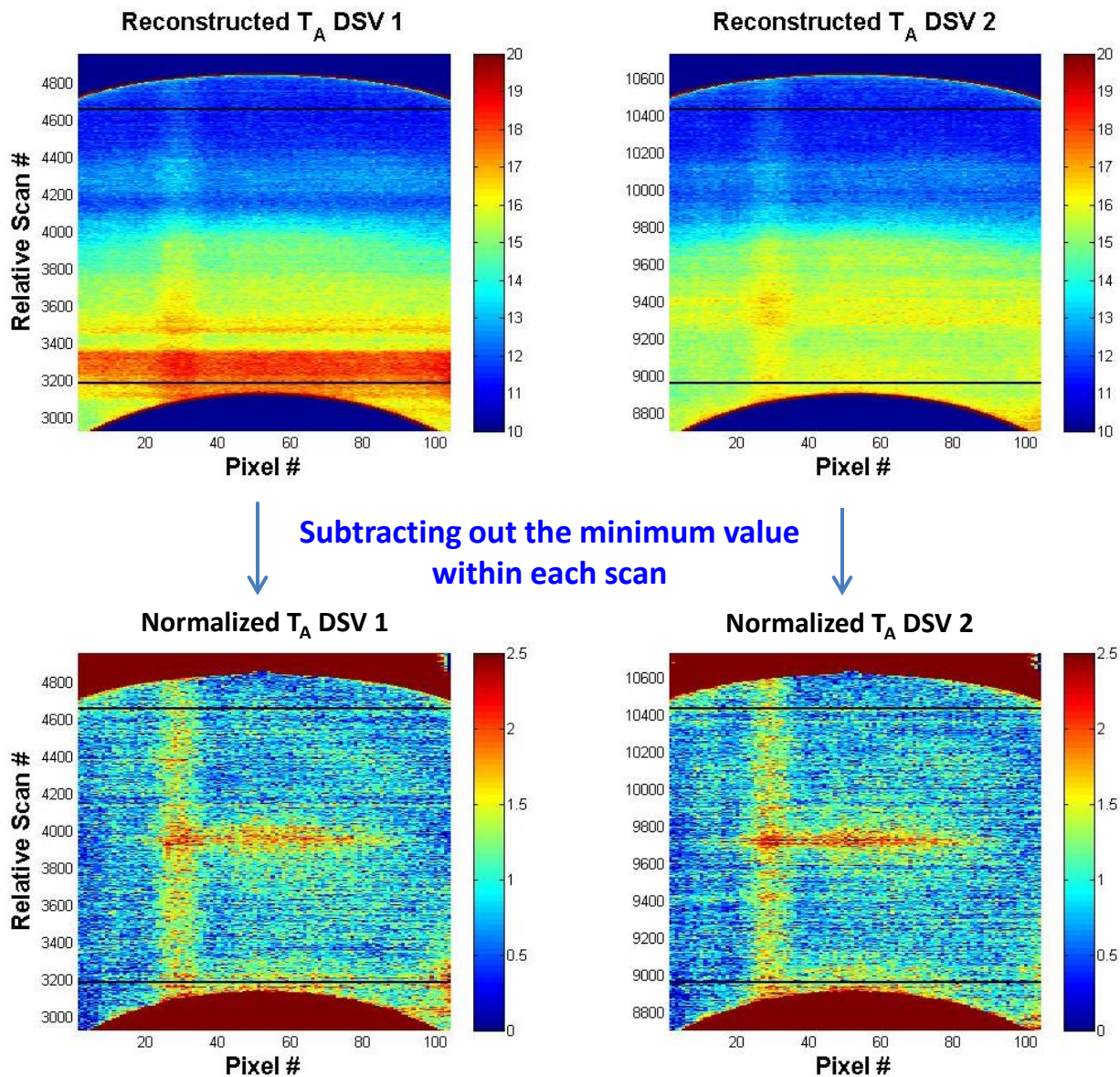
Scan Position

Reconstructed T_A DSV 6



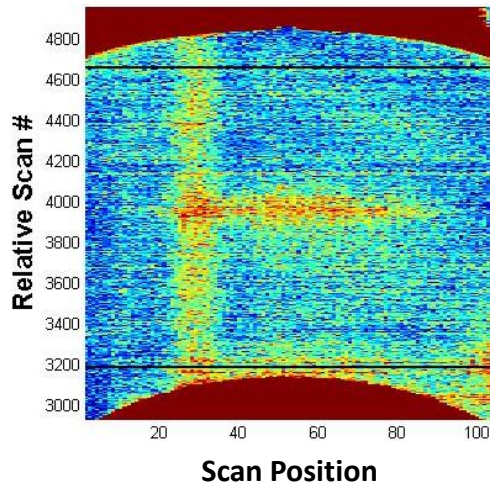
Scan Position

Deep Space Views for 19 V-Pol

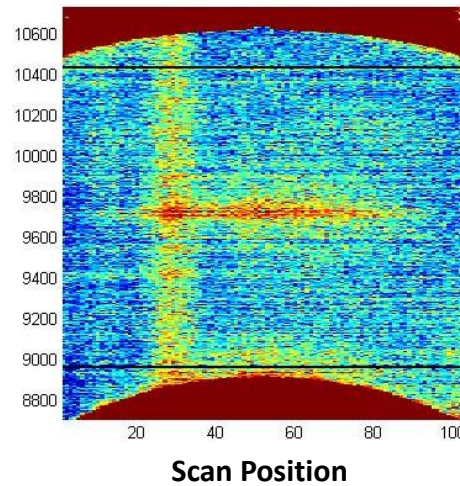


Deep Space Views for 19 V-Pol

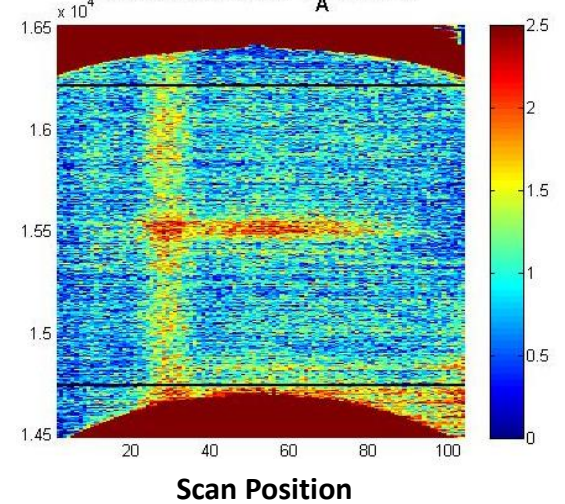
Reconstructed T_A DSV 1



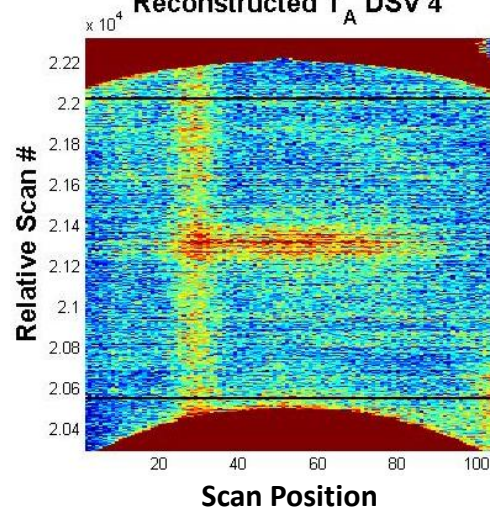
Reconstructed T_A DSV 2



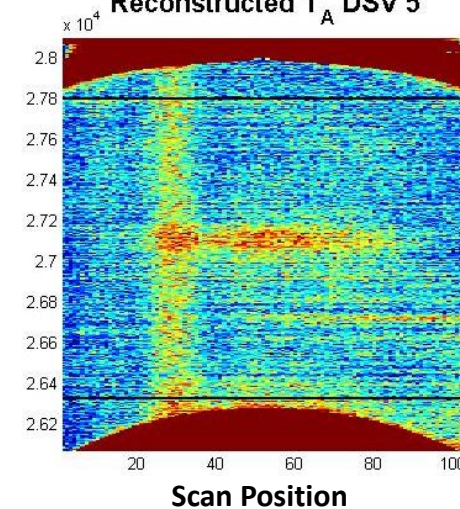
Reconstructed T_A DSV 3



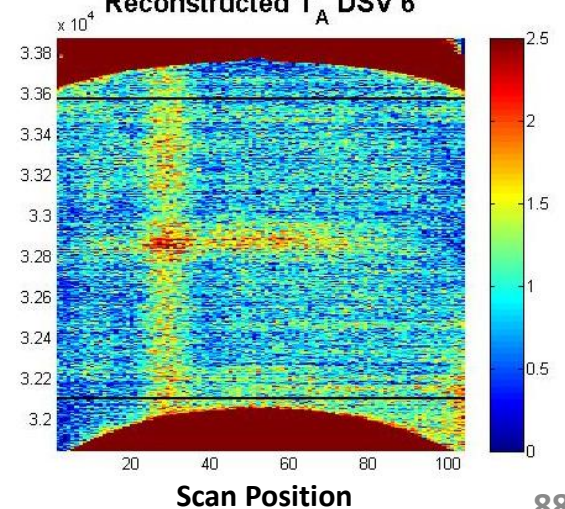
Reconstructed T_A DSV 4



Reconstructed T_A DSV 5



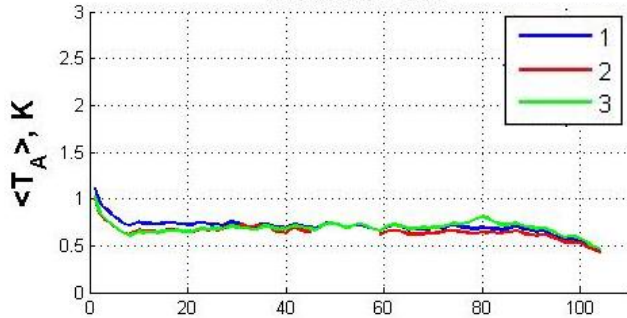
Reconstructed T_A DSV 6



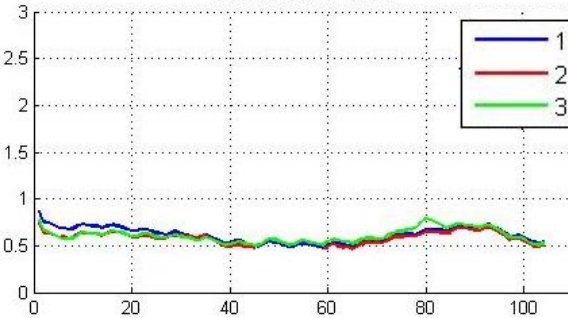
DSCM Sets

Limited Range Data

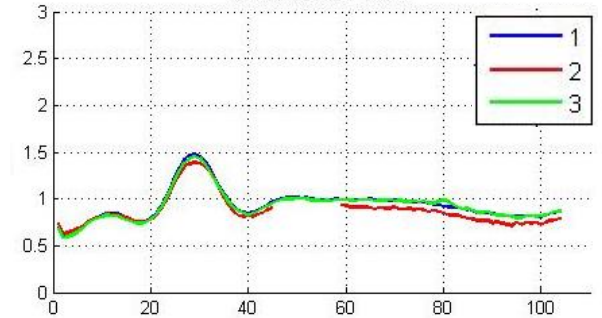
Channel: 10V



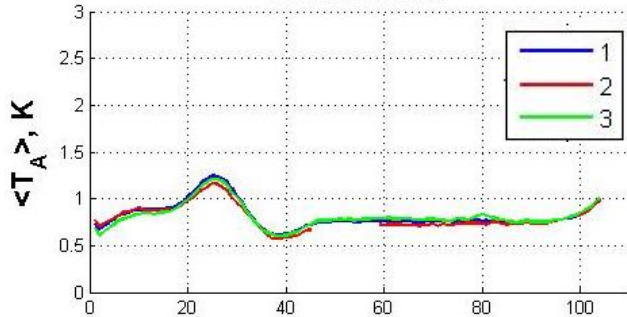
Channel: 10H



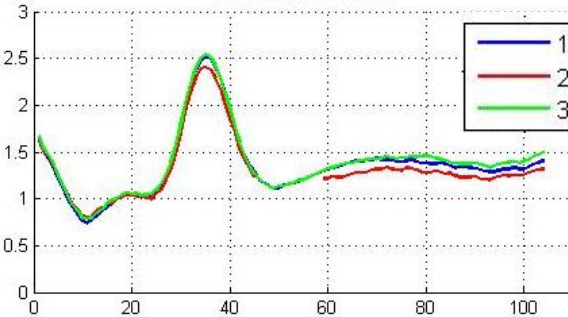
Channel: 19V



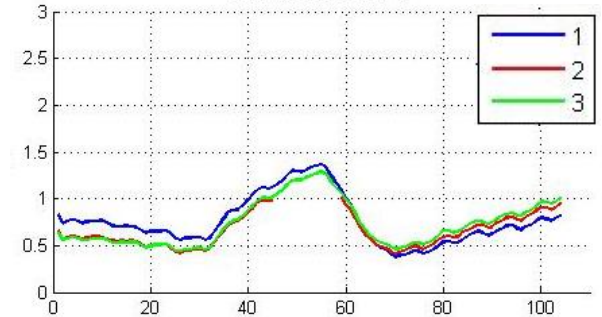
Channel: 19H



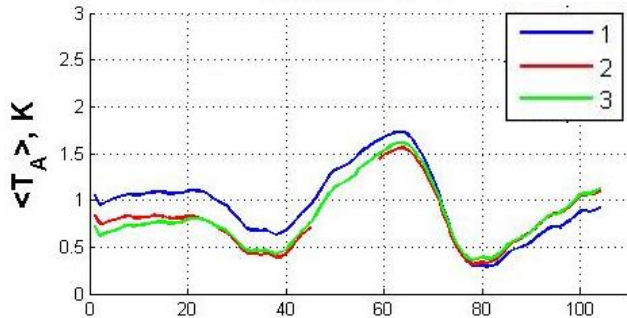
Channel: 21V



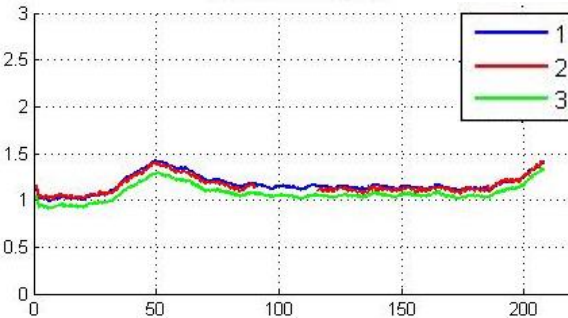
Channel: 37V



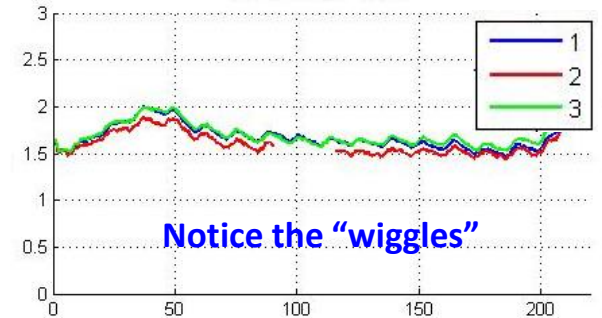
Channel: 37H



Channel: 86V



Channel: 86H



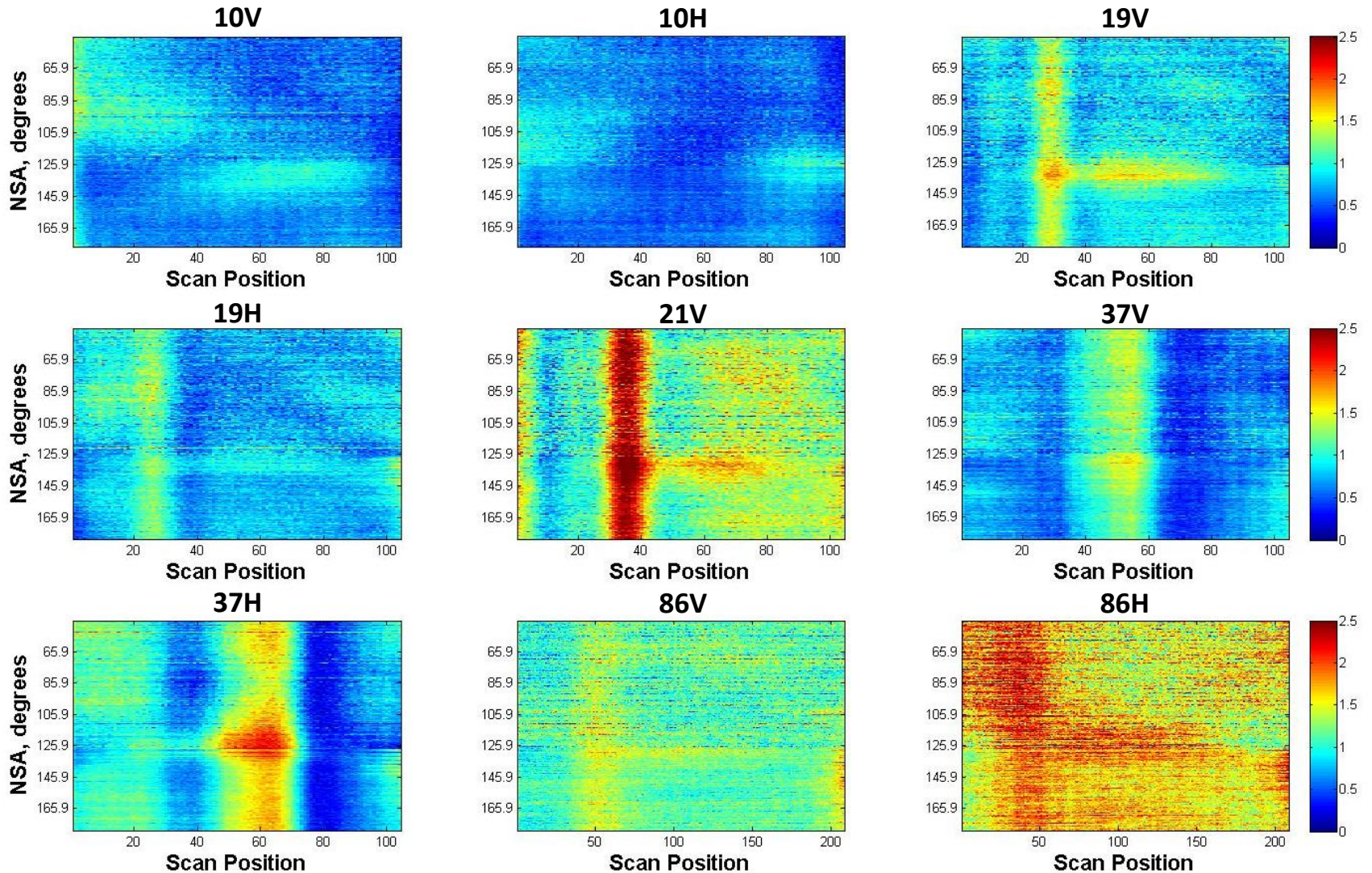
Notice the "wiggles"

Scan Position

Scan Position

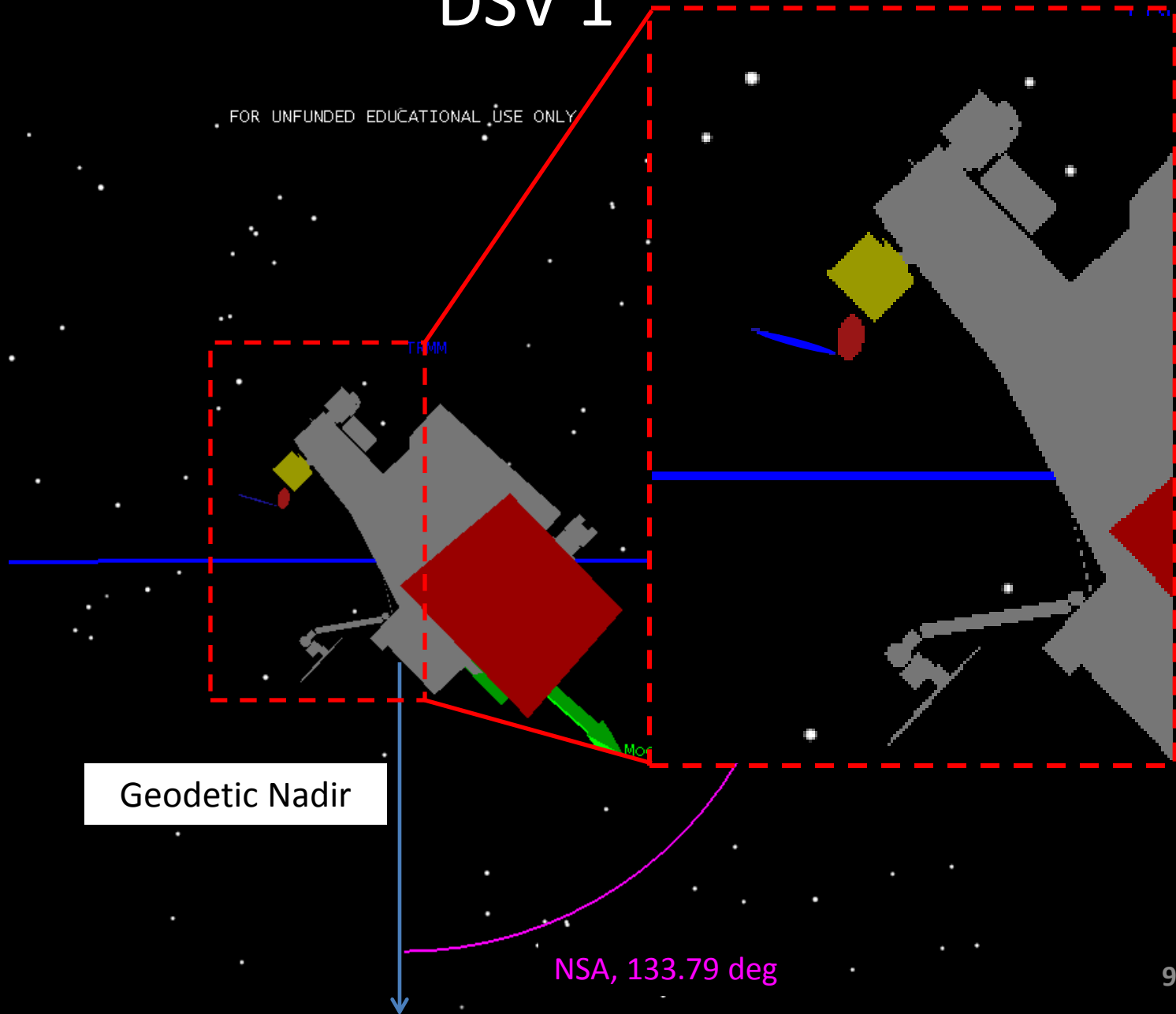
Scan Position

DSCM Set 1 – Averaged w.r.t. NSA



DSV 1

FOR UNFUNDED EDUCATIONAL USE ONLY



Geodetic Nadir

NSA, 133.79 deg

Conclusion & Future Work

- Along-scan analysis is in good agreement with RSS' (2001) analysis but this depends on channel
- Back-lobe / Spillover is present in this analysis and is obvious at an NSA angle of $\sim 133^\circ$
 - Depending on channels can be up to 1.0 K for a given scan position
- Future Work: Post Dissertation
 - Include Year 2015 maneuvers into this analysis

Extra Slides

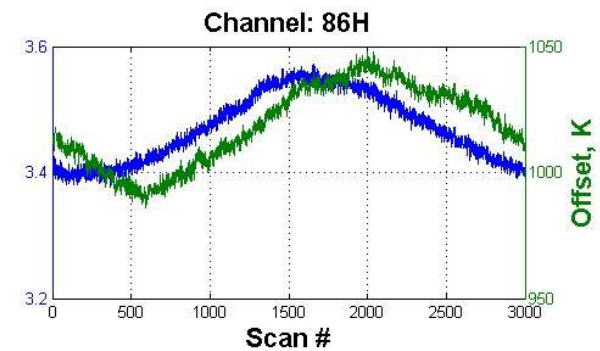
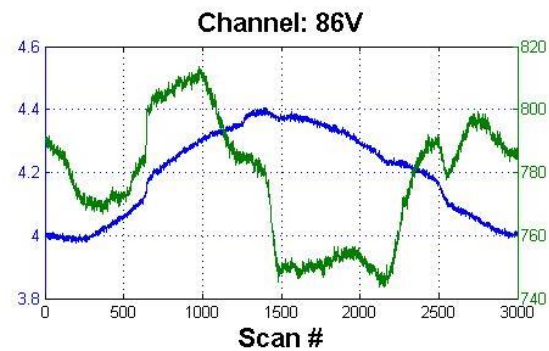
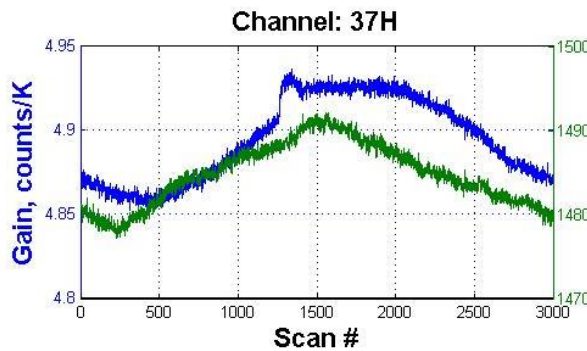
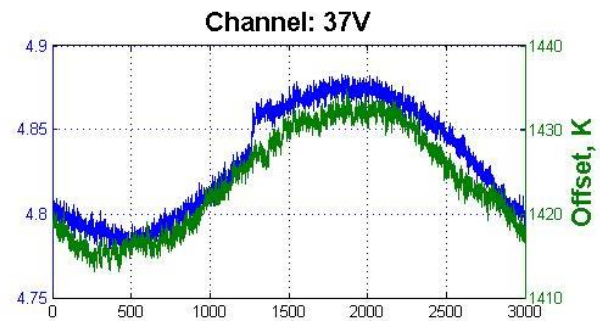
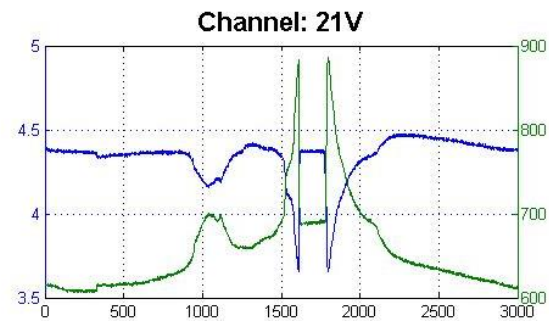
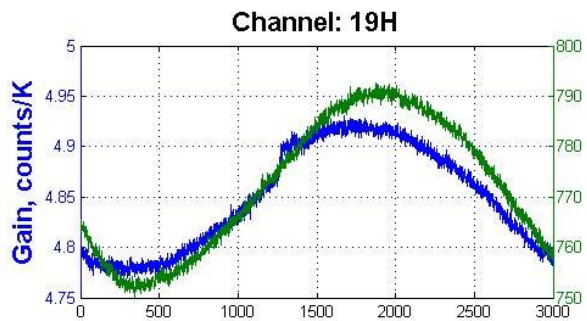
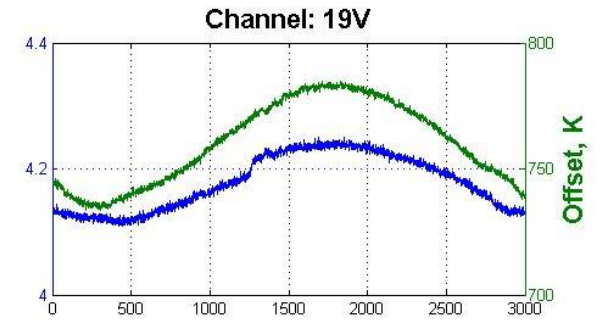
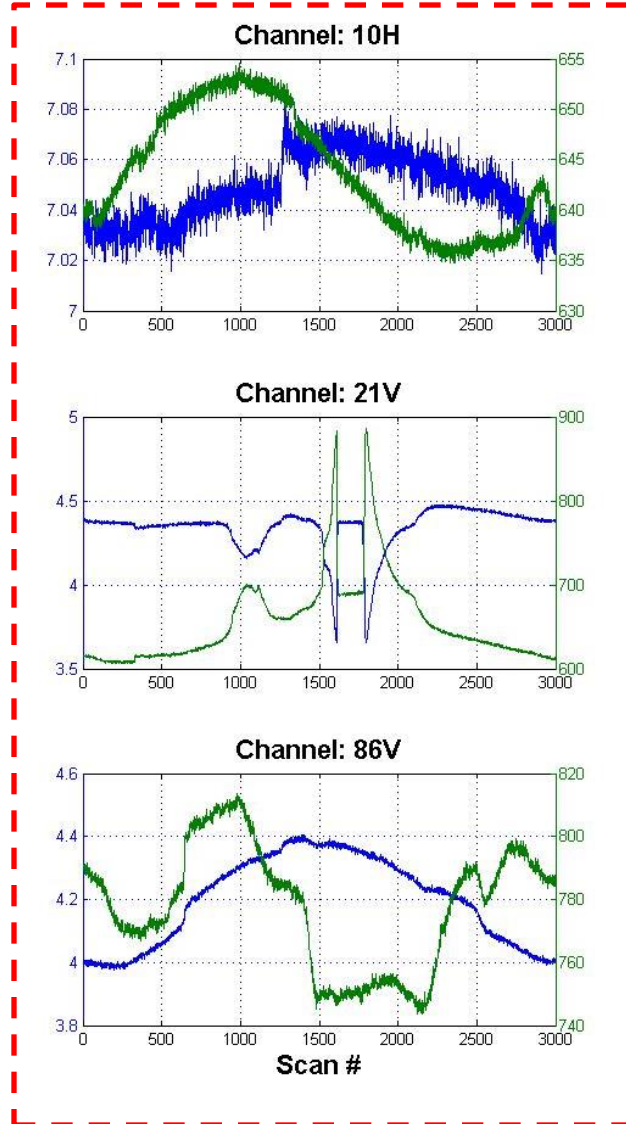
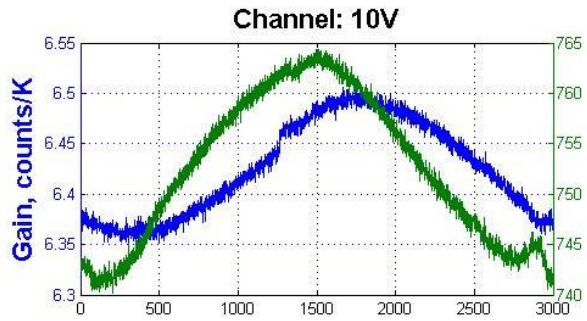
Back Up

Intro

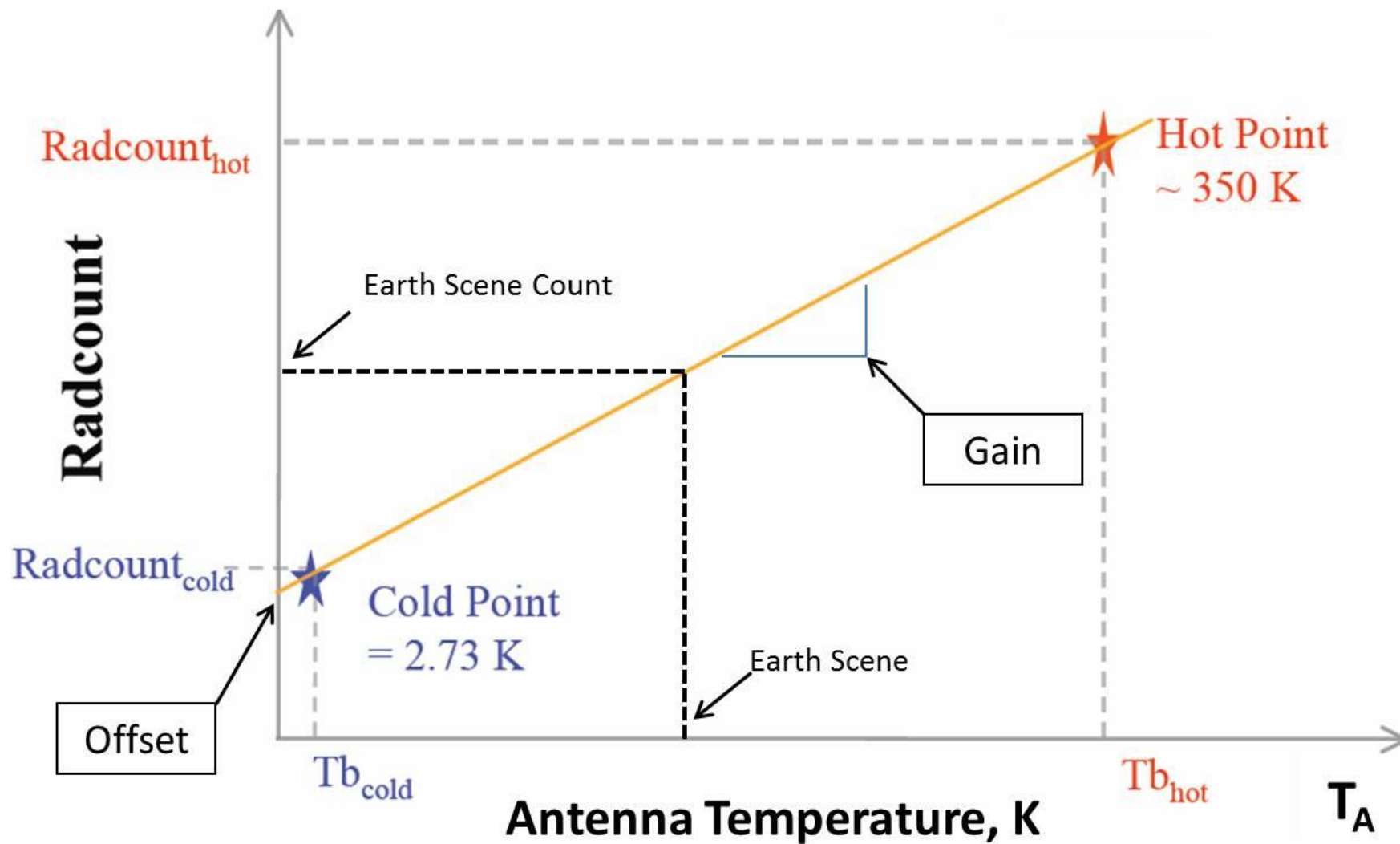
Gain & Offset for All TMI Channels



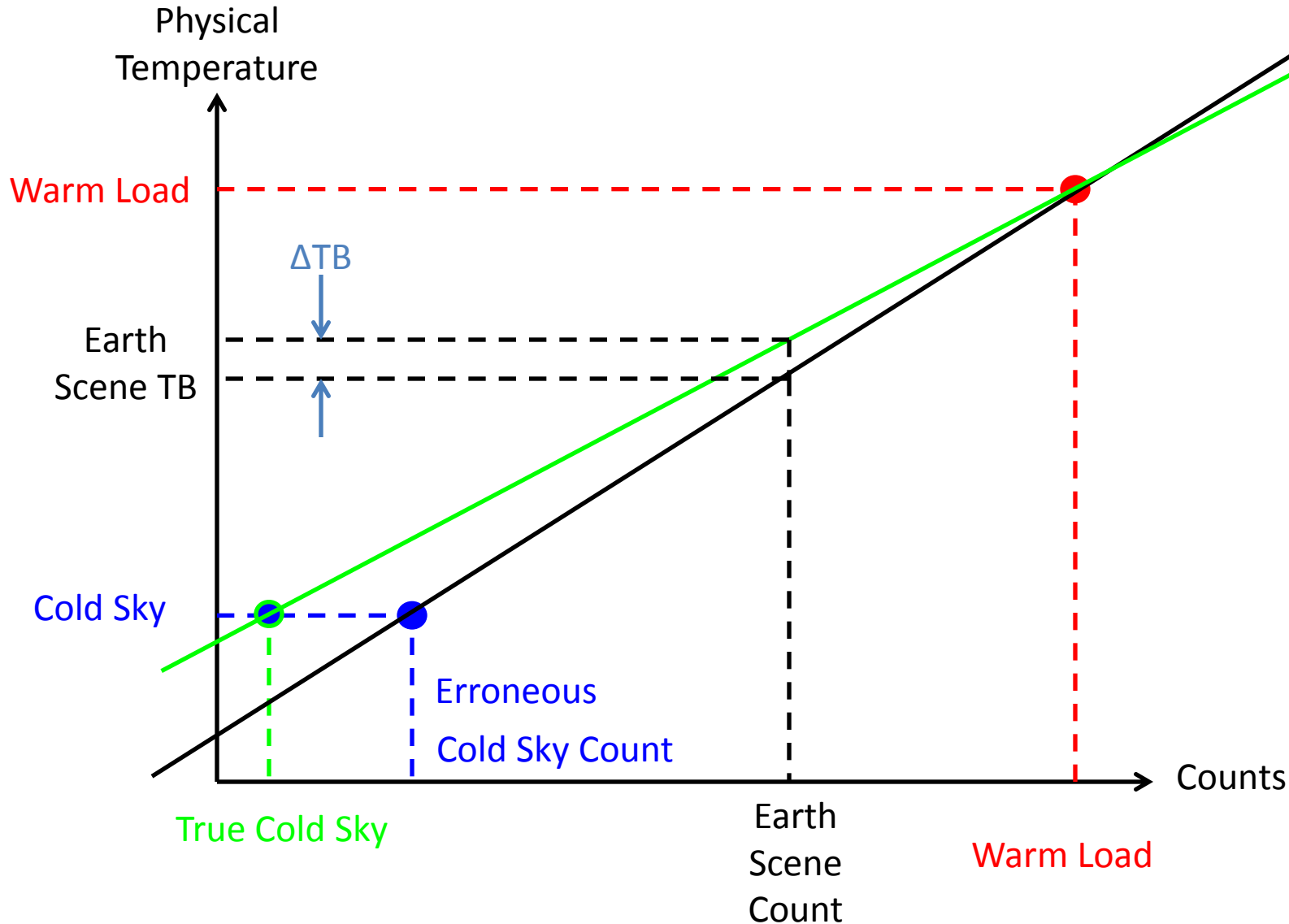
TMI Orbit 601



Two Point Calibration



Transfer Function (Two-Point Calibration)



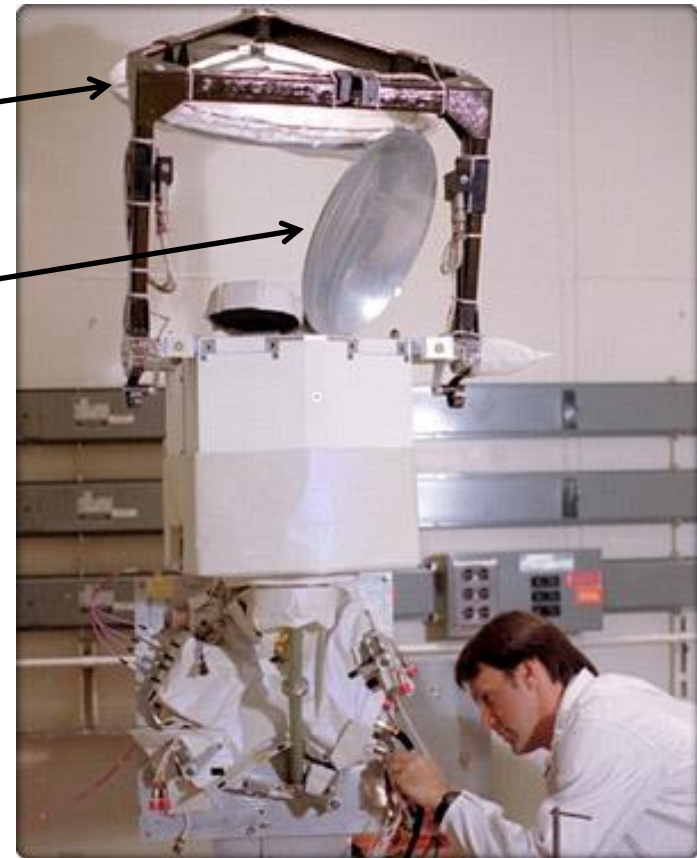
TRMM Microwave Imager (TMI)

Facing Main Reflector (MR)



(a)

Facing Cold Sky Reflector (CSR)



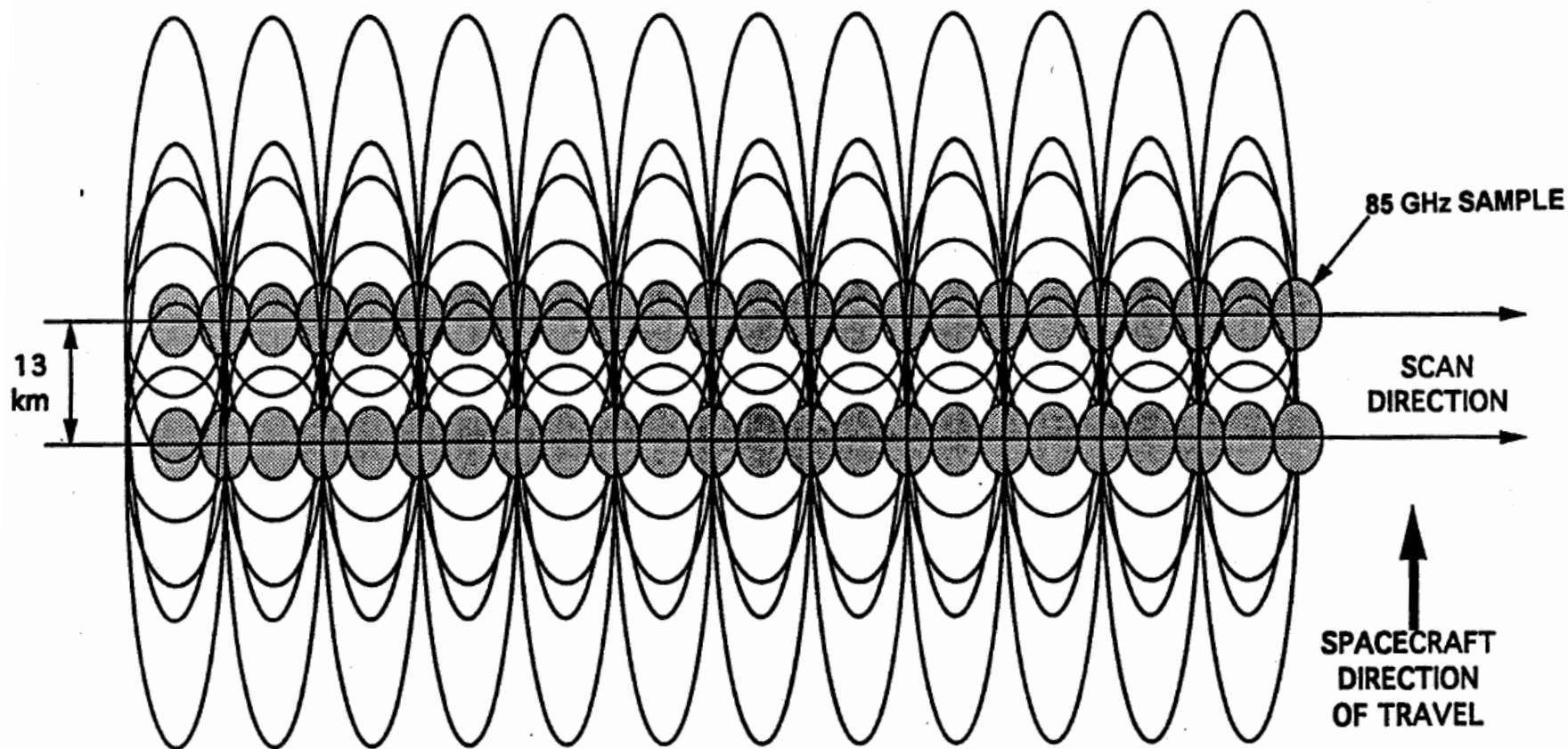
(b)

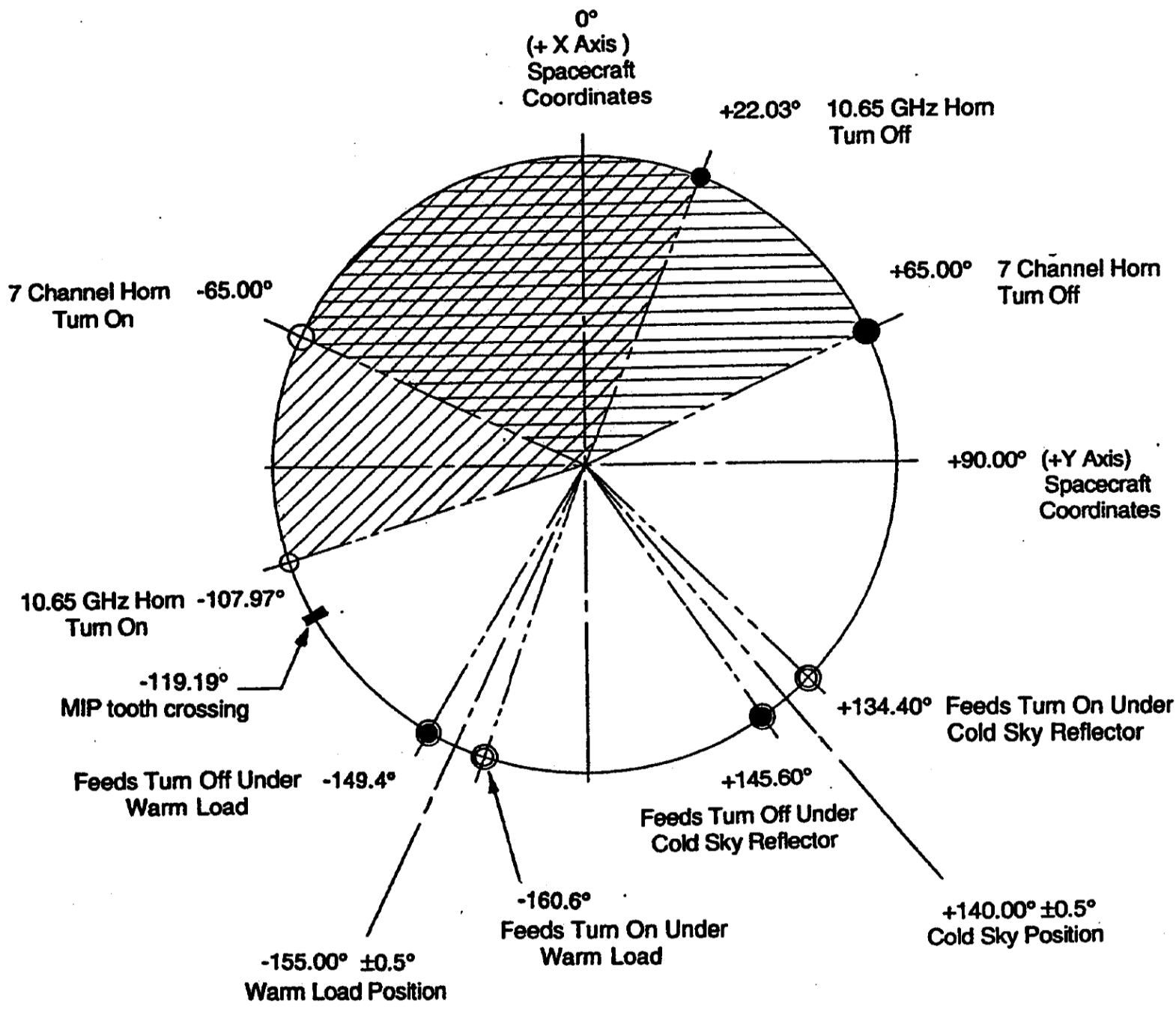
MR

CSR

TMI SAMPLING PATTERN

HUGHES



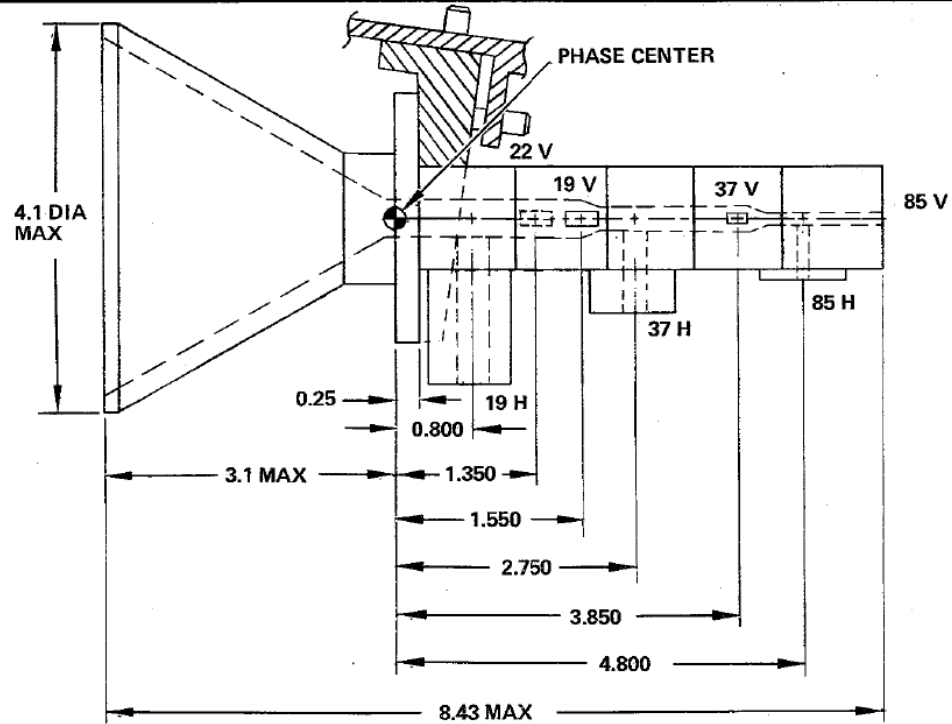


SSM/I CDR



SSM/I RADIOMETER FEED SYSTEM

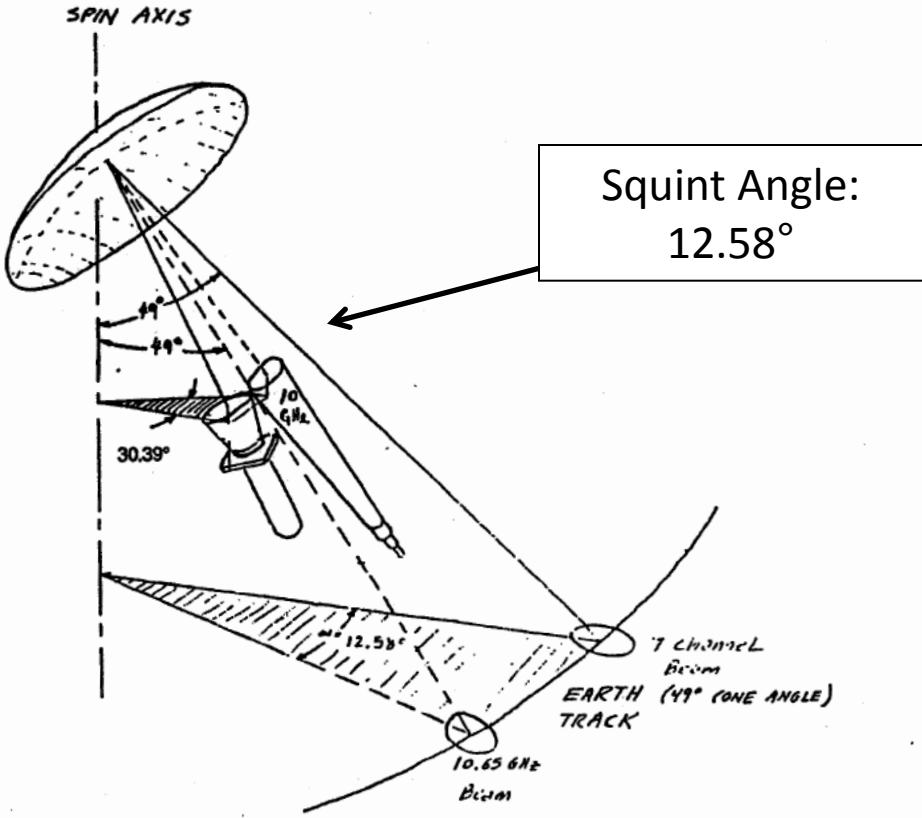
HUGHES



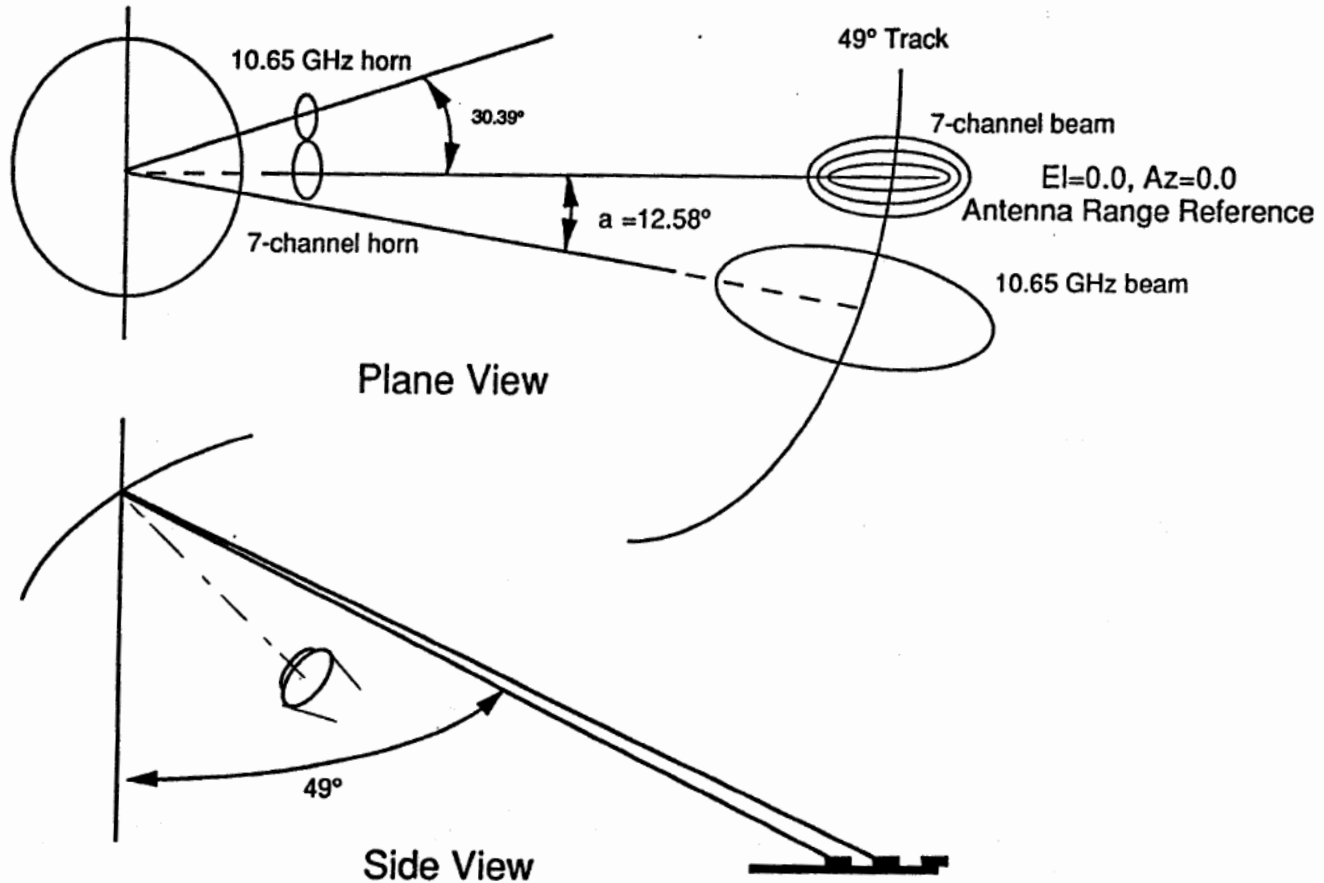
06133-85

10.65 GHz BEAM POSITIONING Isometric View

HUGHES



10.65 GHz BEAM POSITION Plane, Side View

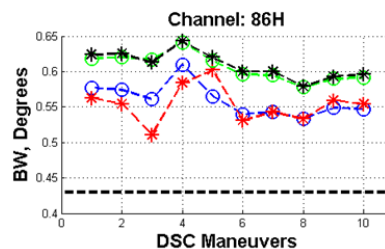
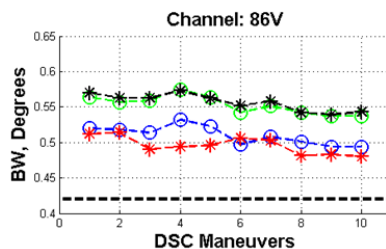
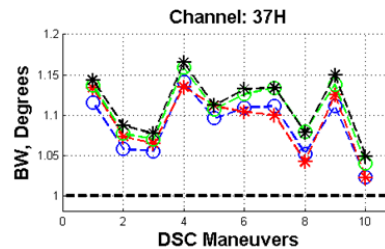
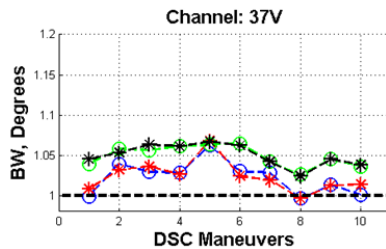
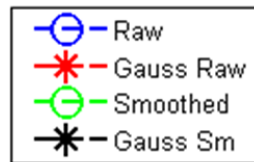
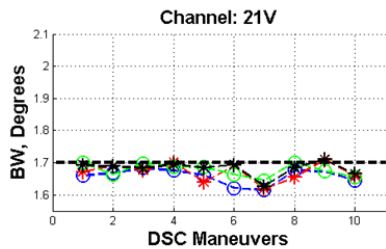
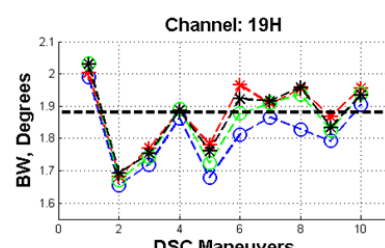
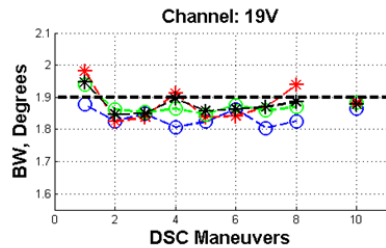
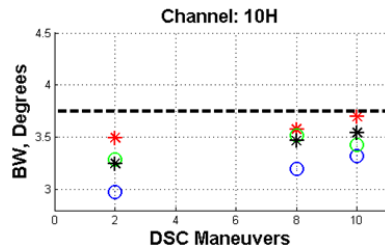
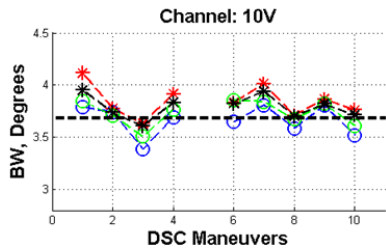


3-14

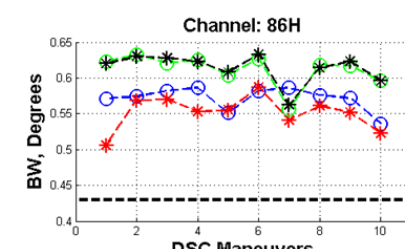
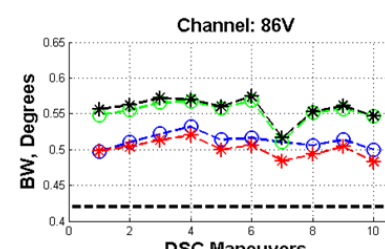
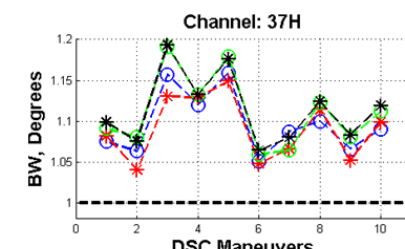
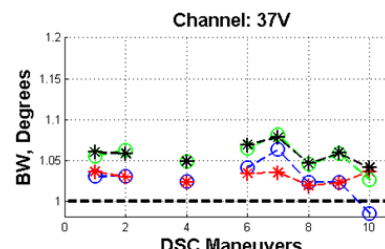
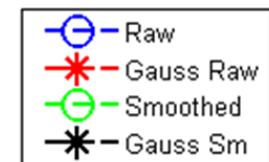
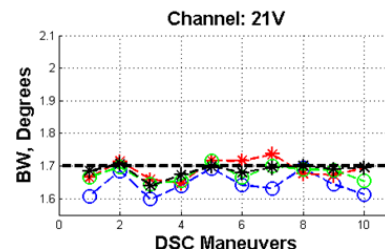
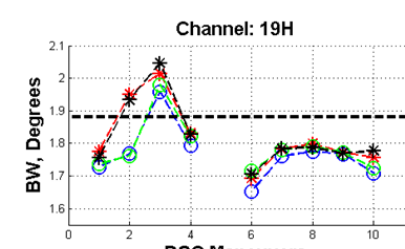
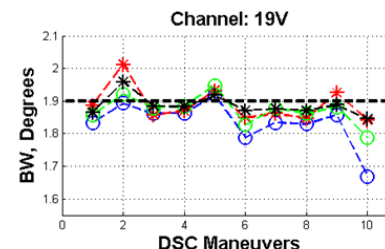
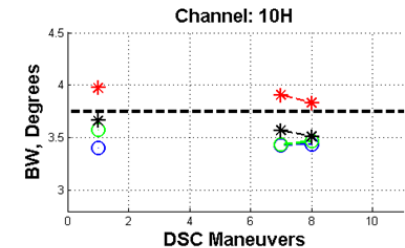
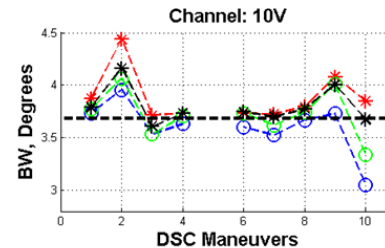
Back Up

Beam Width

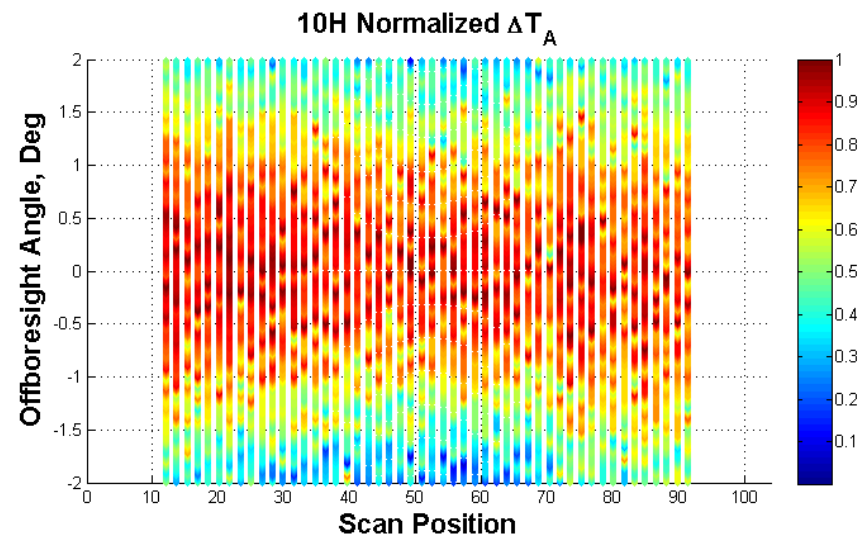
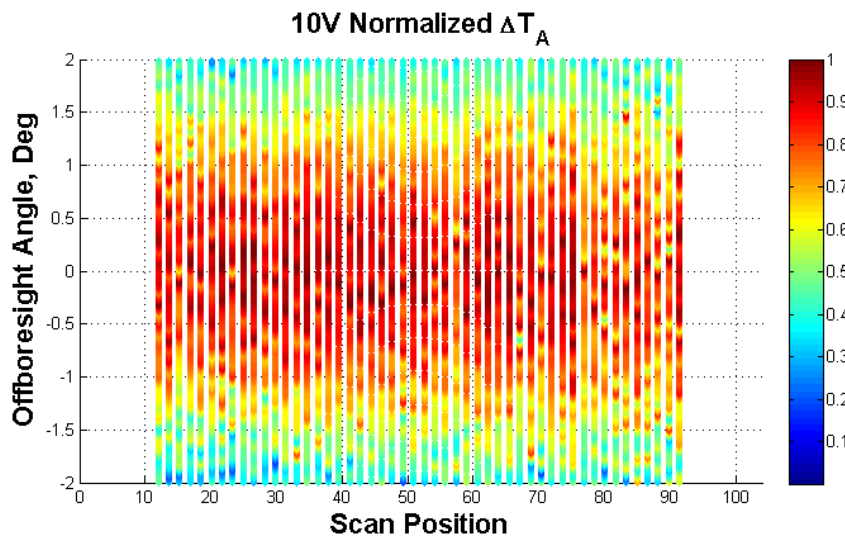
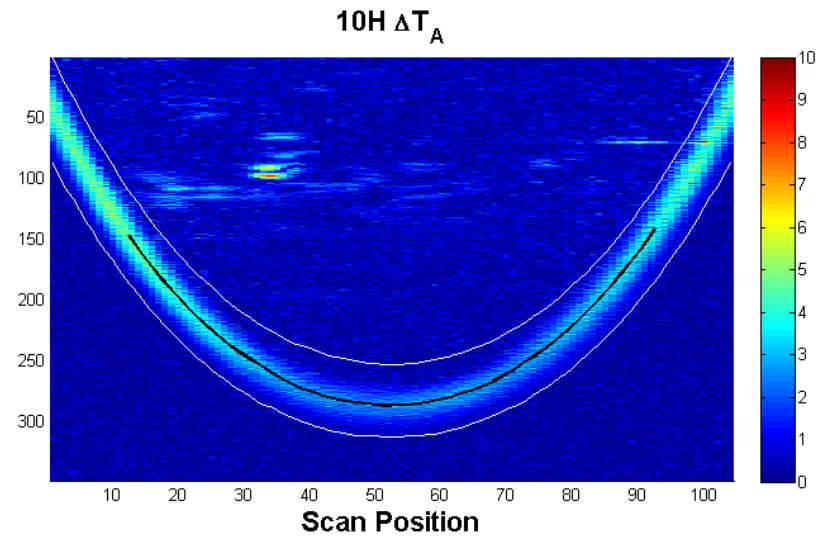
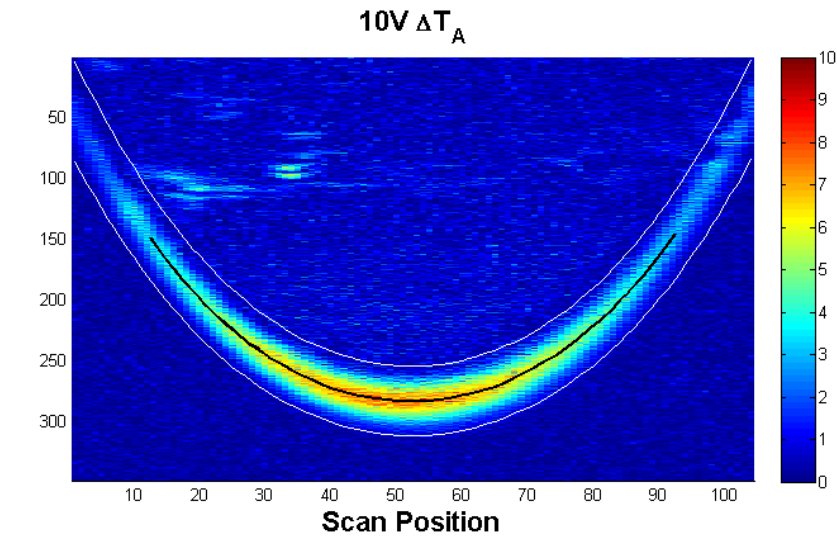
Transition 1



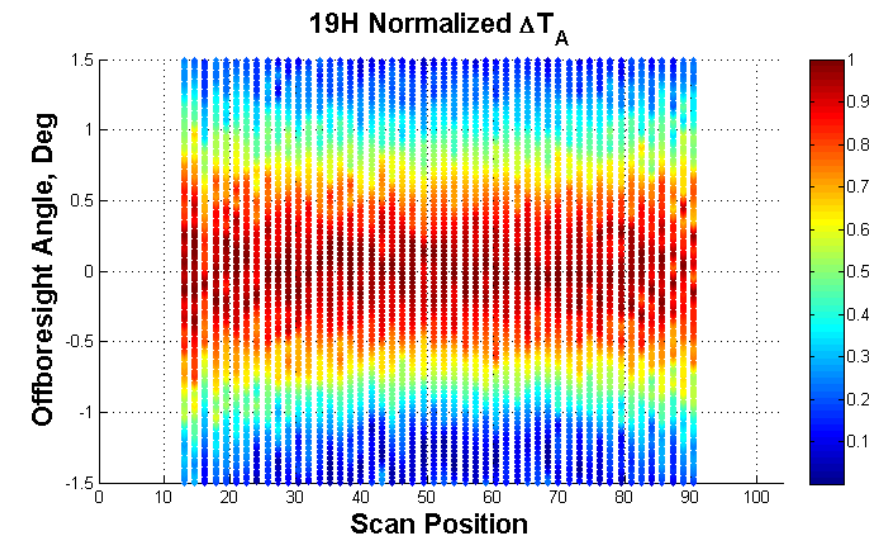
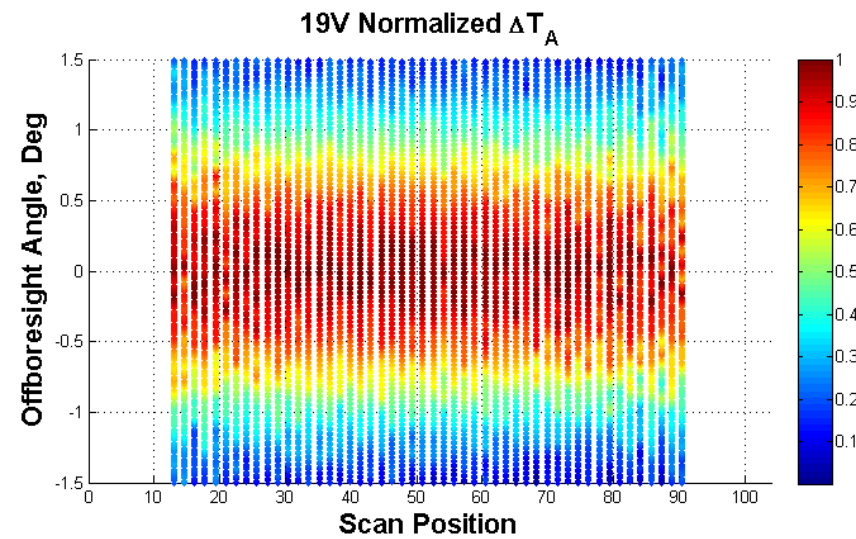
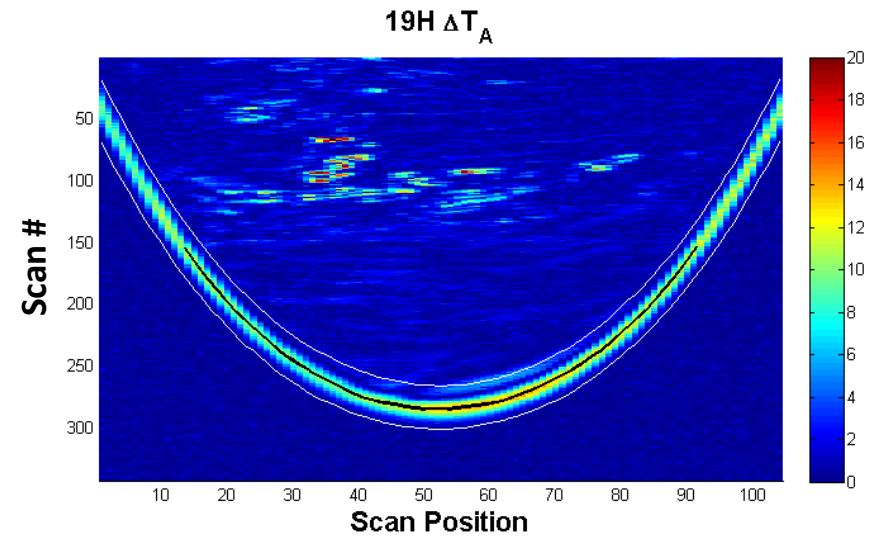
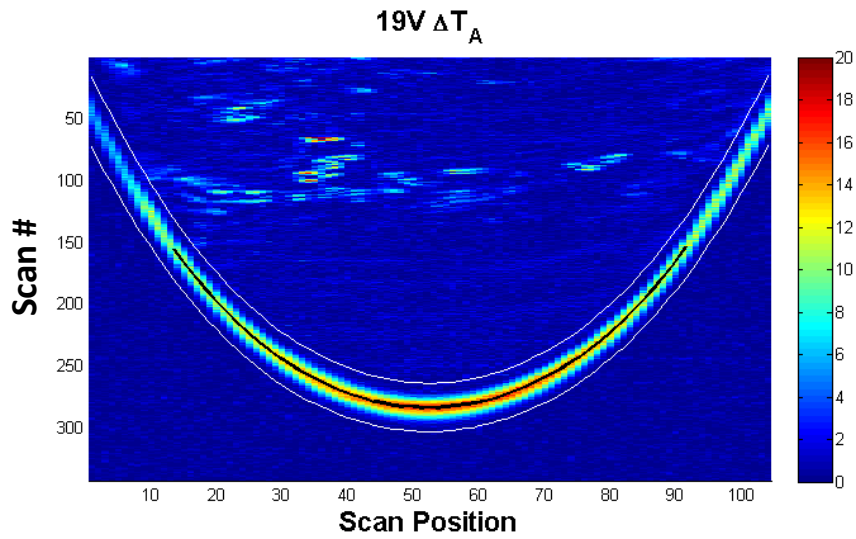
Transition 2



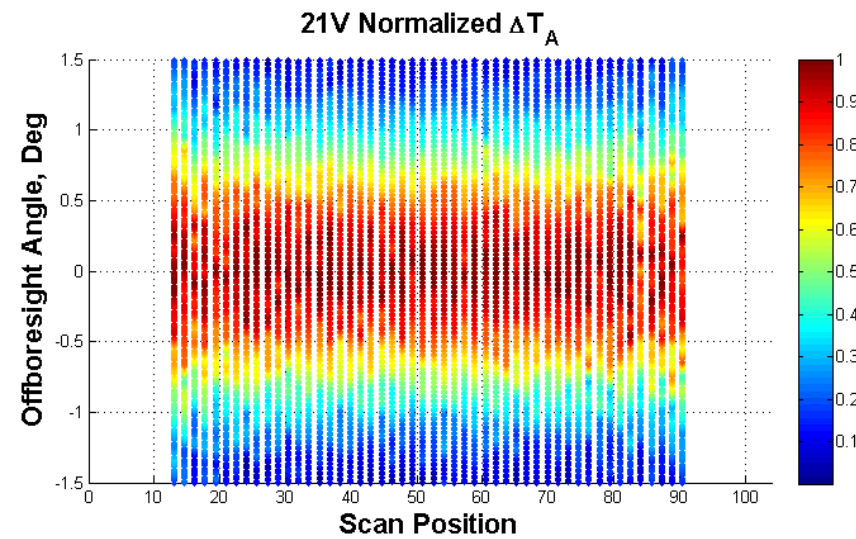
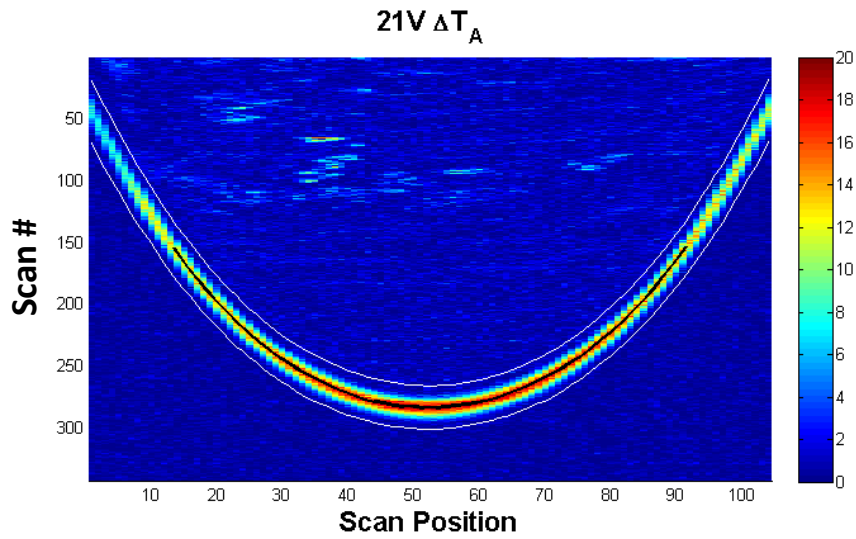
11 GHz Channels



19 GHz Channels



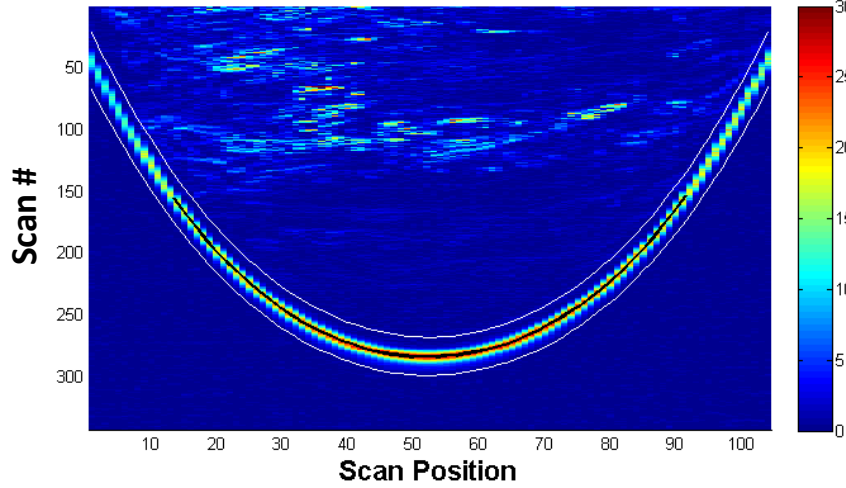
21 GHz Channel



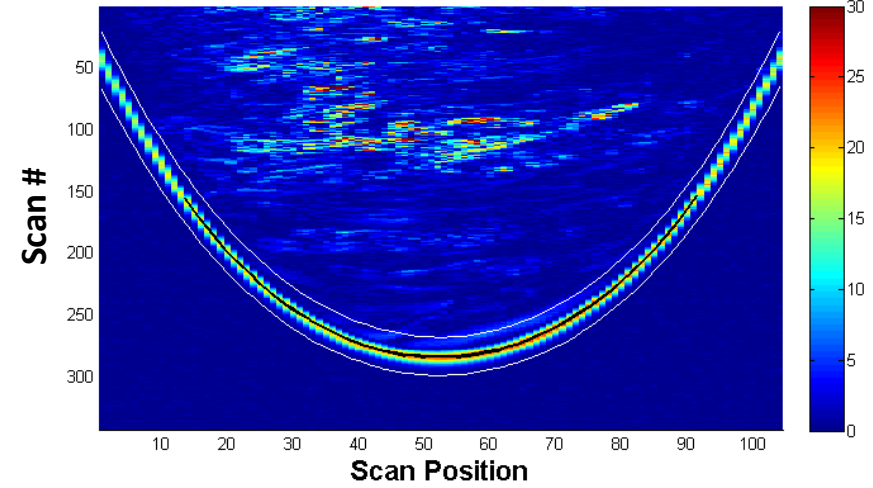
37 GHz Channels



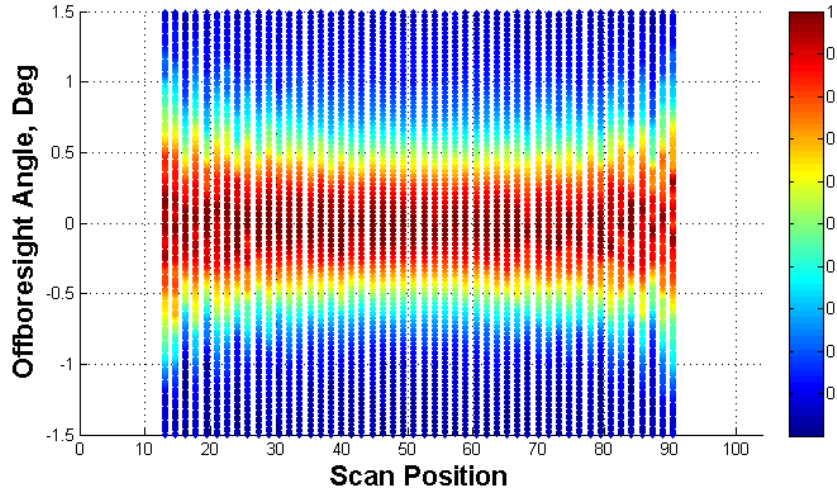
37V ΔT_A



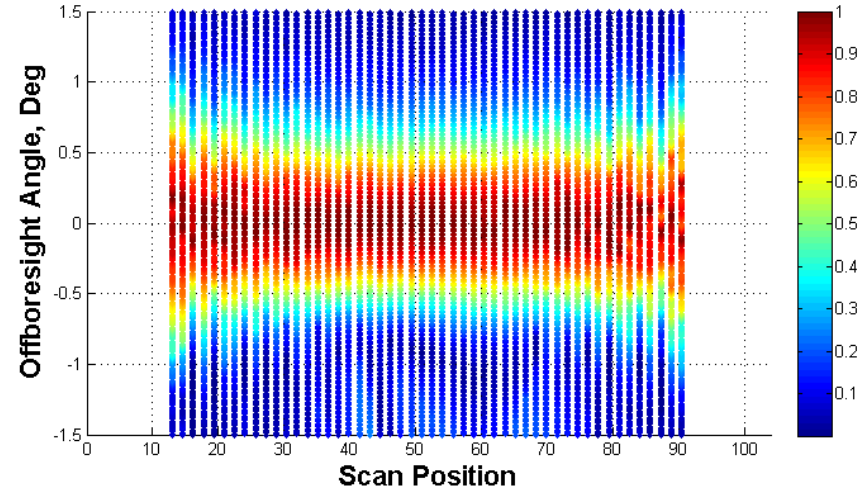
37H ΔT_A



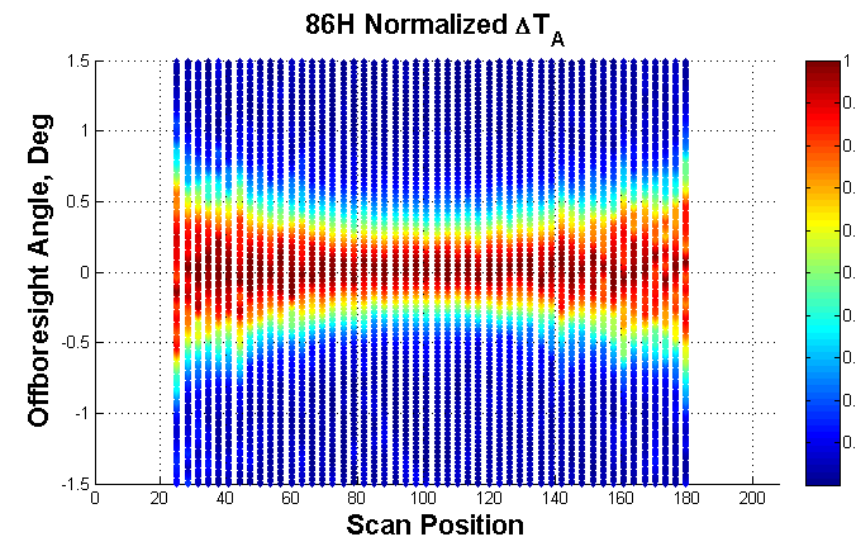
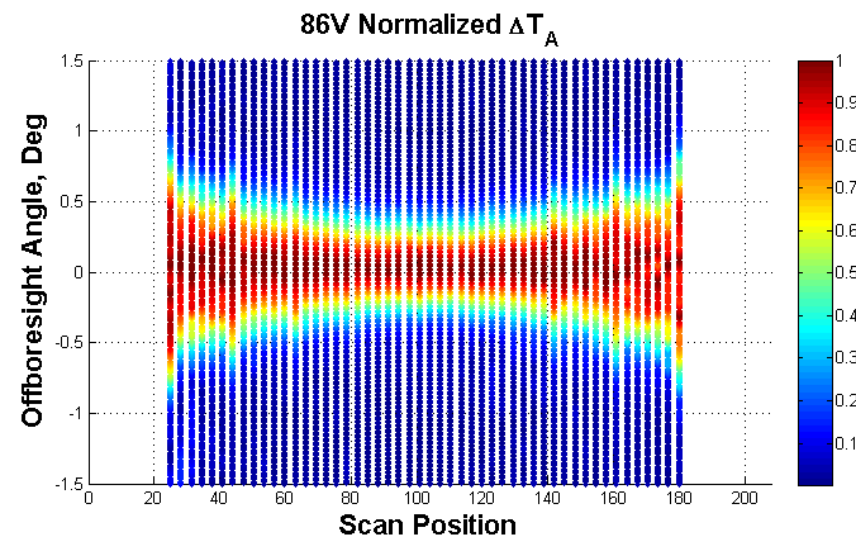
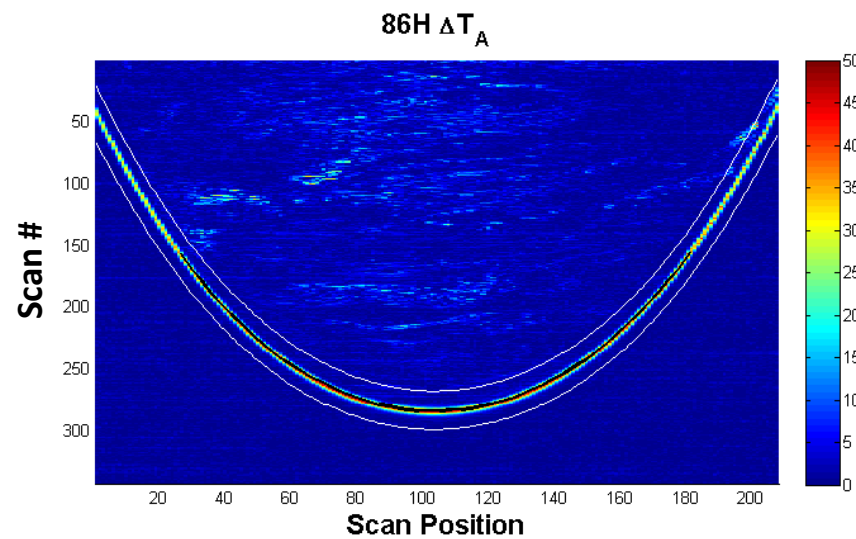
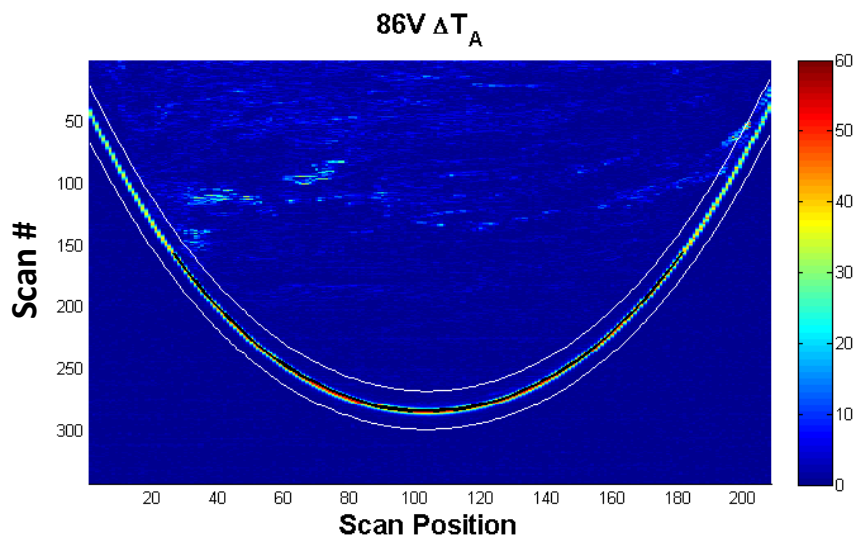
37V Normalized ΔT_A



37H Normalized ΔT_A



86 GHz Channels



Back Up

Boresight Pointing

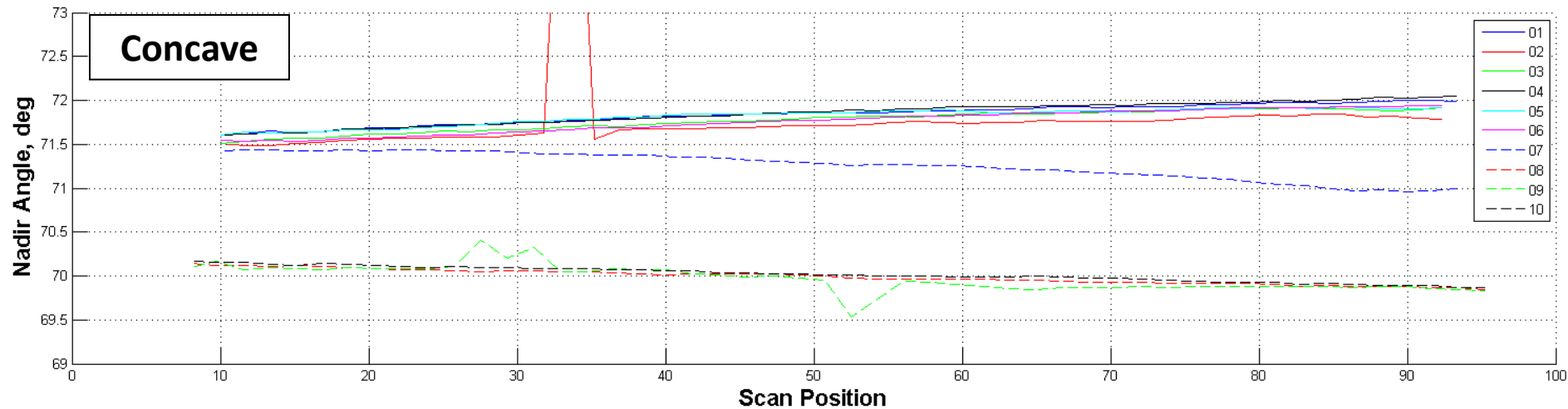
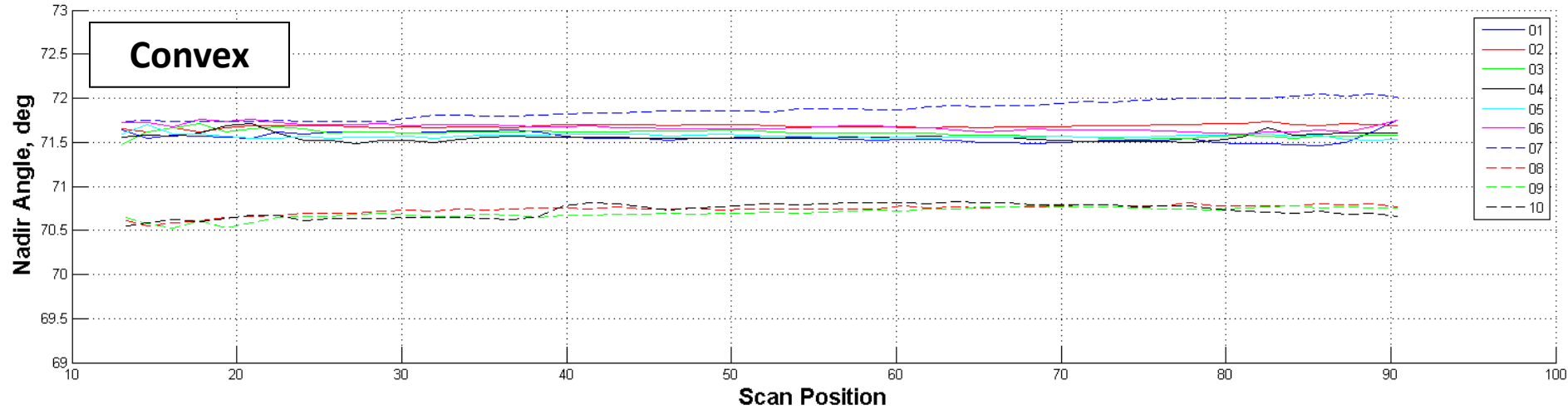
TMI Boresight Table

Channels	Offsets from Shiue Memo (deg)		Offsets from TMI Subsystem Test Doc (deg)	
	Along-track	X-Track	Along-Track	X-Track
10.65 V	0.555	-0.185	0.487	0.09
10.65 H	0.185	0.555	0.568	0.134
19.35 V	0	0	0.06	0.005
19.35 V	0	0	0.05	0.005
21.30 V	0	0	0.059	-0.025
37.00 V	0	0.1	0.073	-0.006
37.00 H	0.1	0	0.069	-0.001
85.50 V	0.1	0	0.049	-0.030
85.50 H	0.05	0.05	0.065	-0.010

TMI Subsystem Test Doc: Nov 07, 1994 (Outdoor test range)

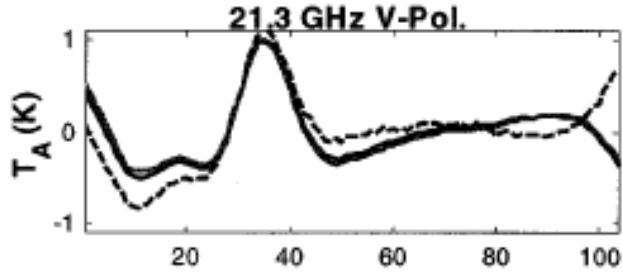
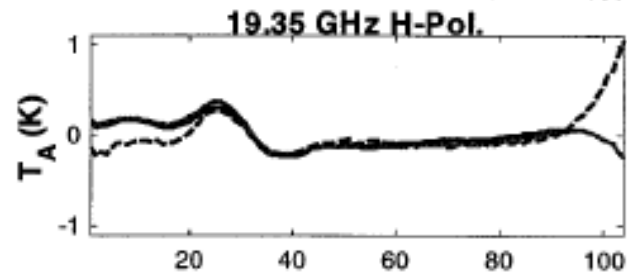
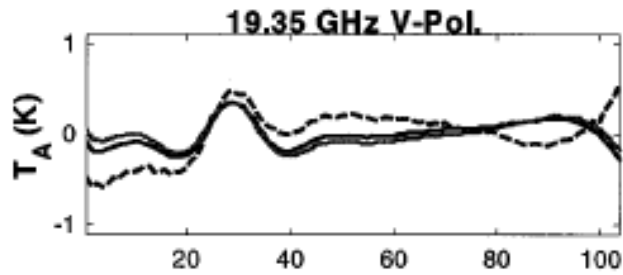
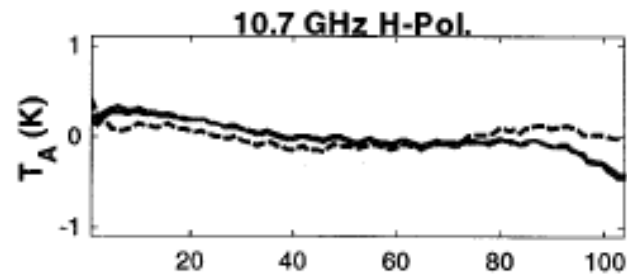
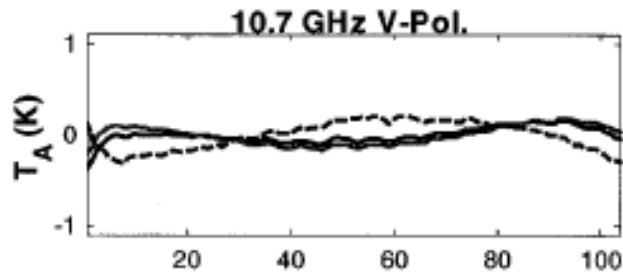
Shiue Memo: 12-11-1997 (Measured by Hughes)

Convex & Concave Comparisons for 19 V-pol (DSCMs 1 to 10)

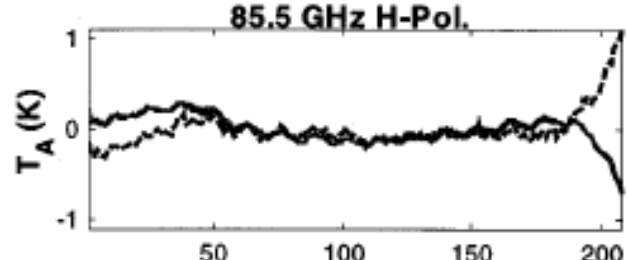
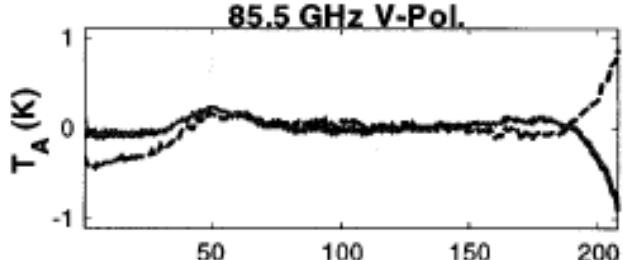
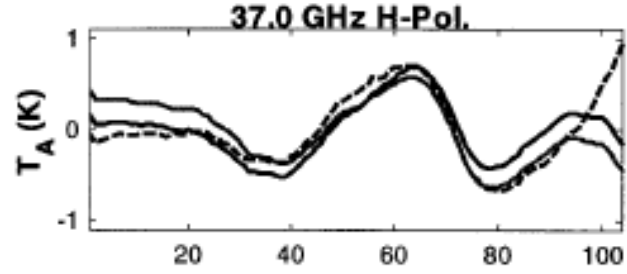
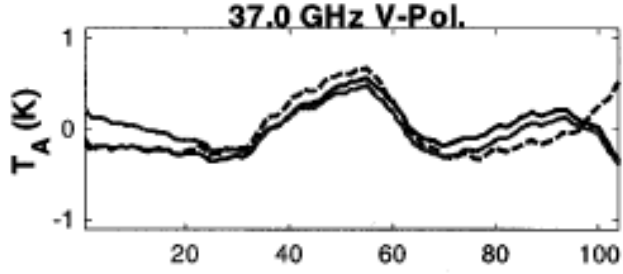


Back Up

Along-scan Bias



This is Wentz' Along-scan bias analysis for TMI's 9 channels. Comparison of the average along-scan error derived from ocean observations and from deep-space observations. The observed T_A anomaly is plotted versus scan position. The solid black and gray curves come from ocean observations for yaw orientations of 0 and 180, respectively, during 1998. The dashed curves come from deep-space observations during January 1998

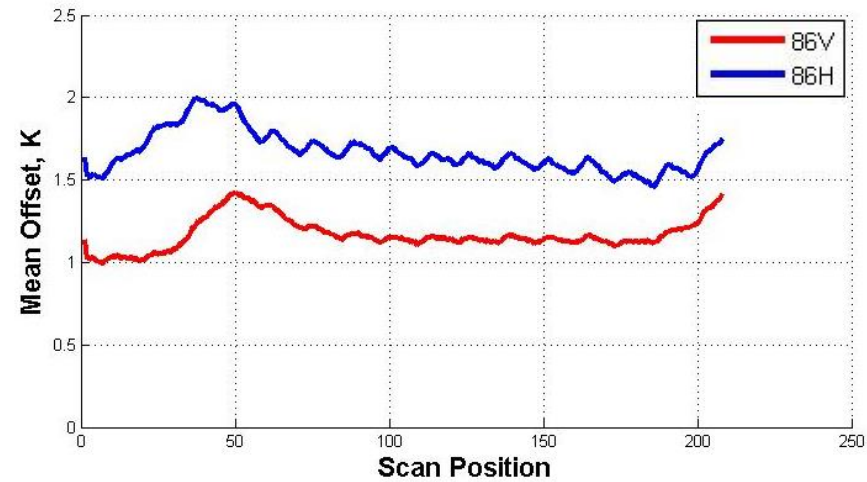
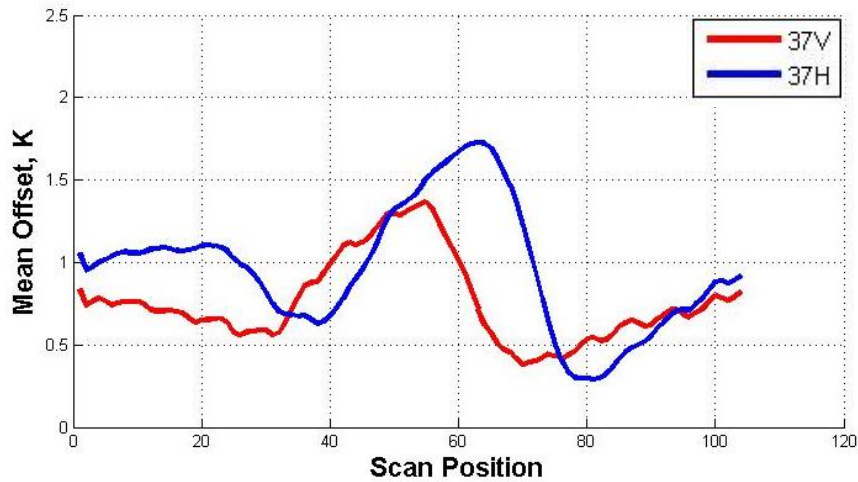
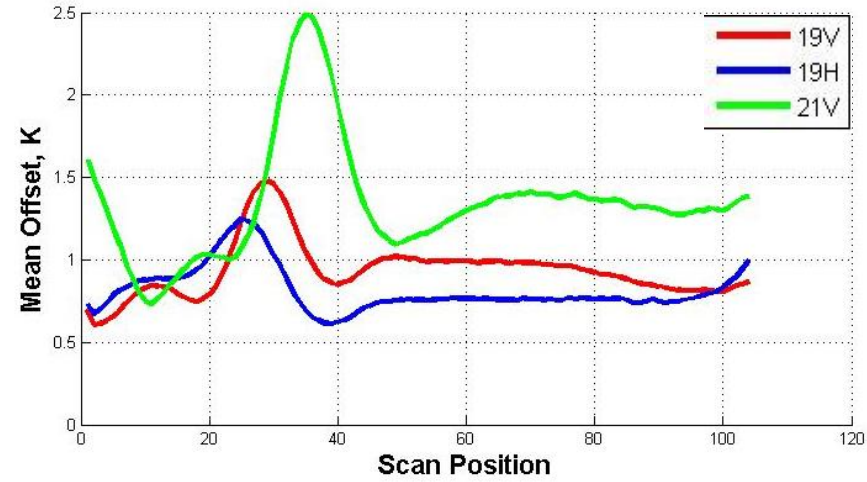
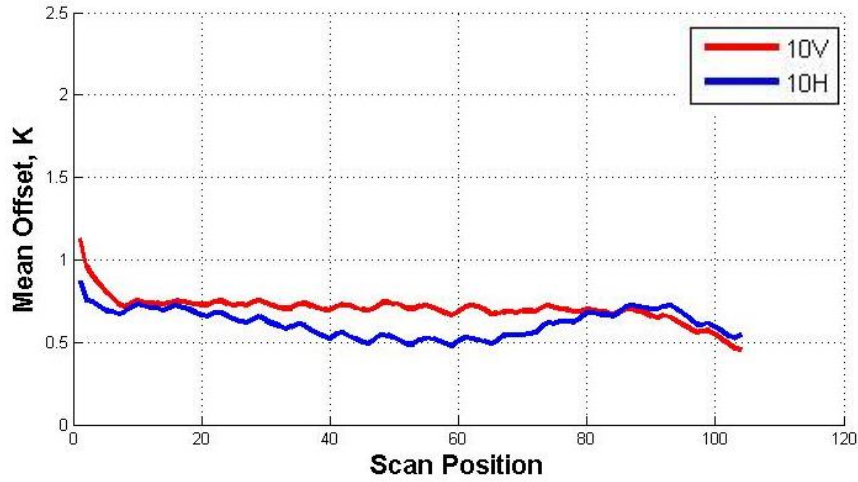


Scan Position

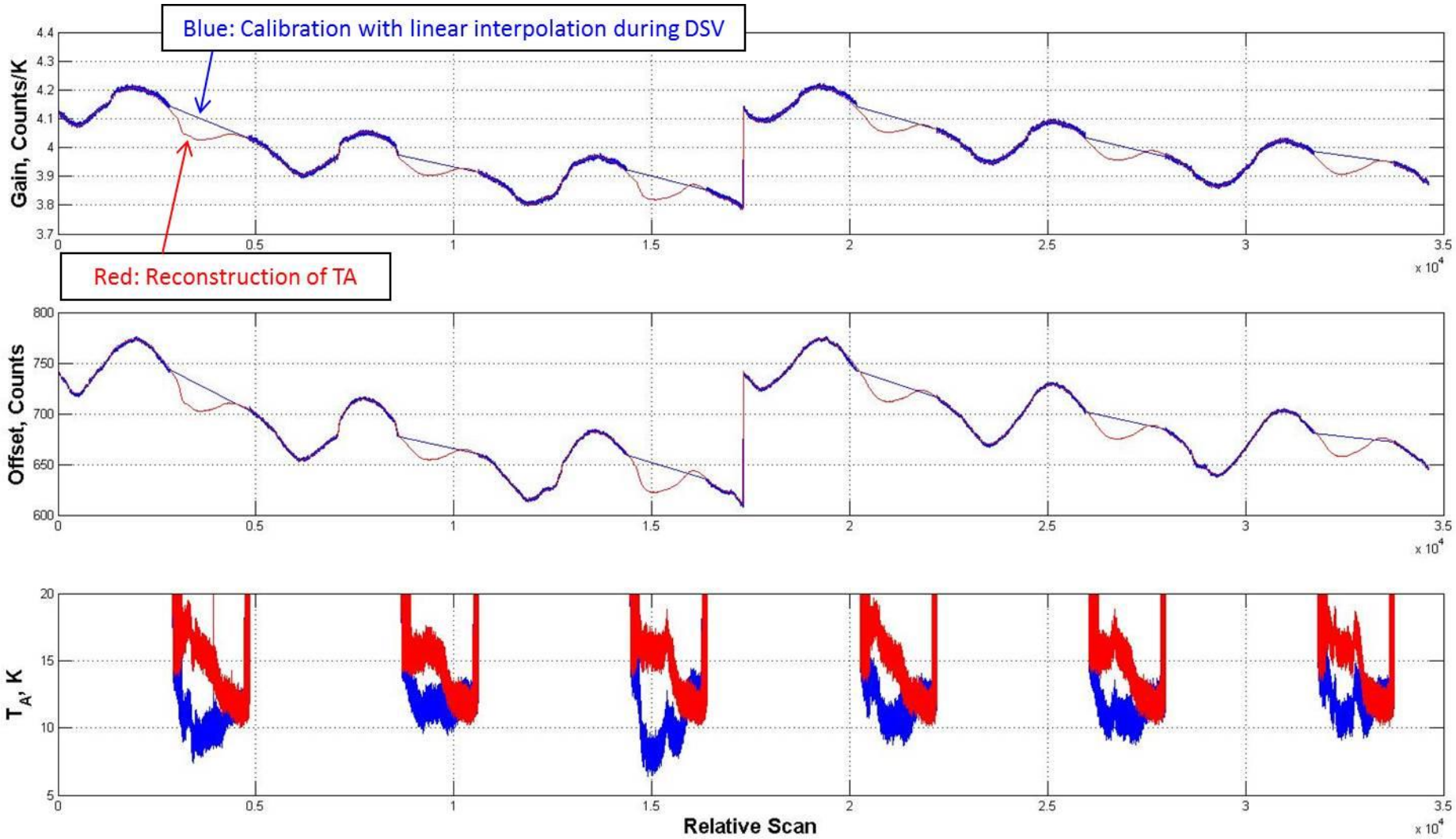
Scan Position

Along Scan Bias

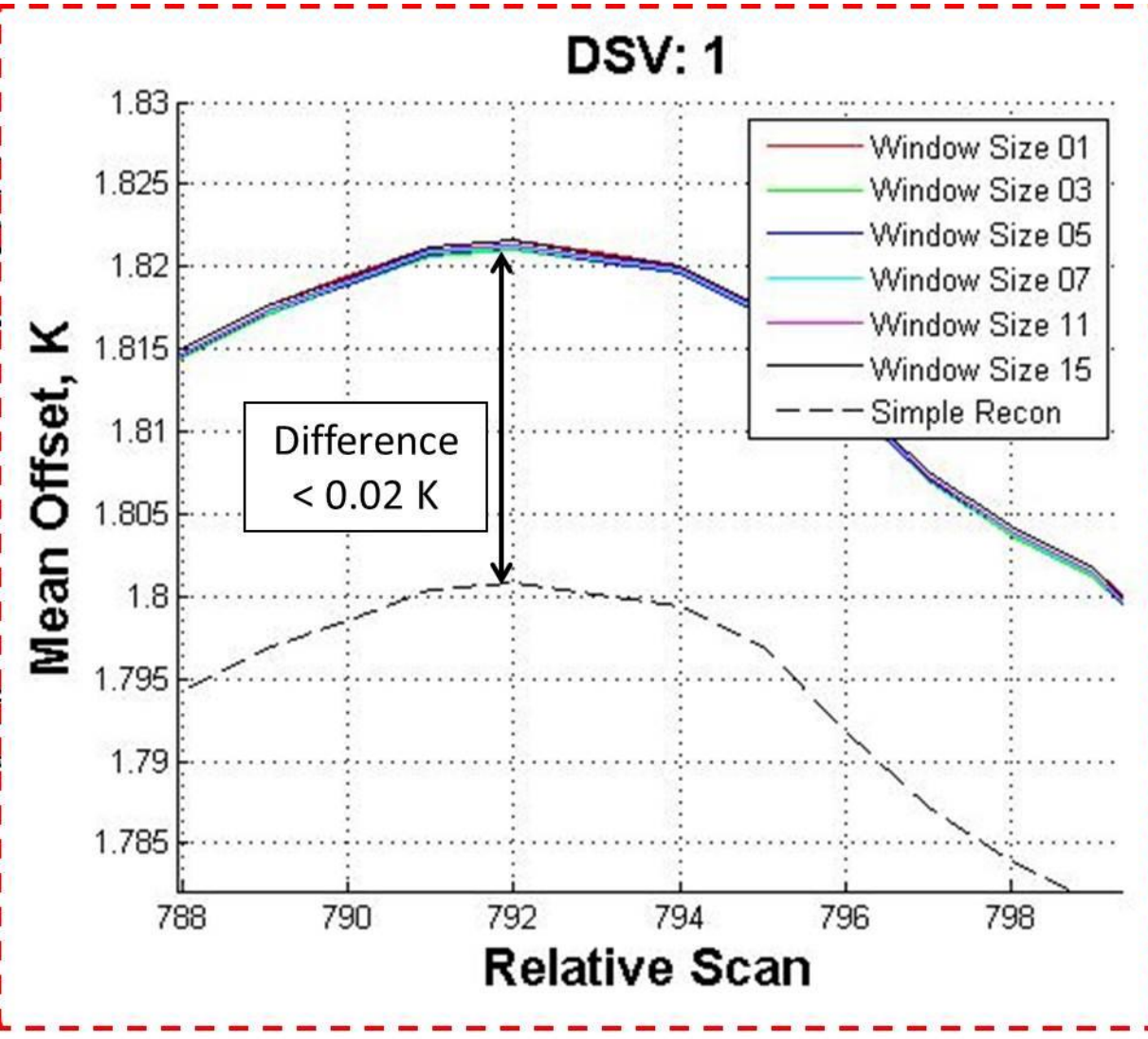
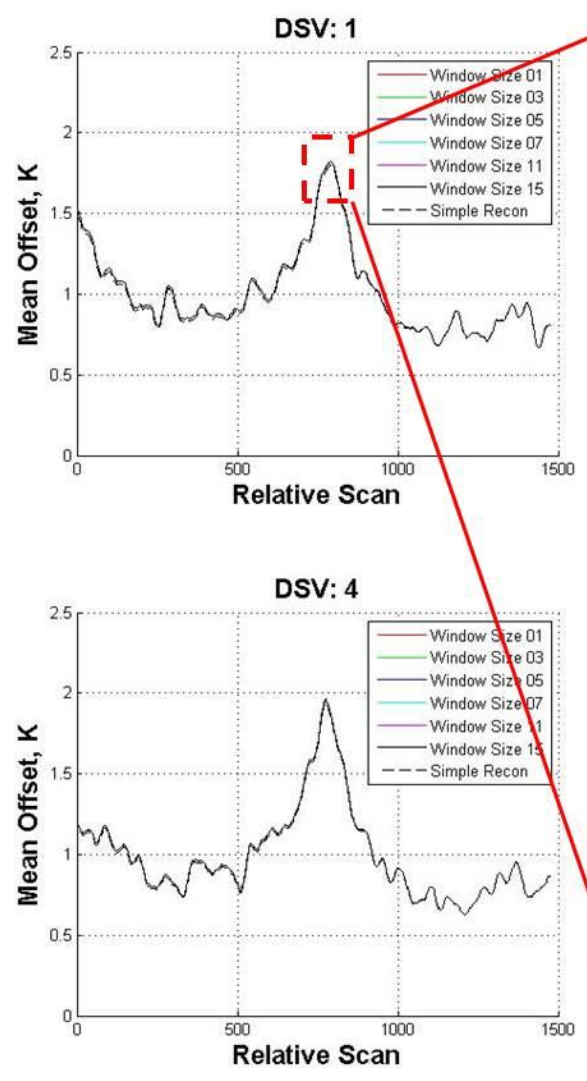
Full Range Data for DSCM
Set 1



19 V-pol



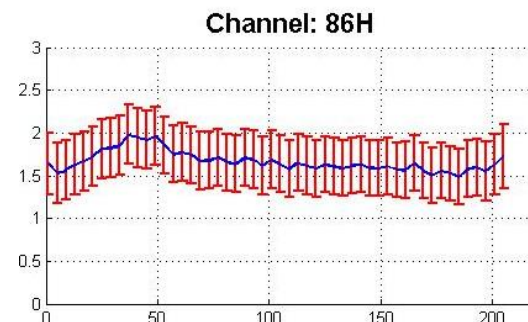
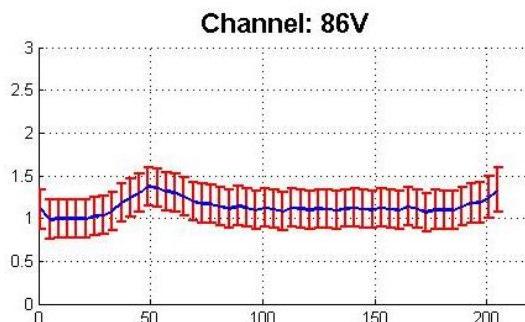
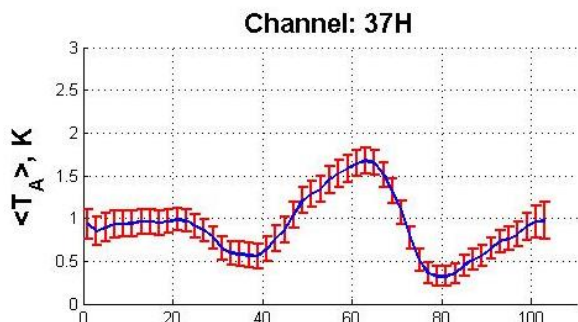
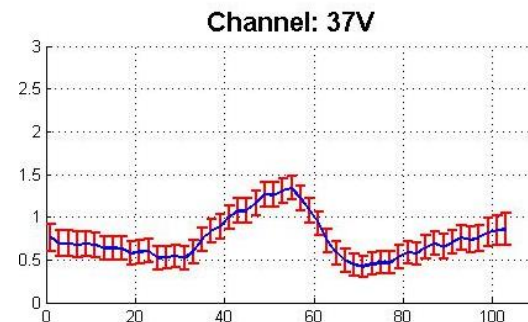
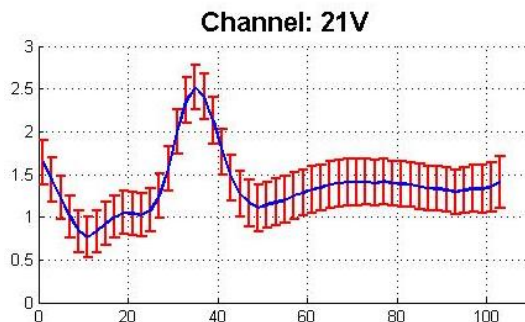
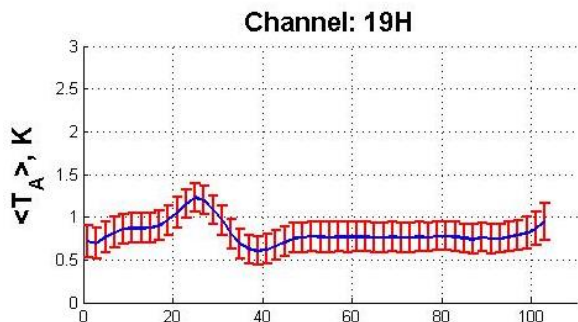
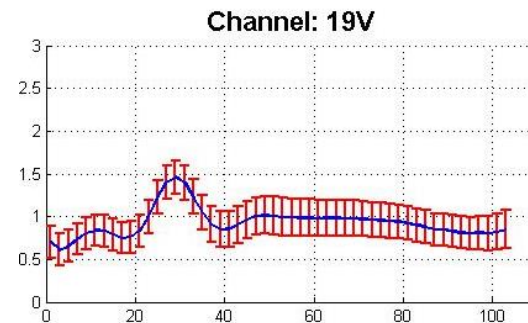
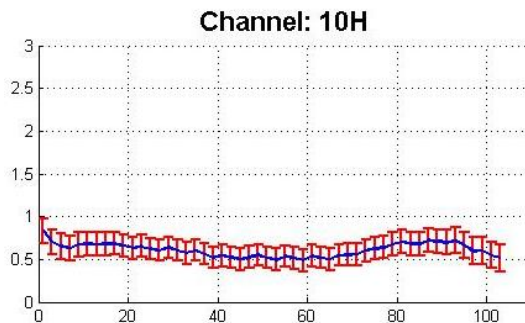
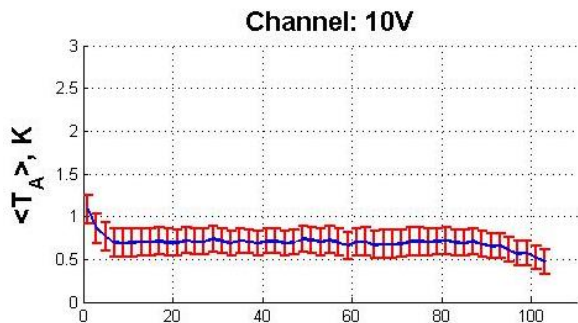
Insensitivity of Along-Scan Analysis to Reconstruction Errors



Combined DSC Sets

Limited Range Data

Bars length = 1σ

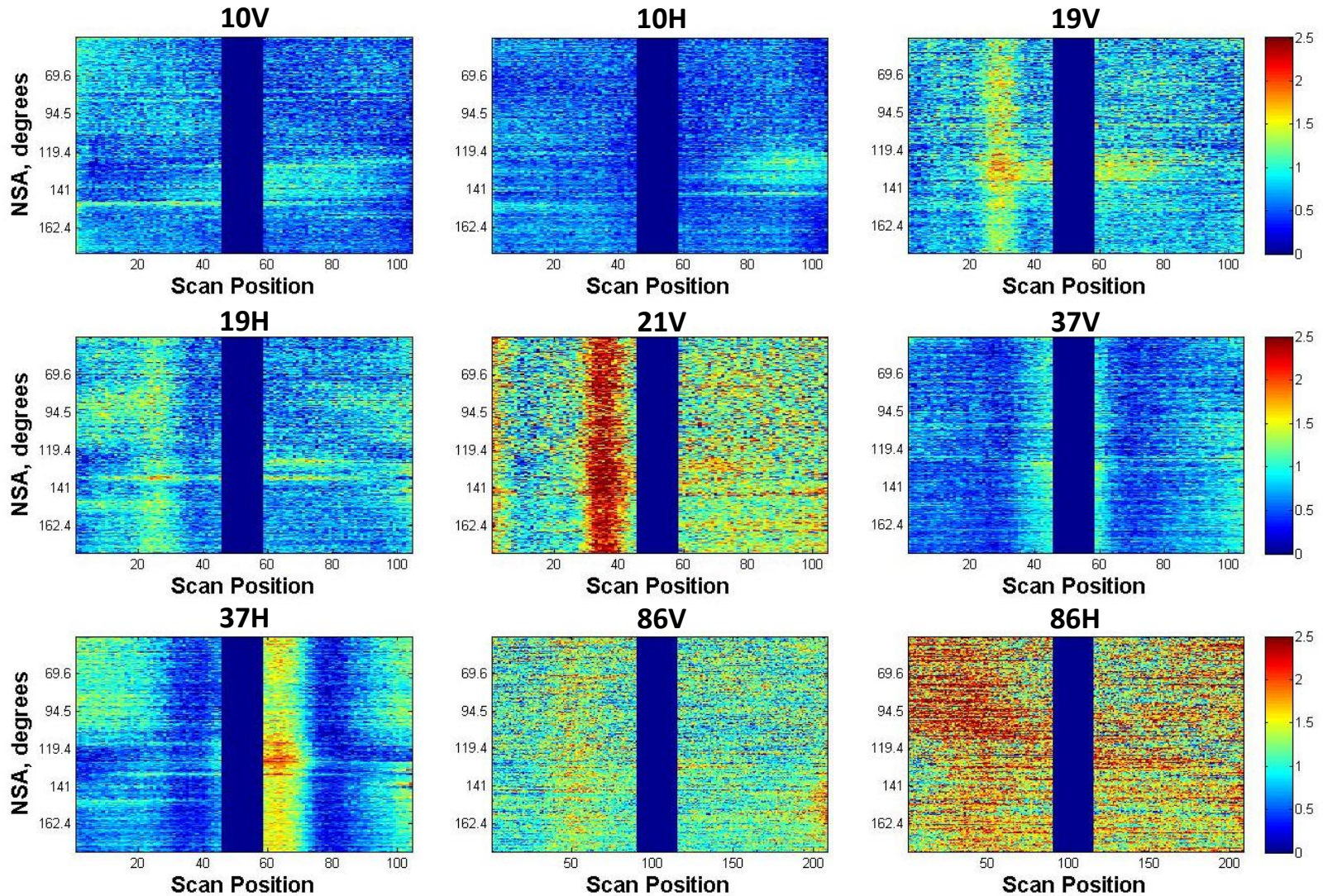


Scan Position

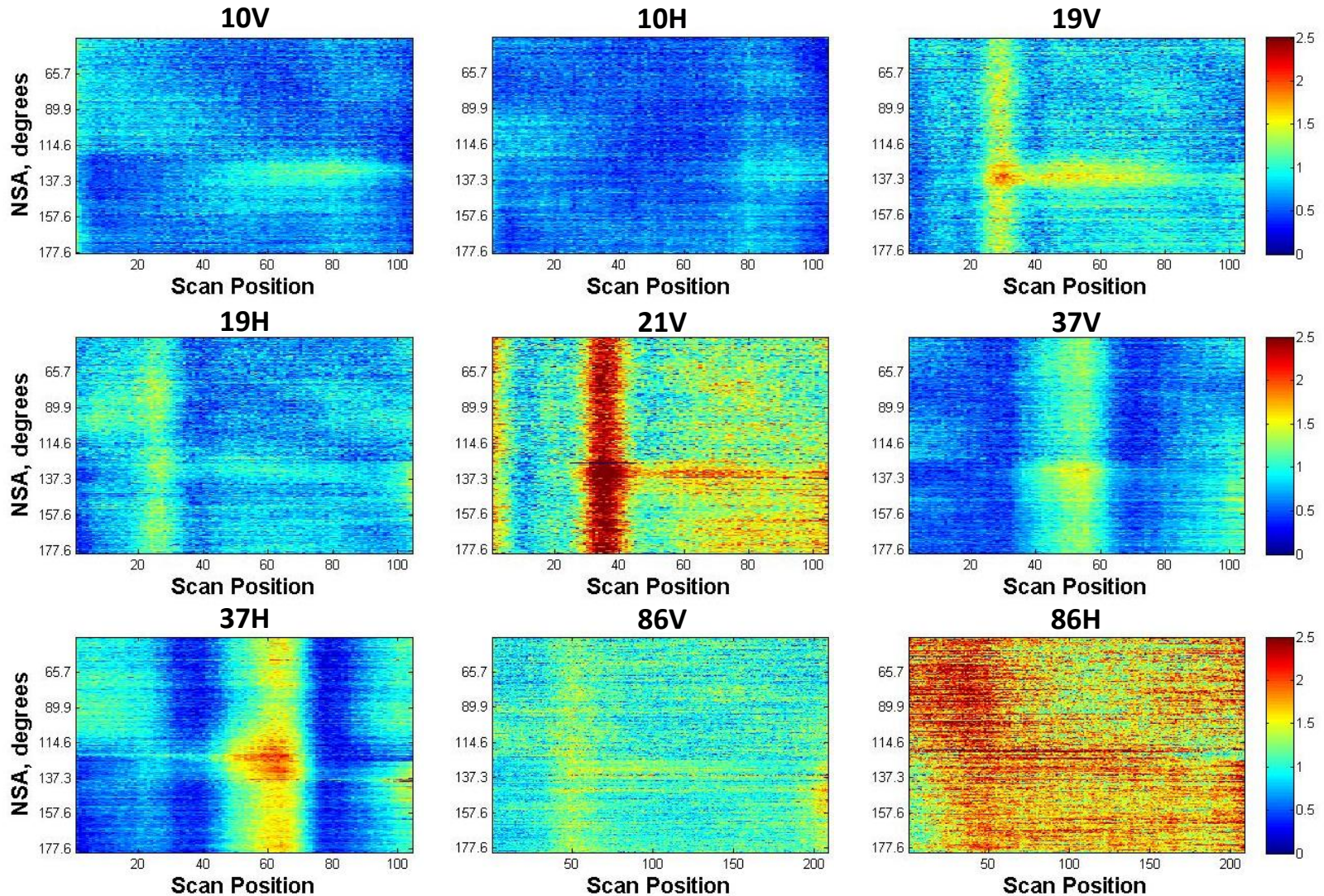
Scan Position

Scan Position

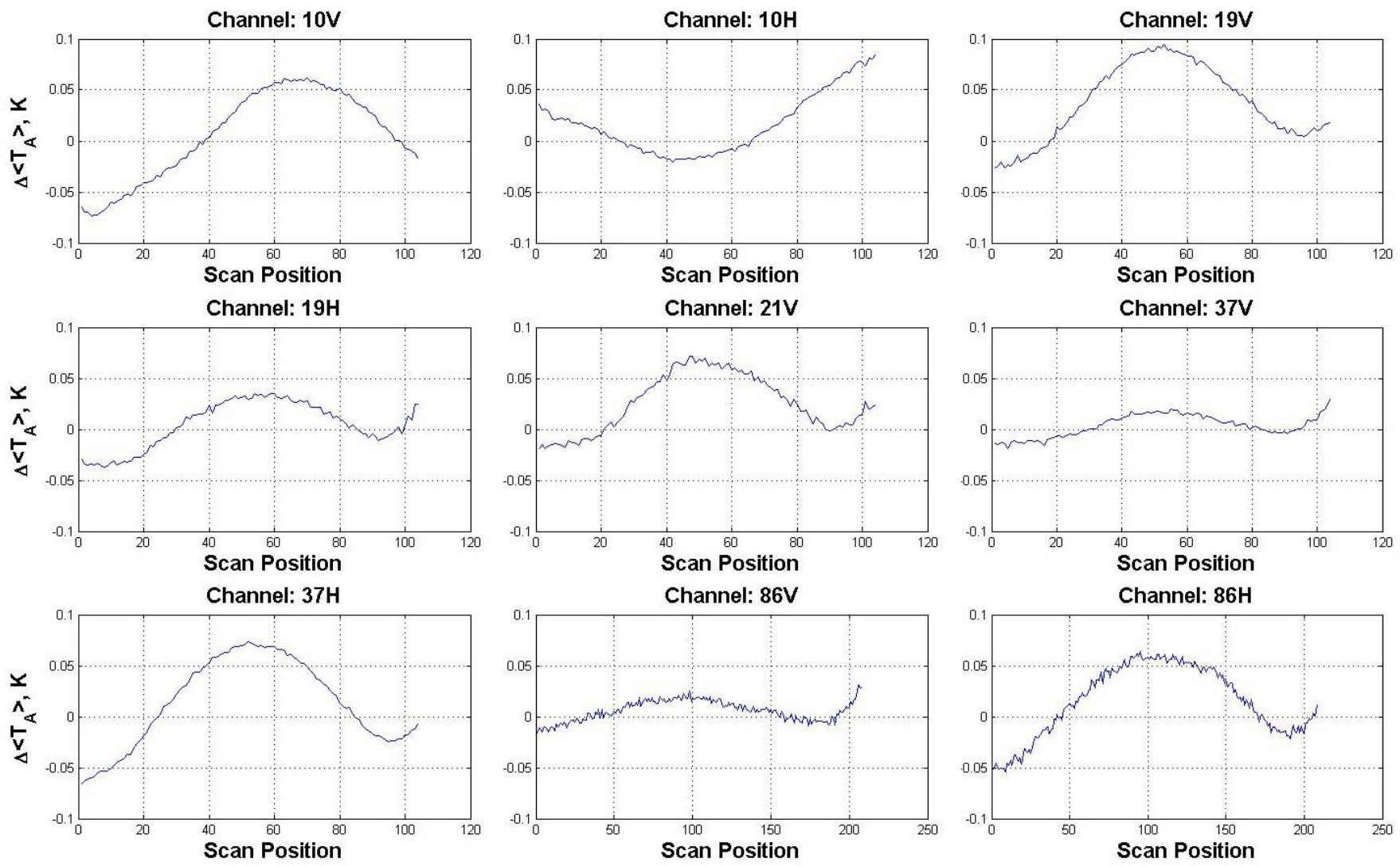
DSCM Set 2 – Averaged w.r.t. NSA



DSCM Set 3 – Averaged w.r.t. NSA



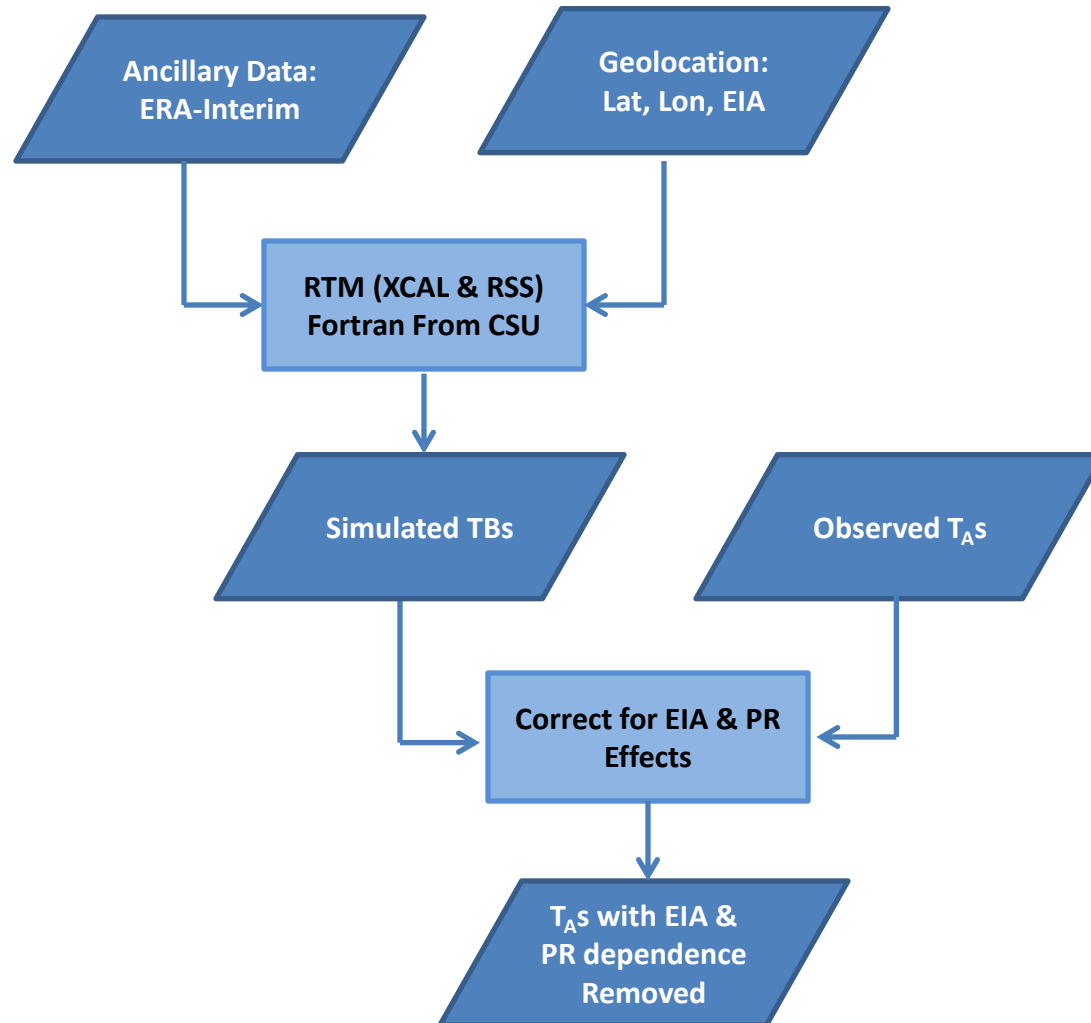
Comparing Biases for Range of Scans

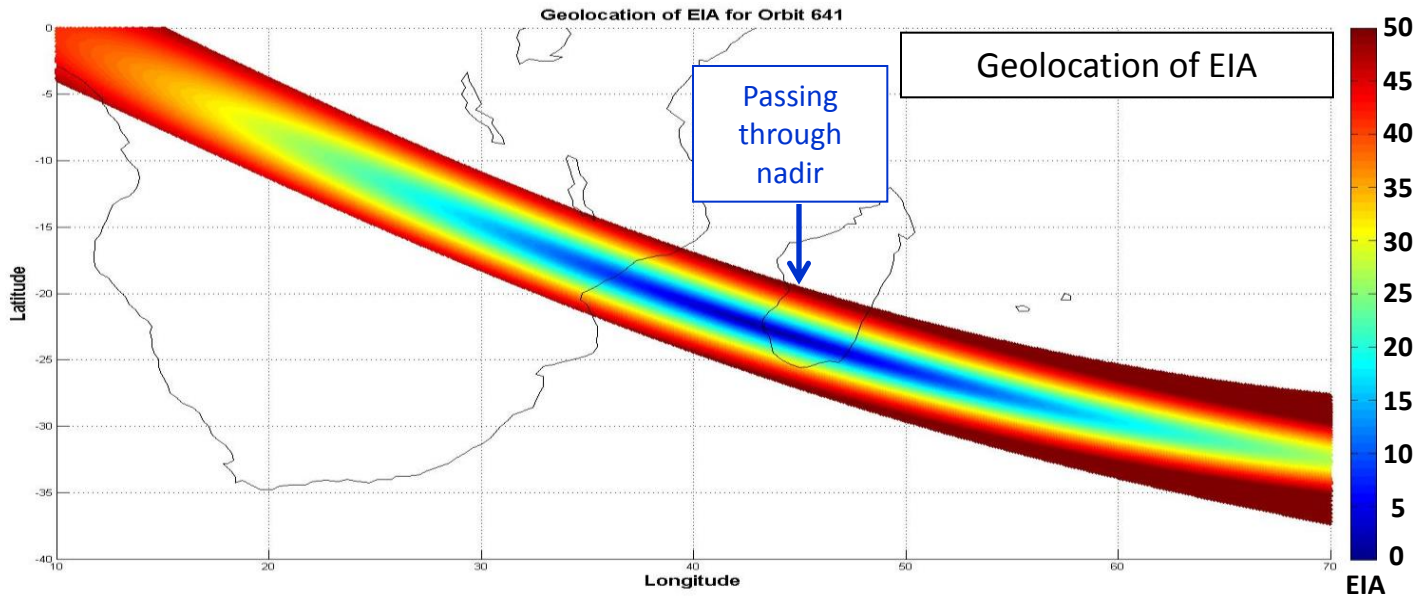
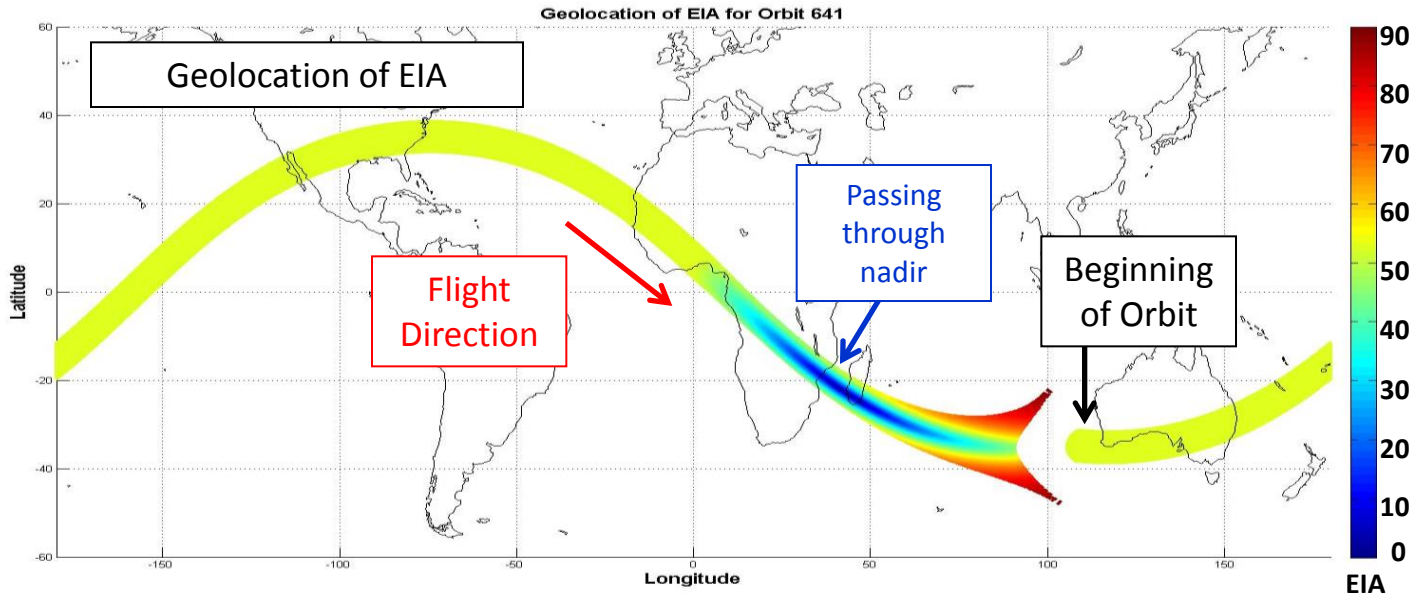


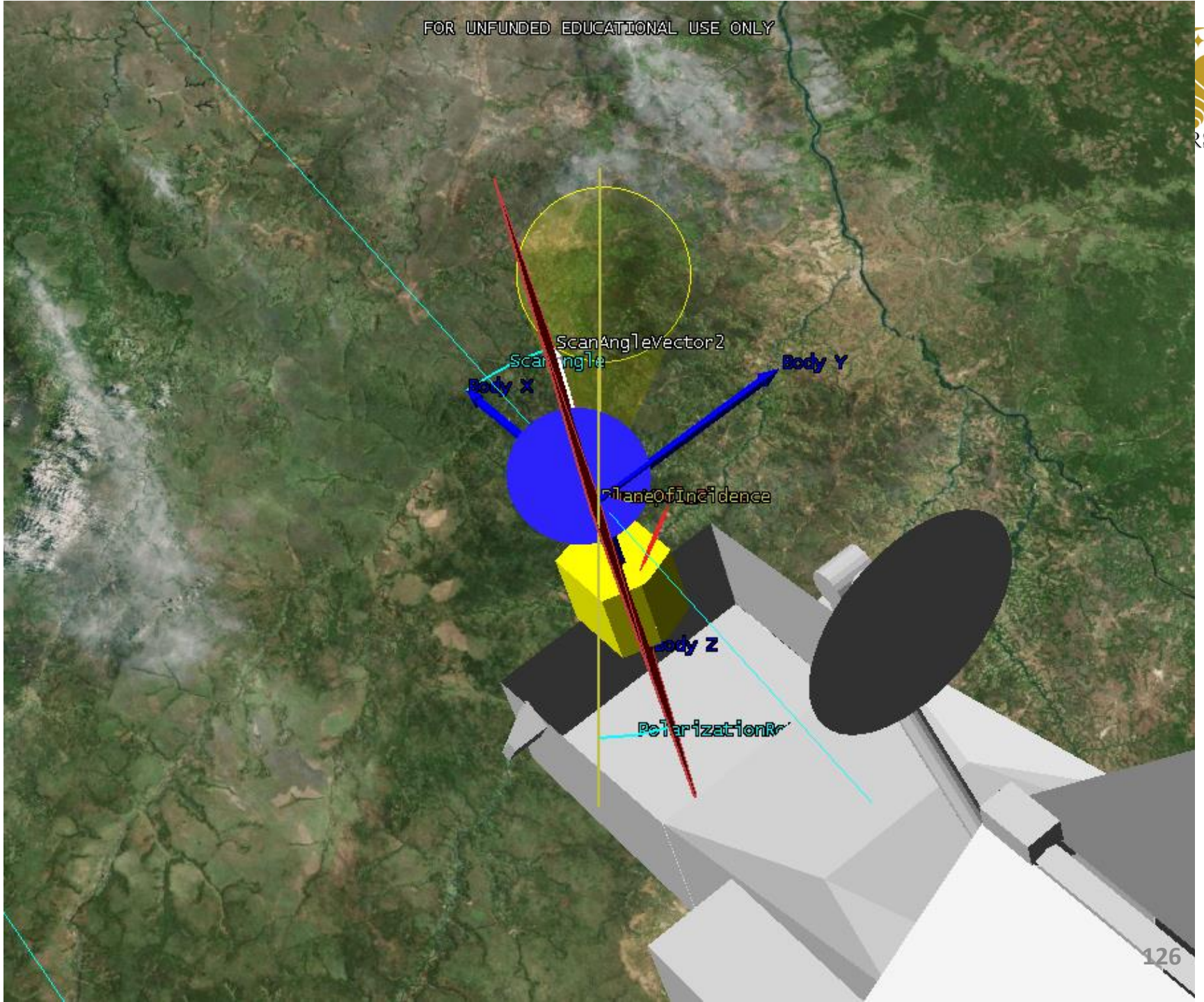
Back Up

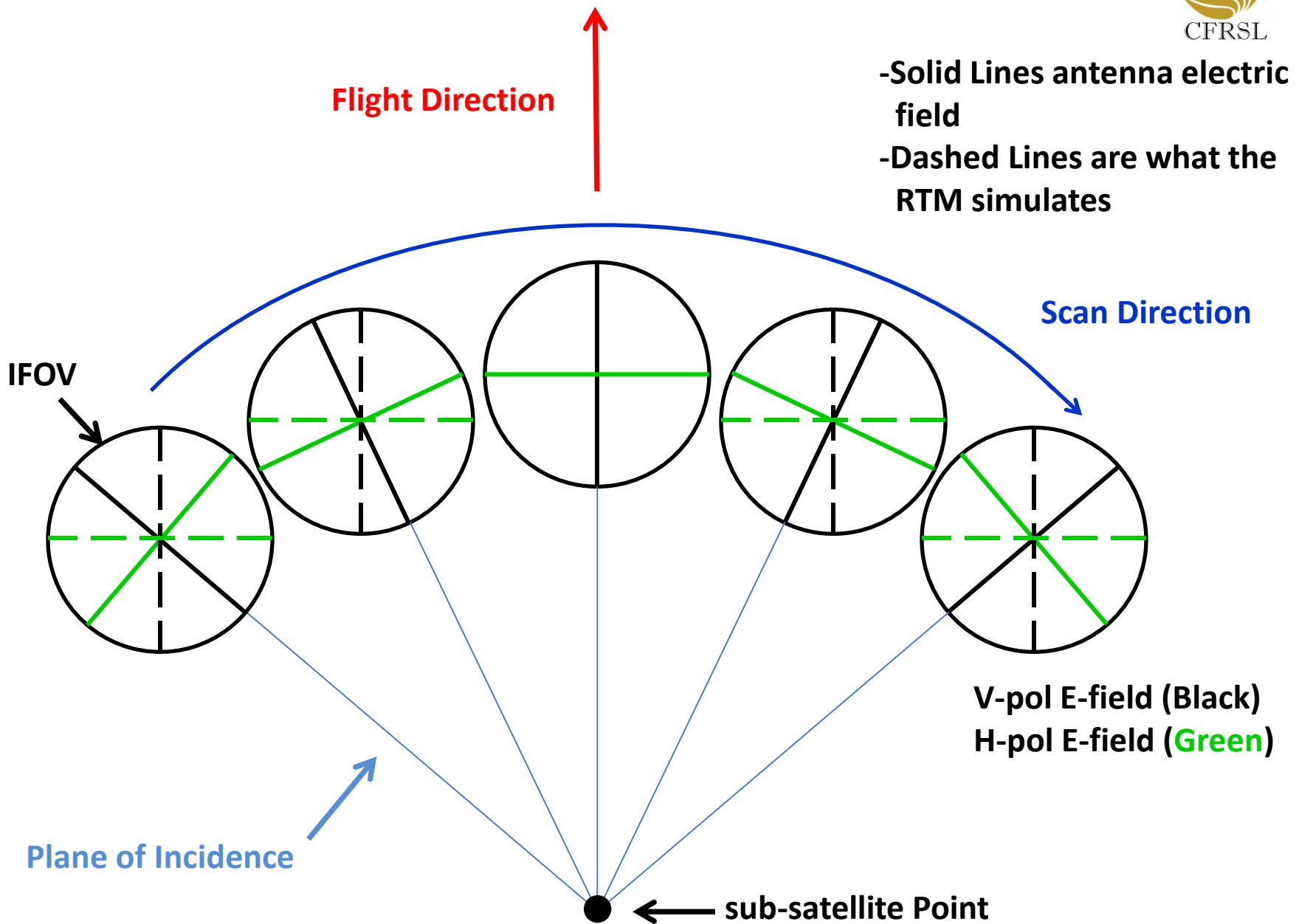
Second Stokes Analysis

SS Analysis Over Ocean Flow Chart



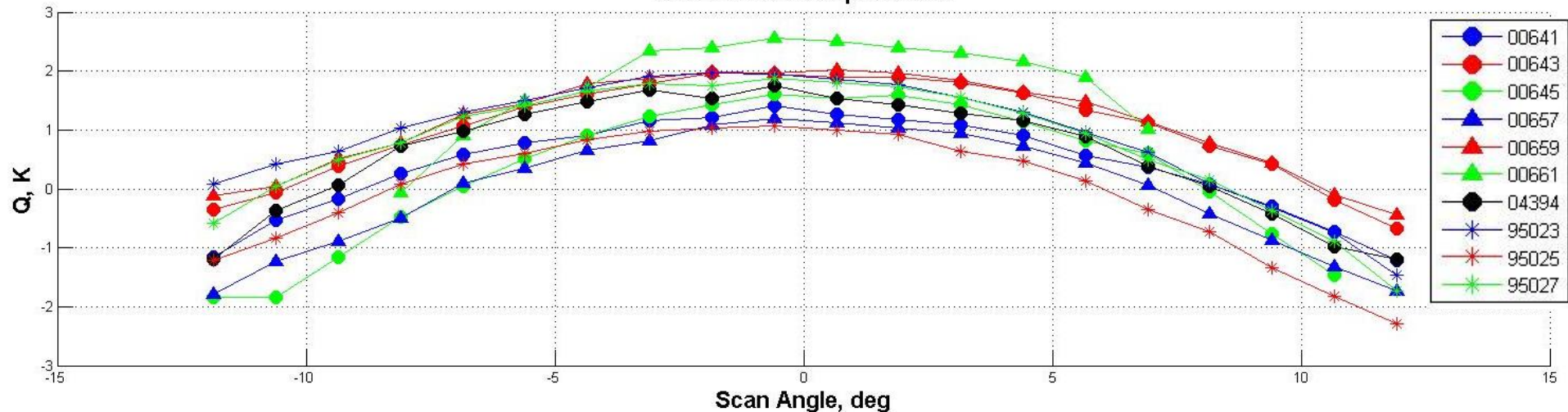




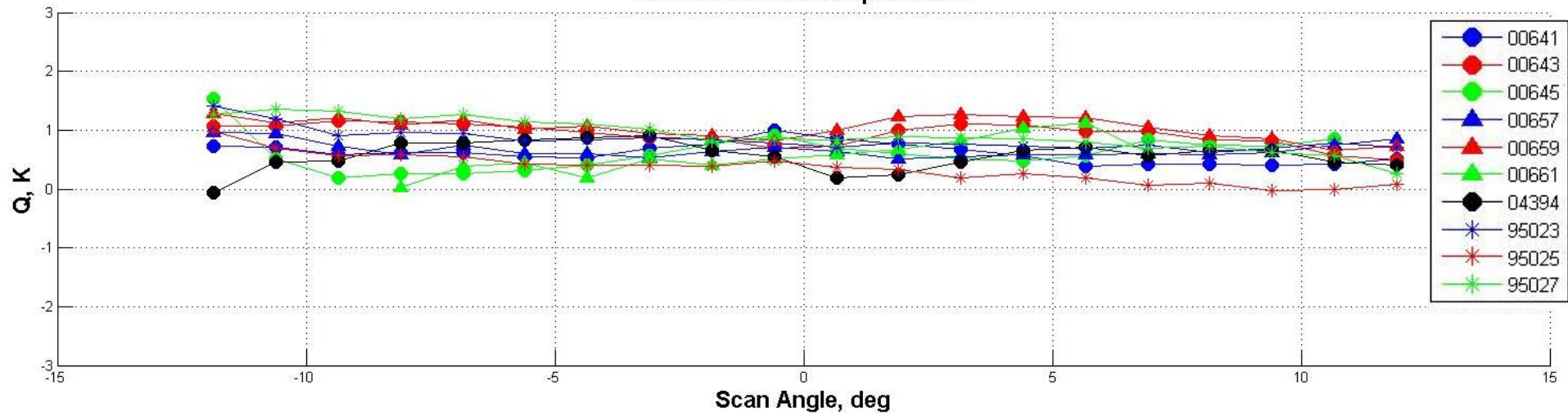


Before & After Correction: 11 GHz

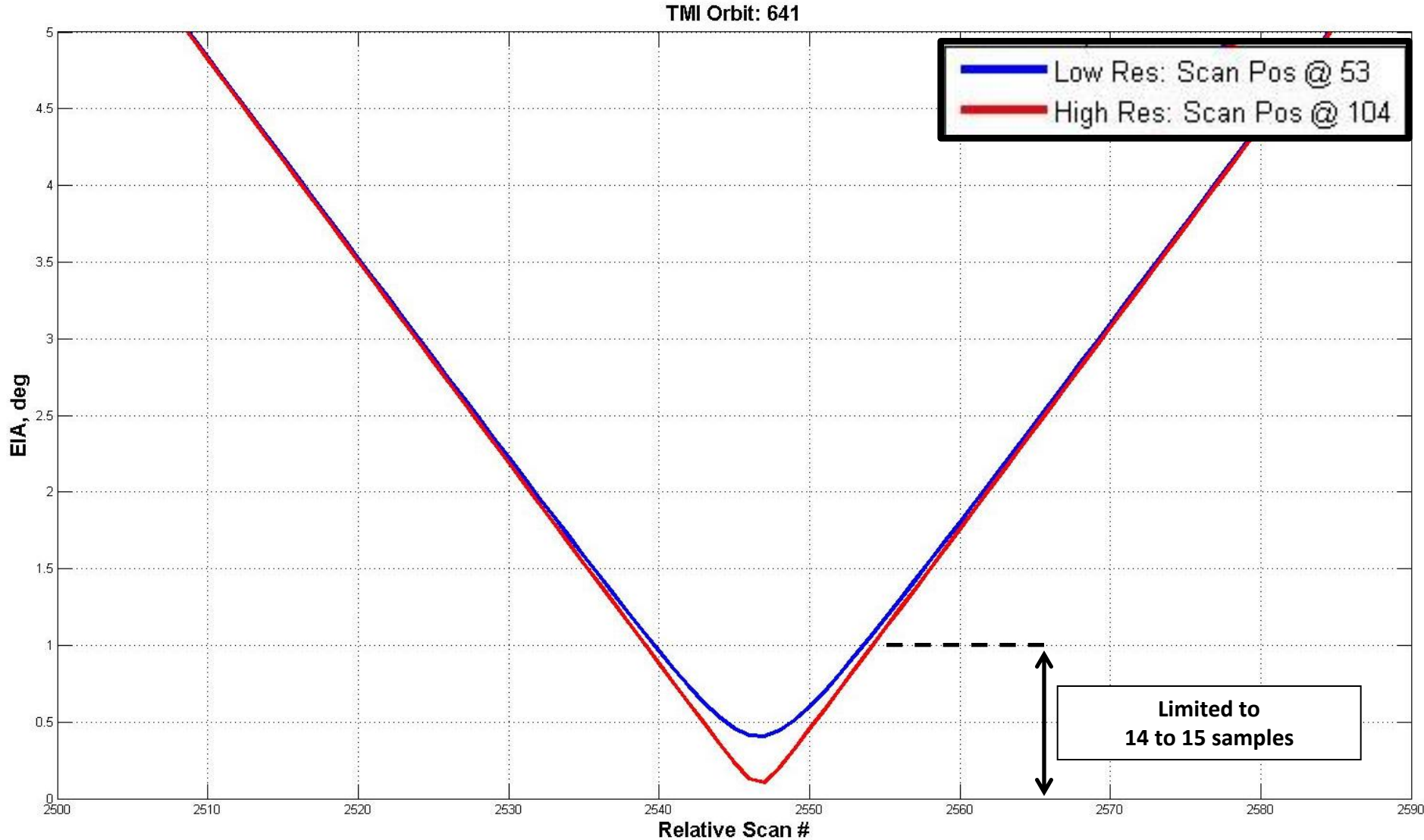
With PR & EIA Dependence



Without PR & EIA Dependence



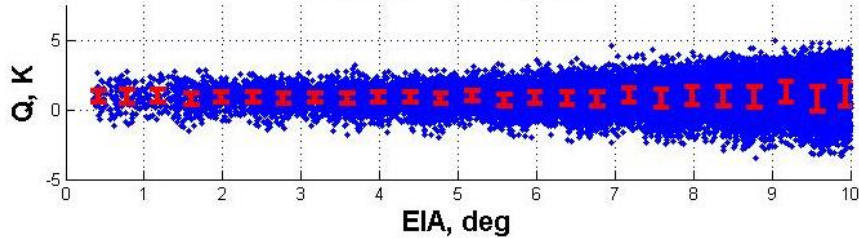
Sweeping Through Nadir



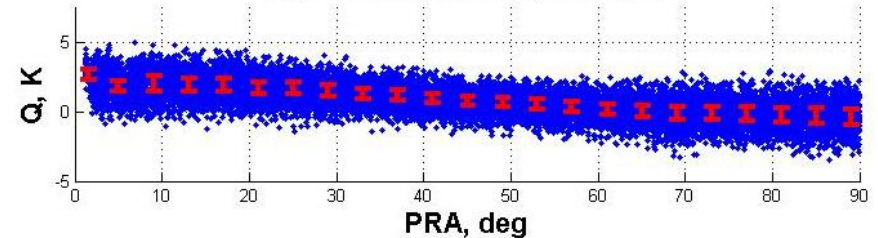
High Res Scan Angle Increment: 0.63°

11 GHz

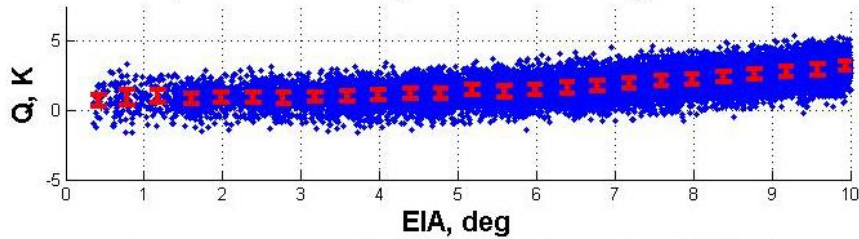
Dependence on EIA, Diff: 0.19



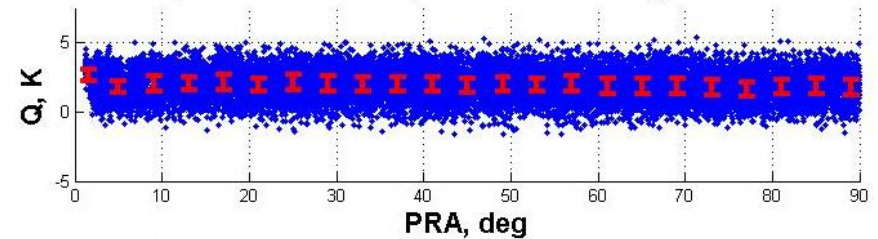
Dependence on PRA, Diff: 3.04



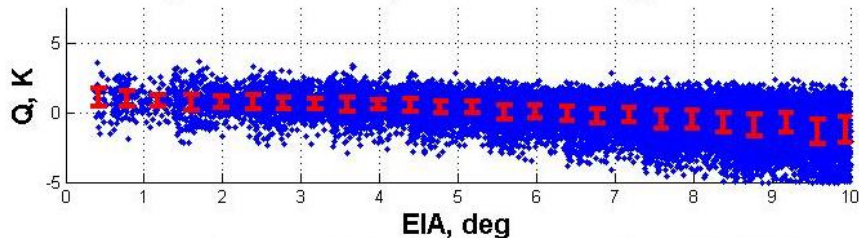
Dependence on EIA, PR corrected only, Diff: 2.55



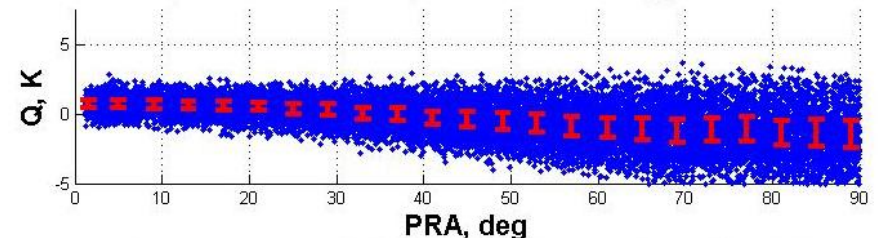
Dependence on PRA, PR corrected only, Diff: 0.87



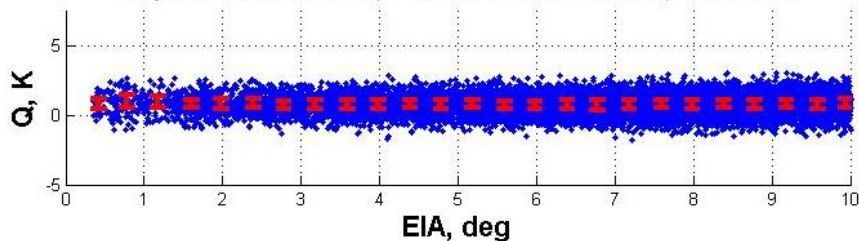
Dependence on EIA, EIA corrected only, Diff: 2.31



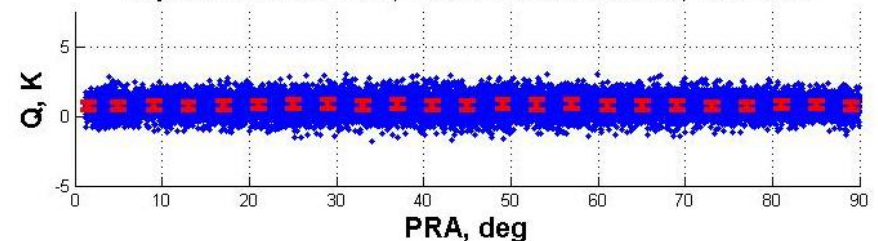
Dependence on PRA, EIA corrected only, Diff: 2.19



Dependence on EIA, EIA & PRA corrected, Diff: 0.05

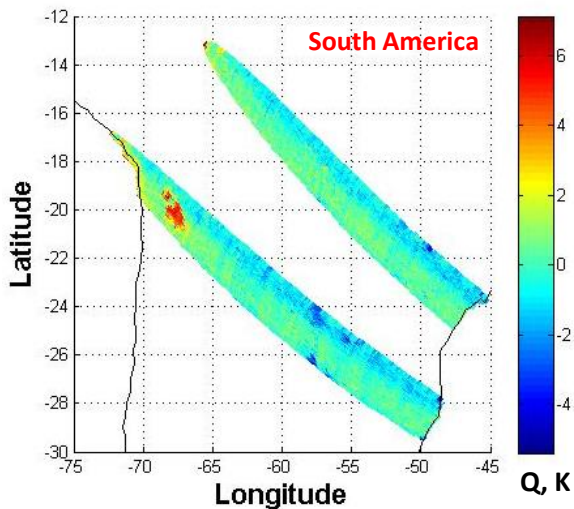


Dependence on PRA, EIA & PRA corrected, Diff: 0.00

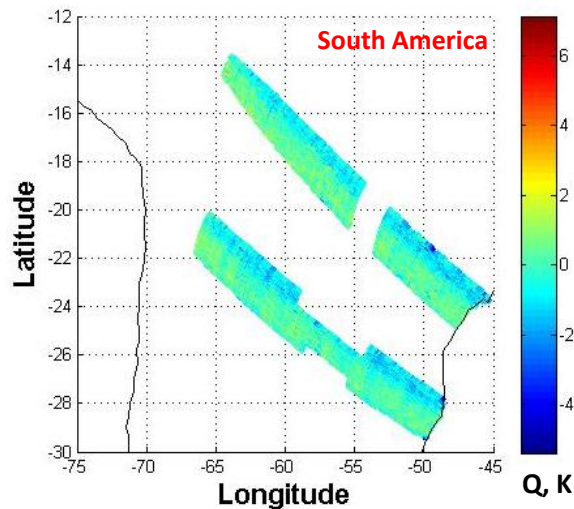


Geolocation of Q Over Land

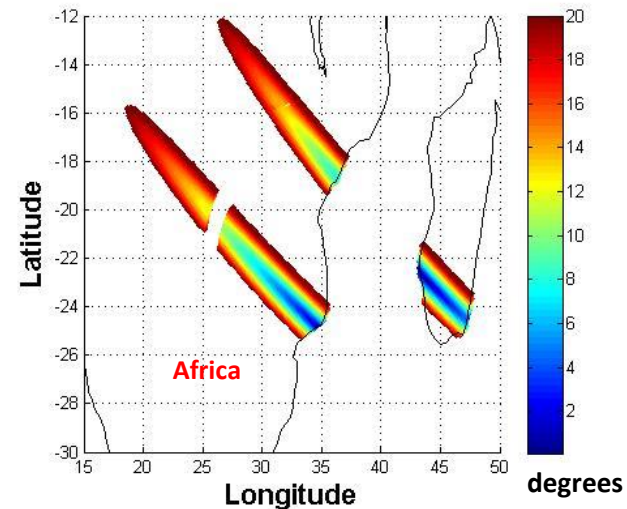
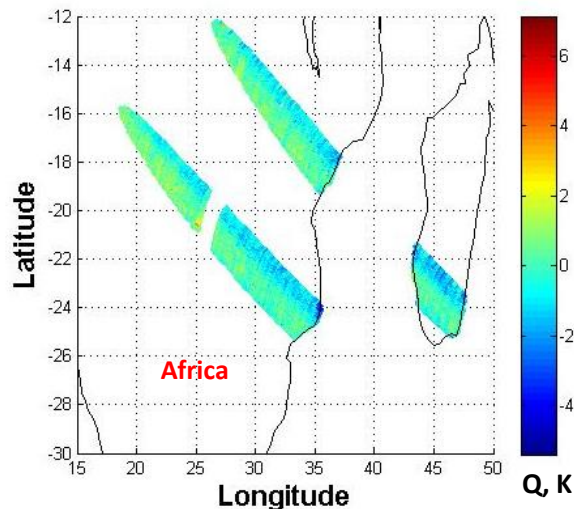
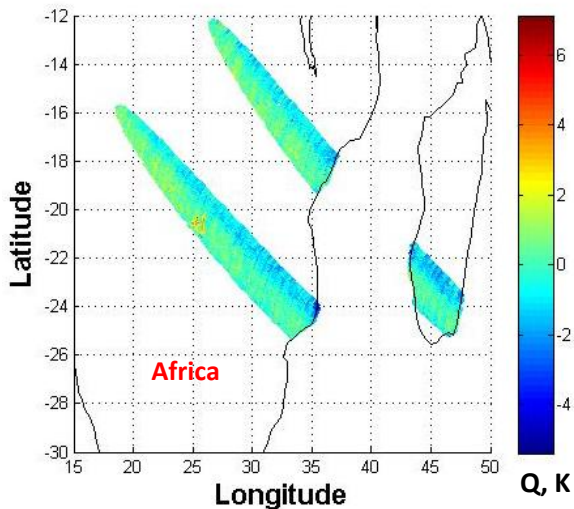
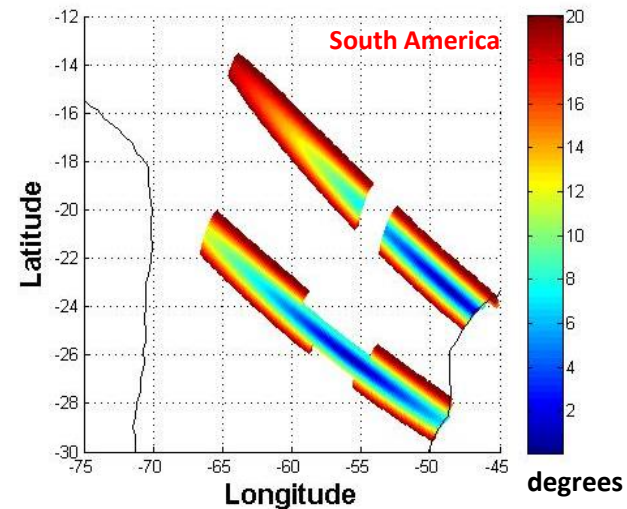
Q at 37GHz Before Removal
Of Contaminated Areas



Q at 37GHz After Removal
Of Contaminated Areas



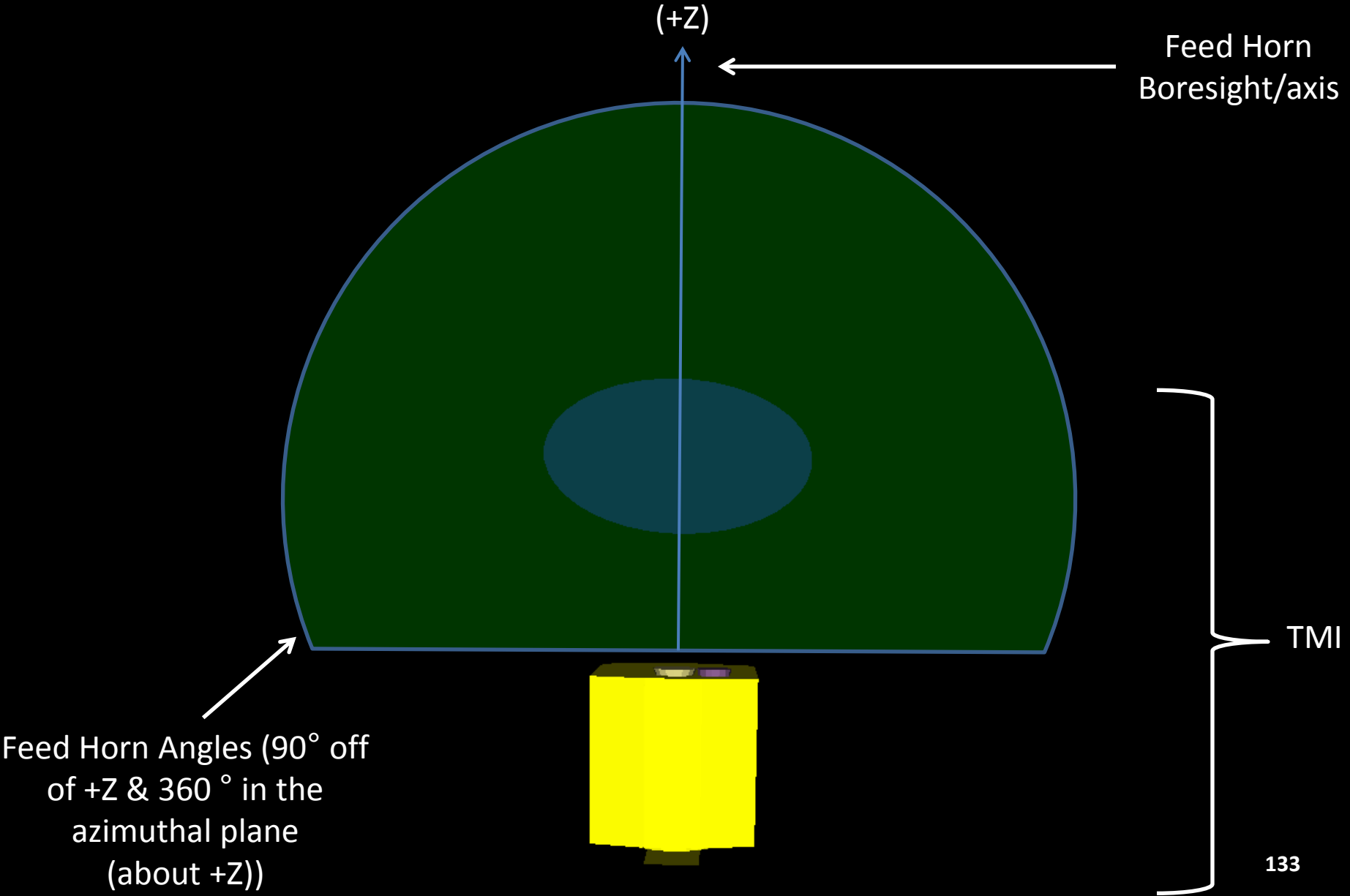
EIA After Removal Of
Contaminated Areas



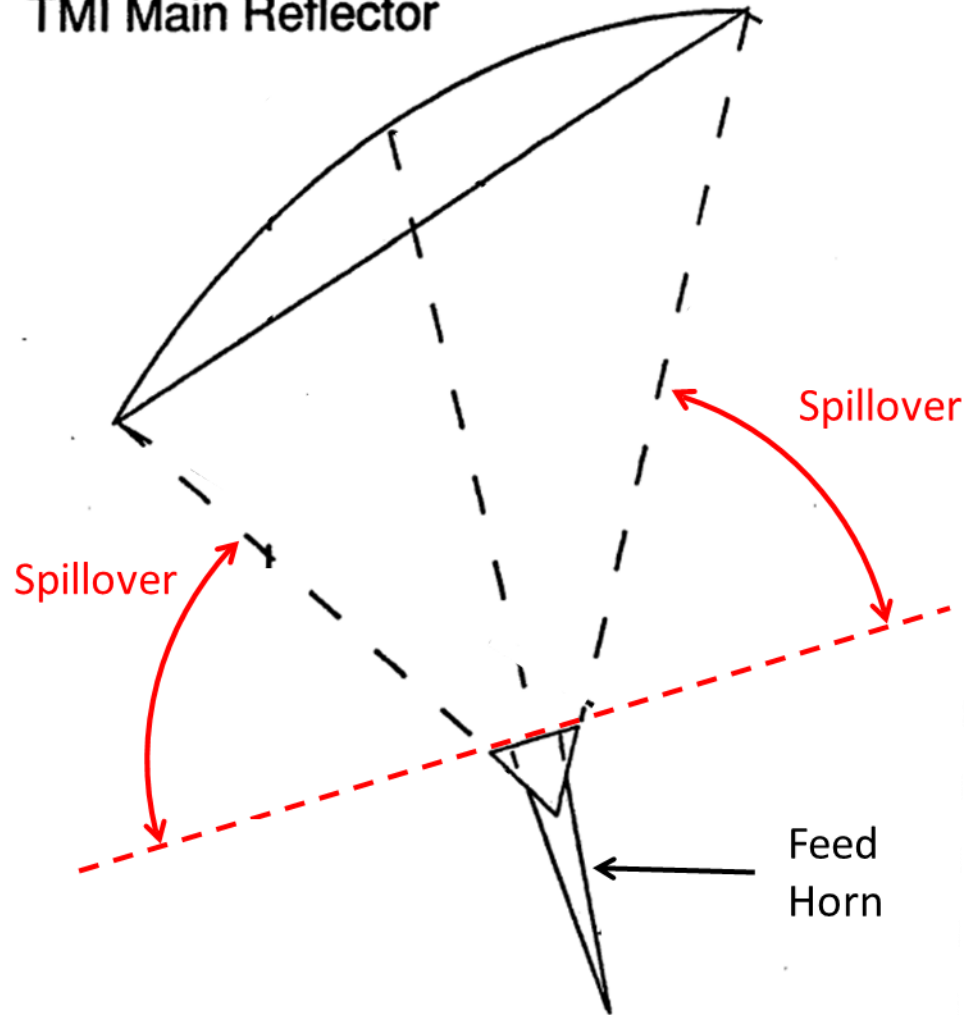
Back Up

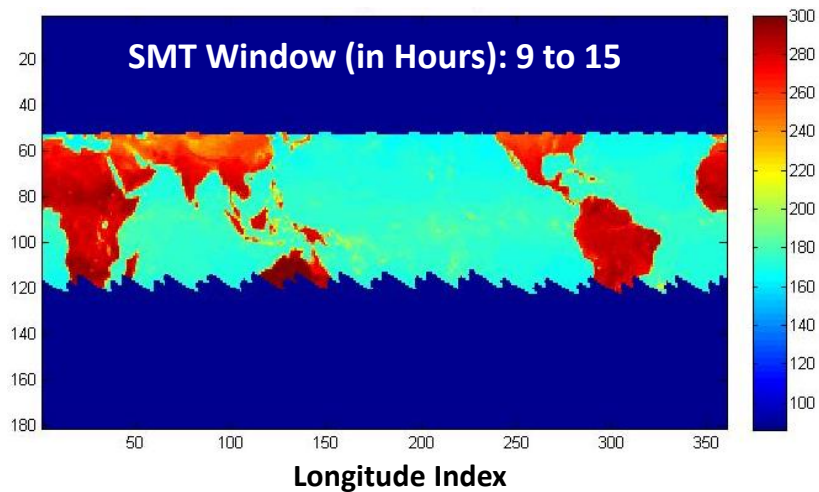
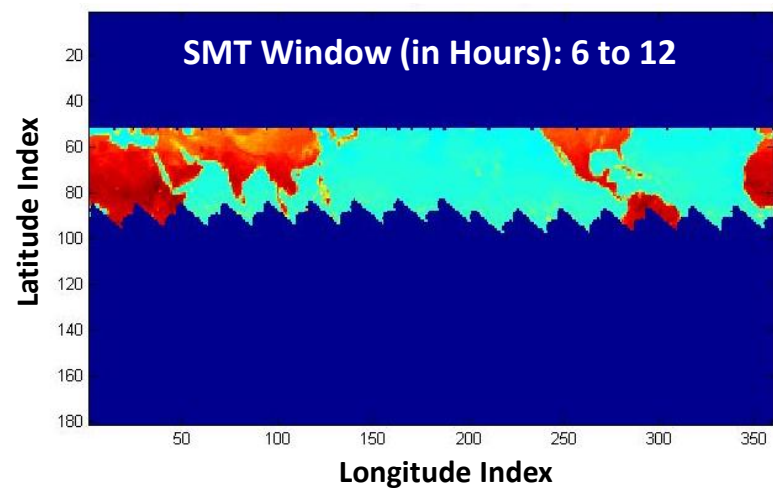
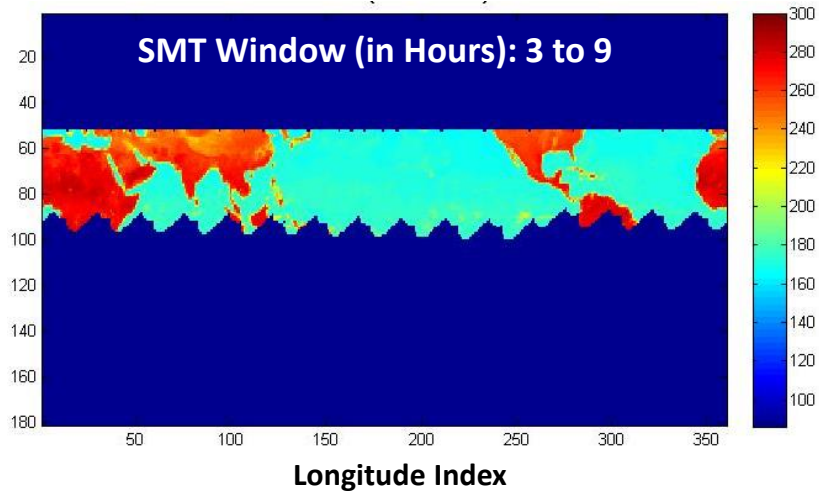
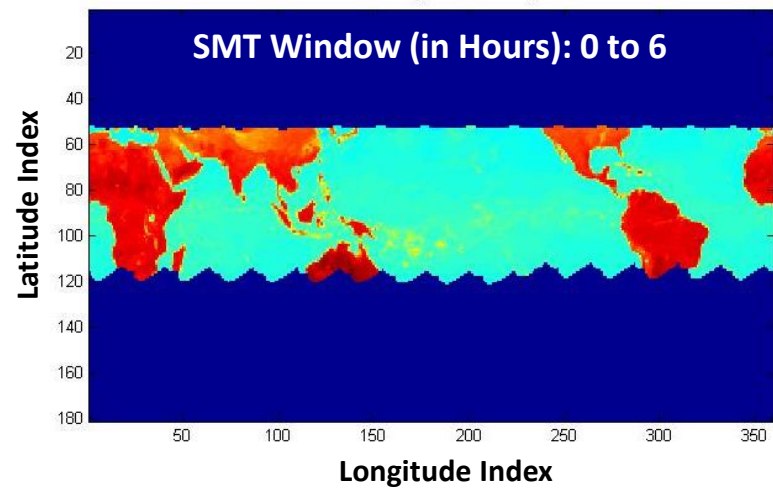
Emissivity

Angles Feed Horn is Defined As

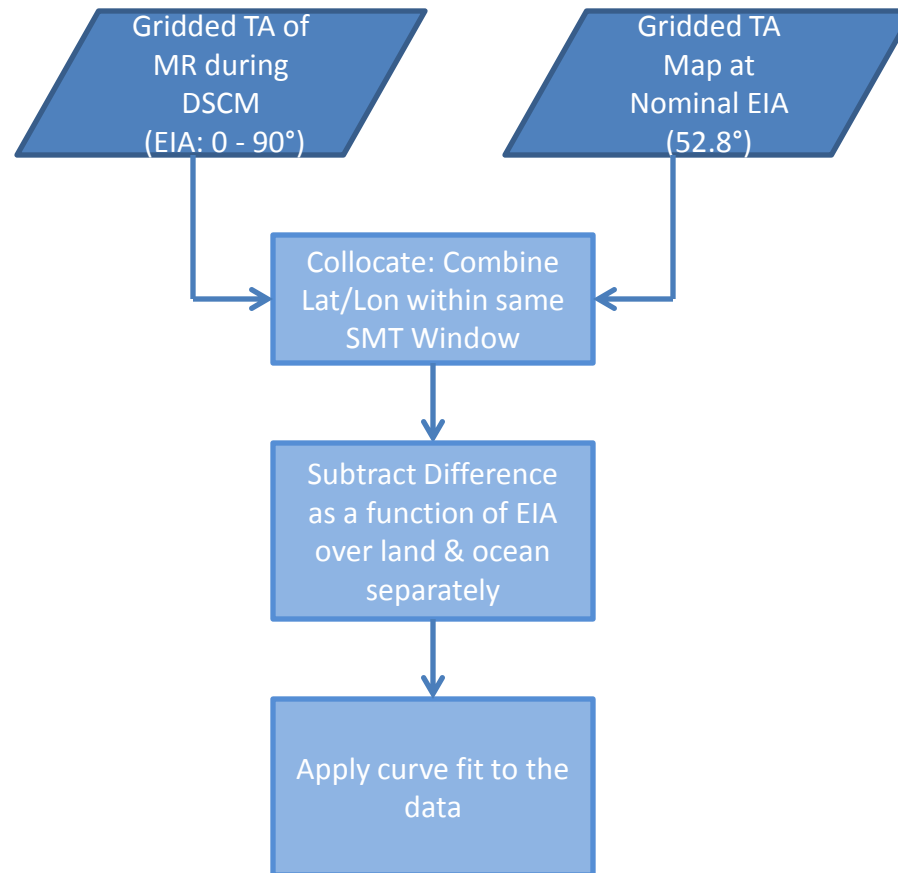


TMI Main Reflector

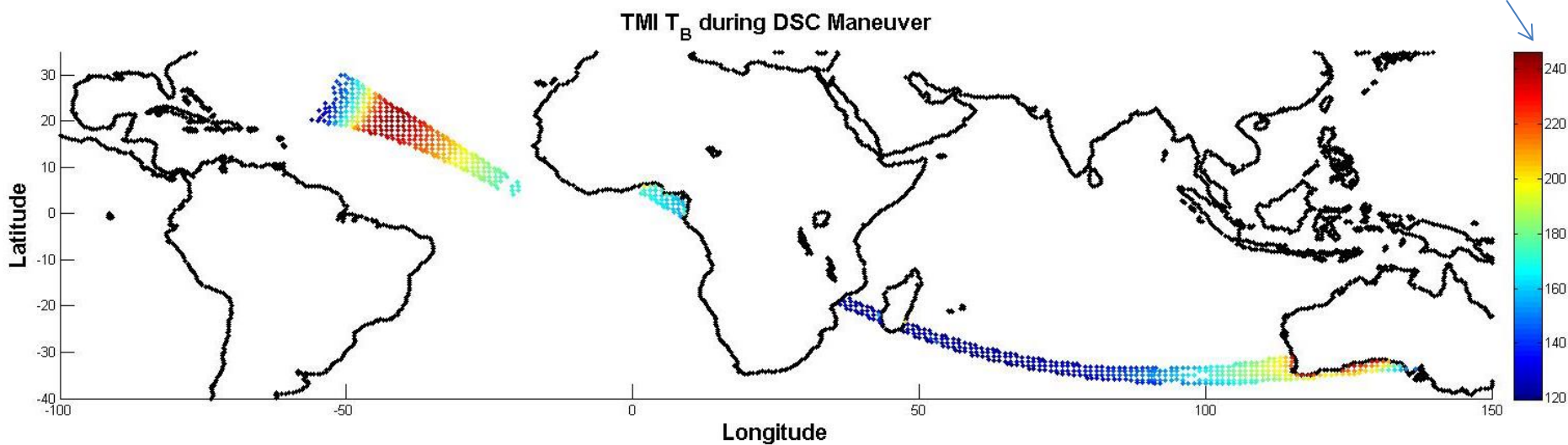
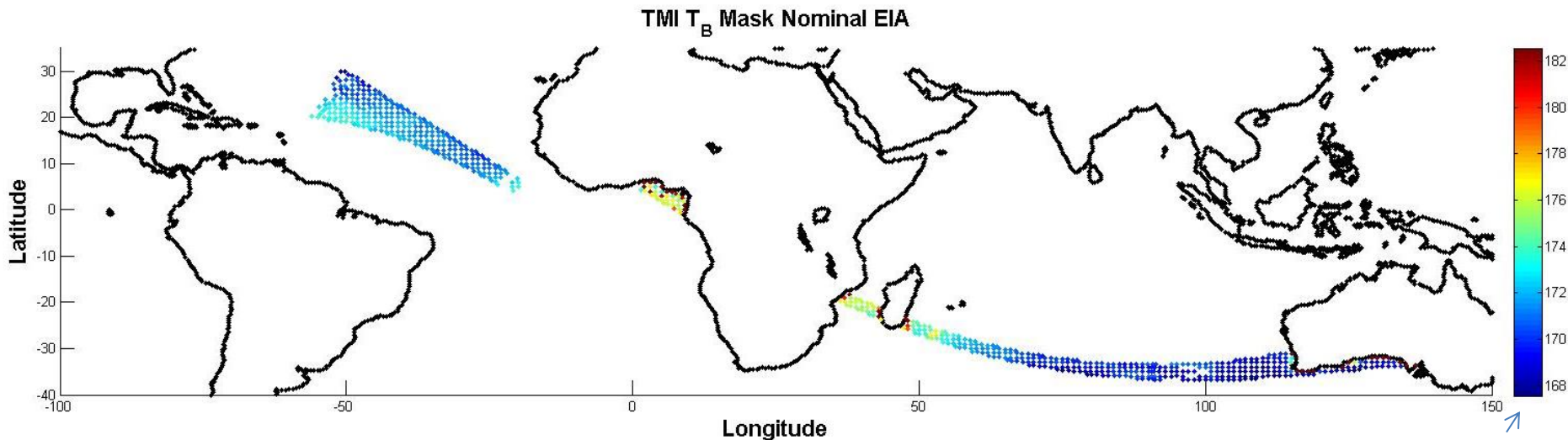




Empirical Method Flow Chart



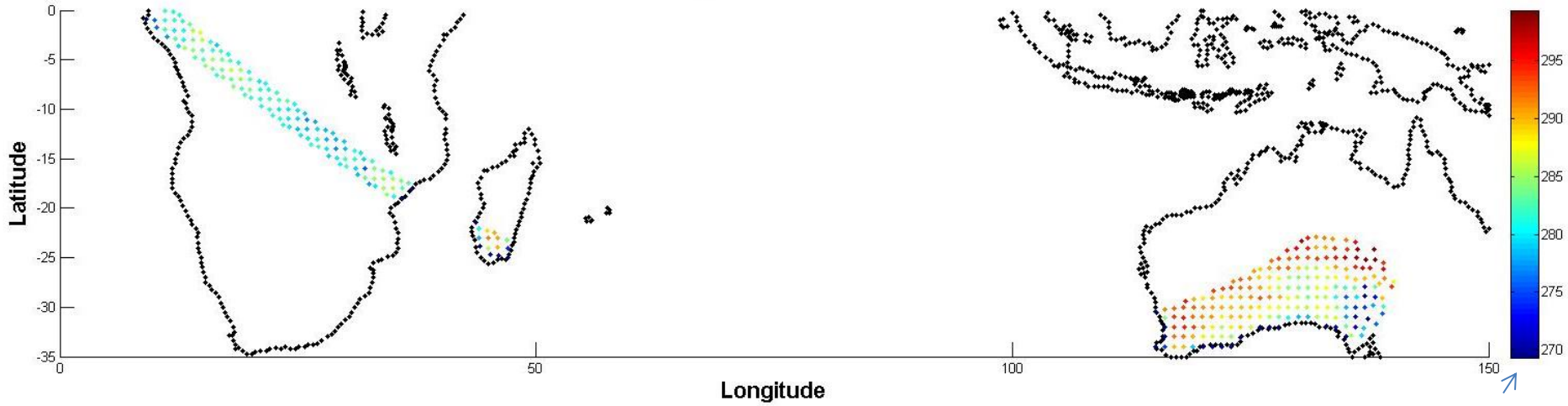
Orbits: 641 & 642 (Ocean)



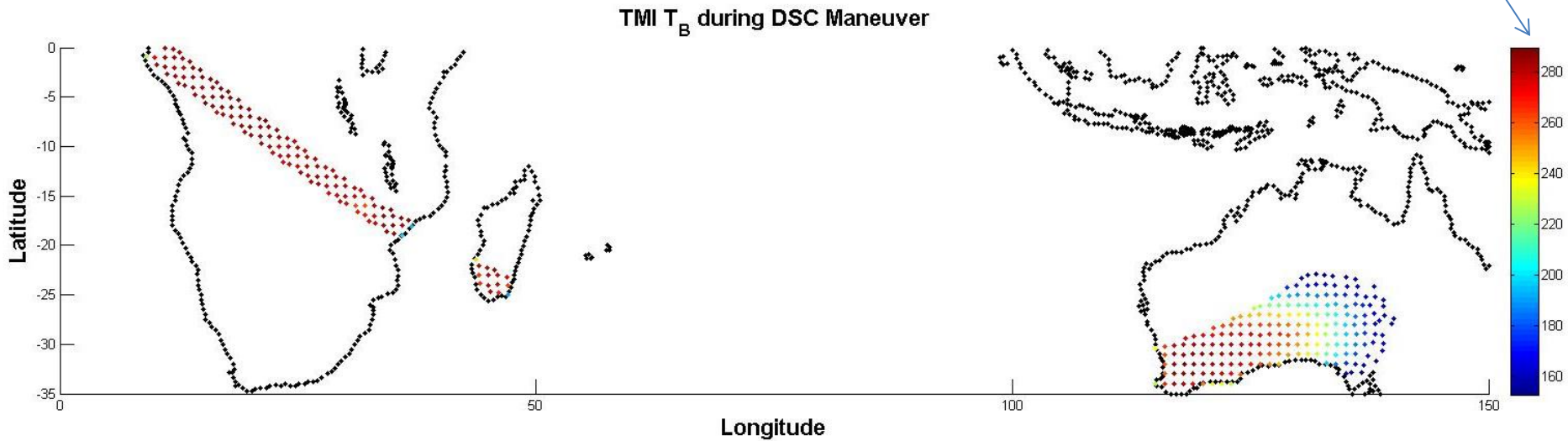
Orbits: 641 & 642 (Land)



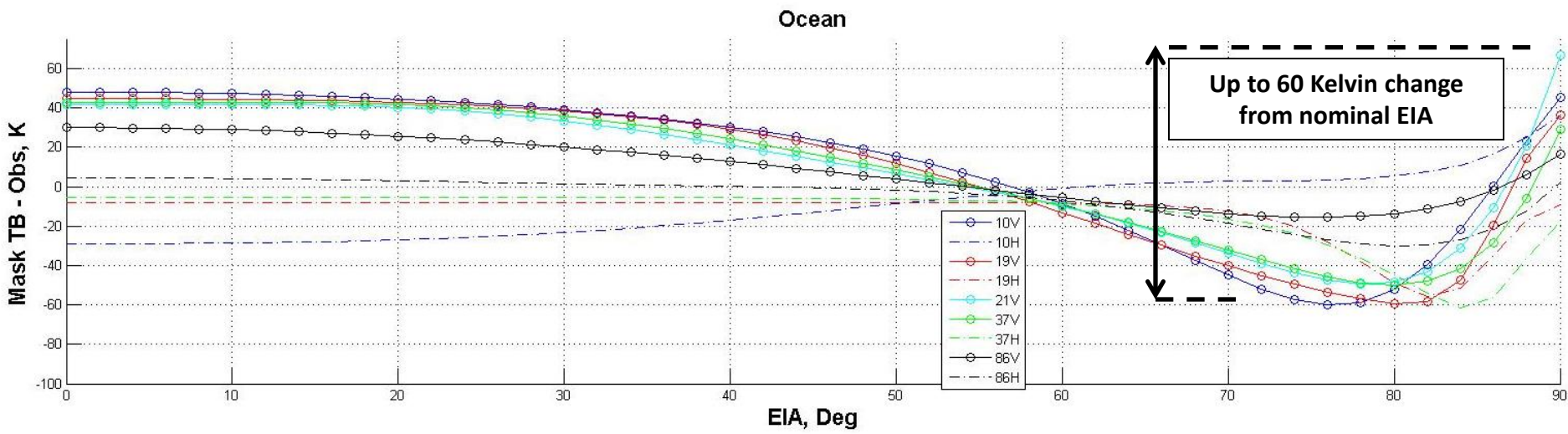
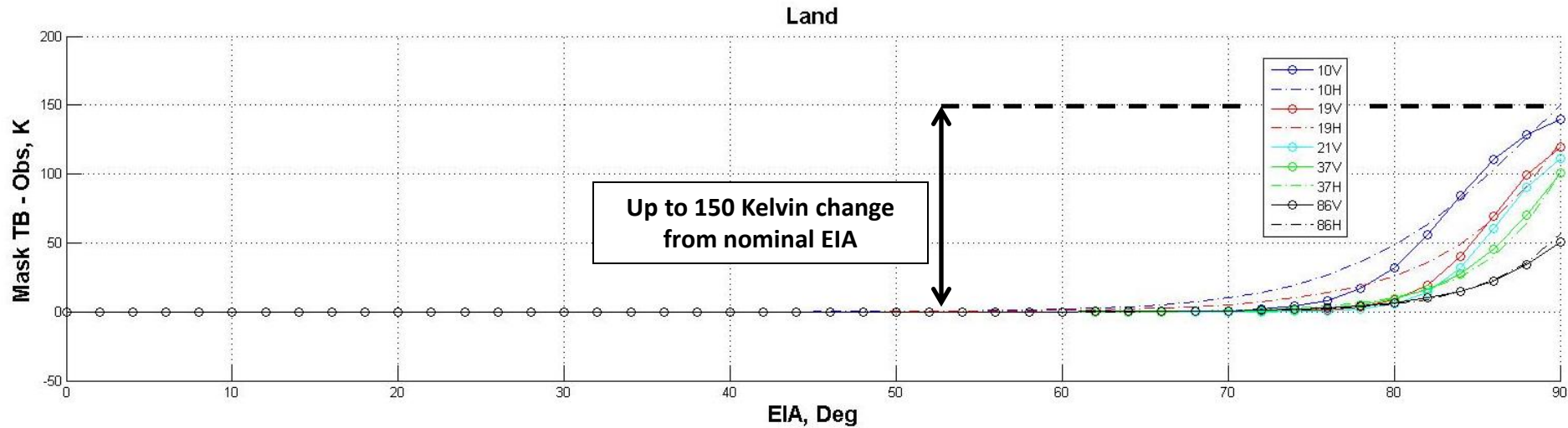
TMI T_B Mask Nominal EIA



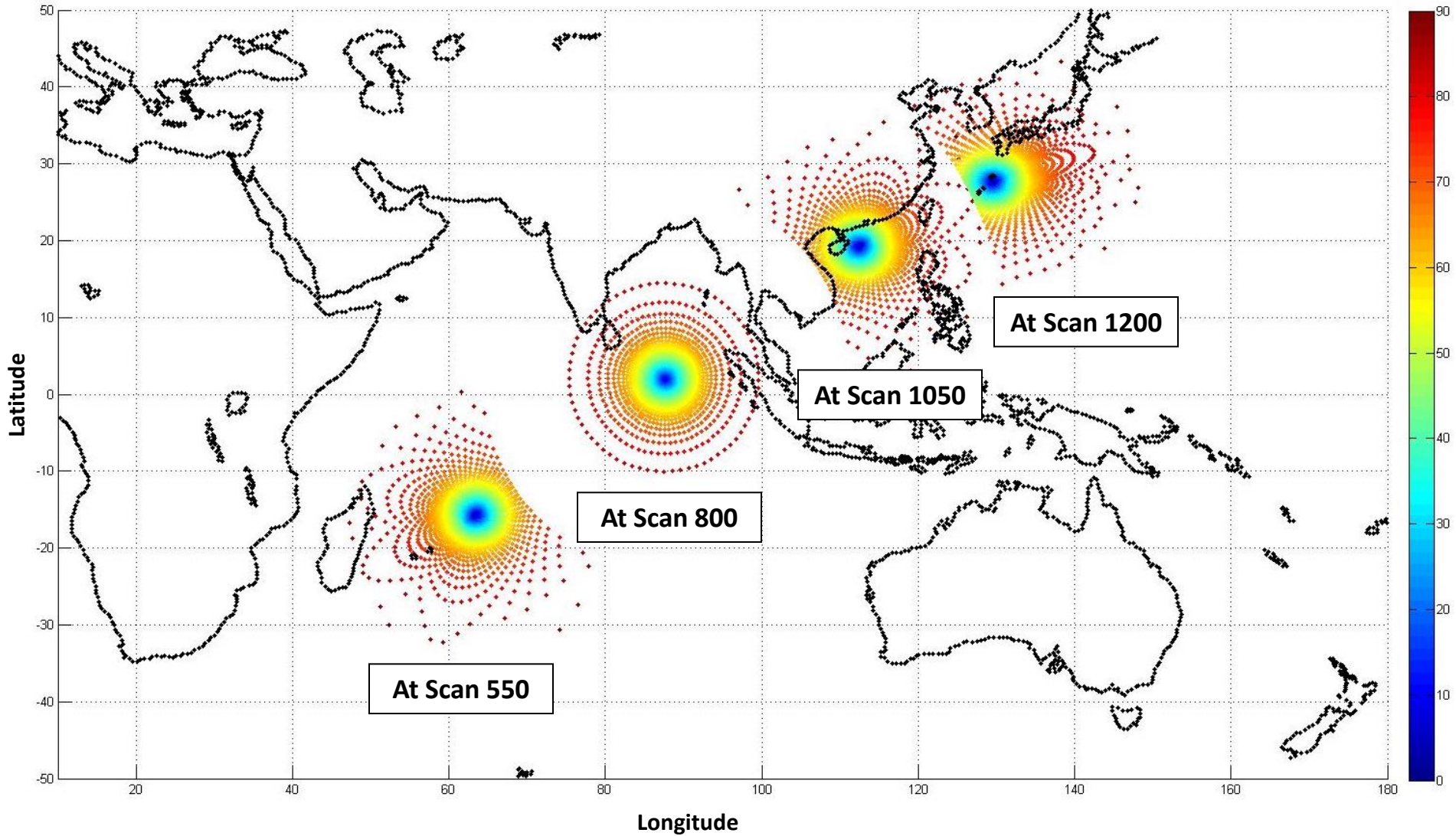
Different color scale



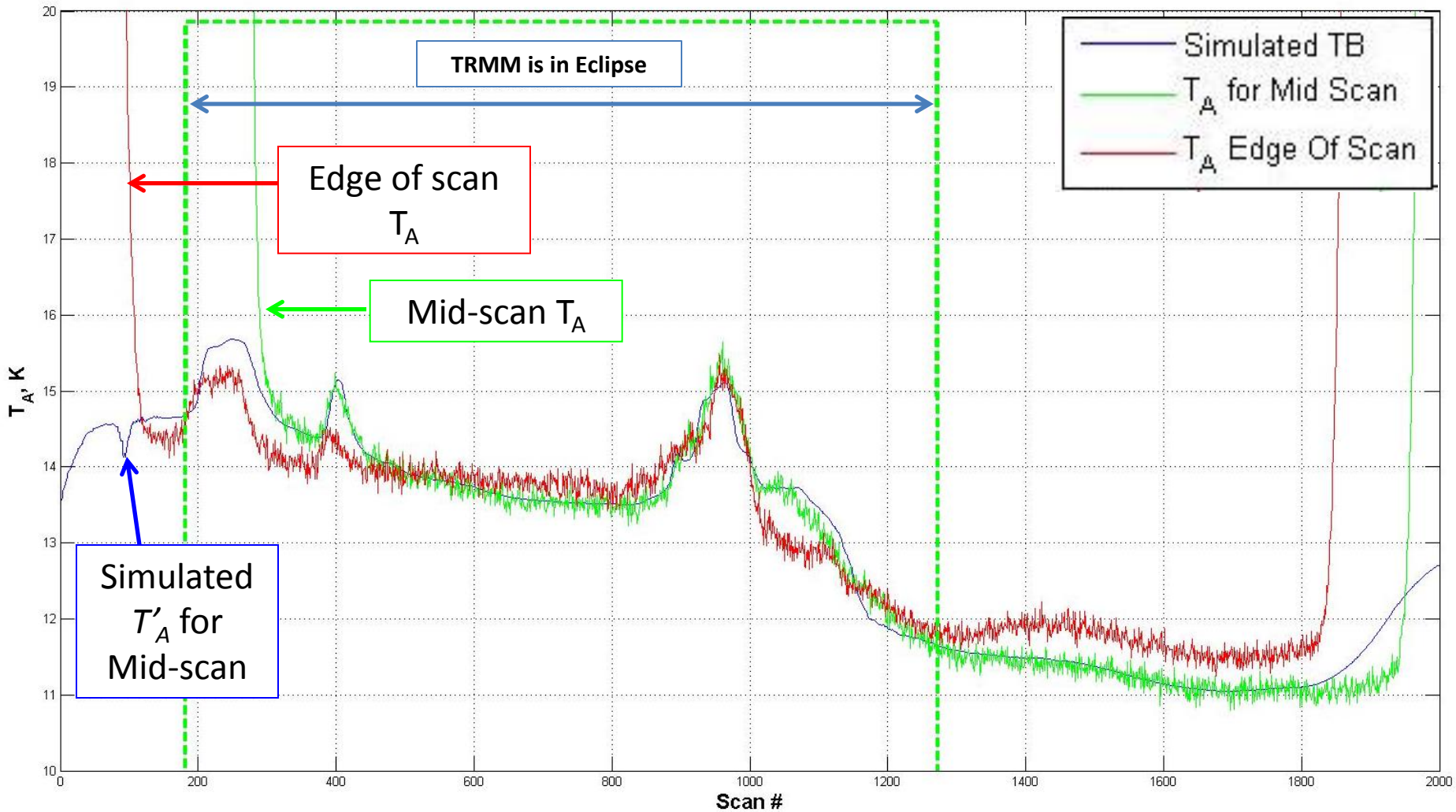
T_B to EIA Empirical Relationship



EIA of Spillover



Matching Simulated T_A to Truth: 10V

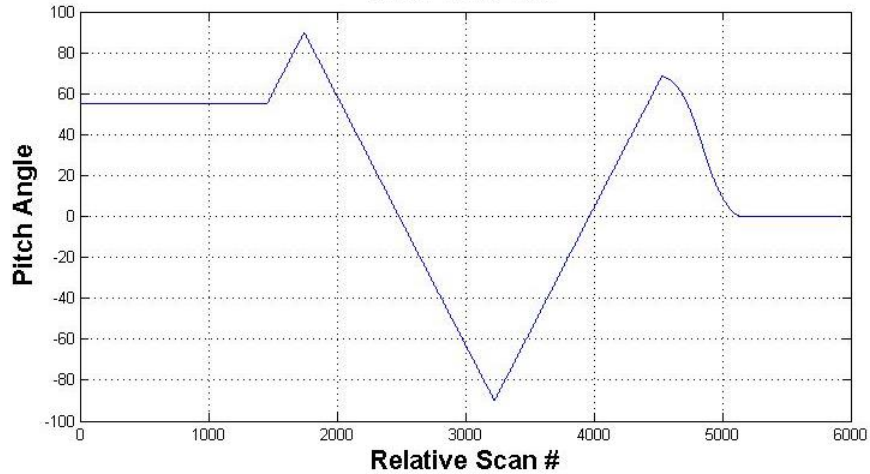


GMI MR Physical Temperature: Inertial Holds



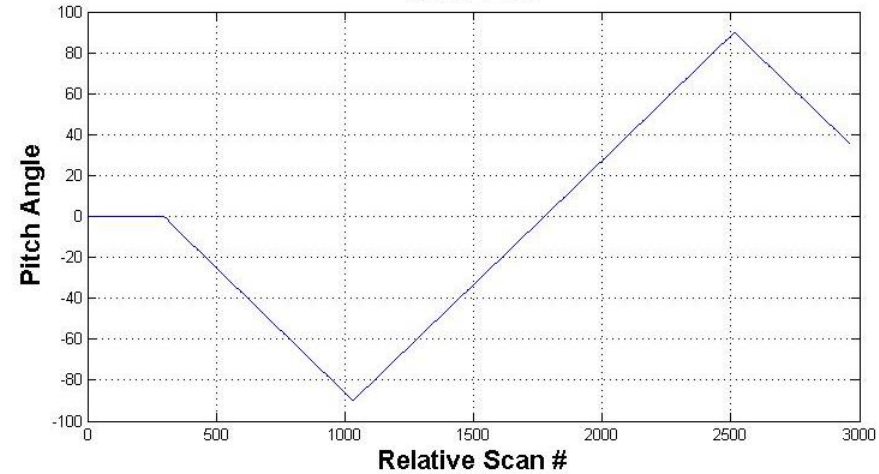
May 20, 2014 Maneuvers

Orbit: 1276-1277

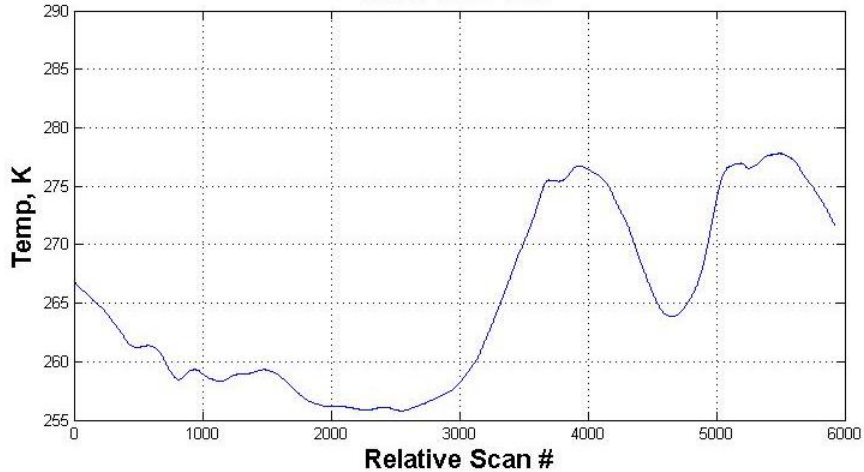


Dec 09, 2014 Maneuvers

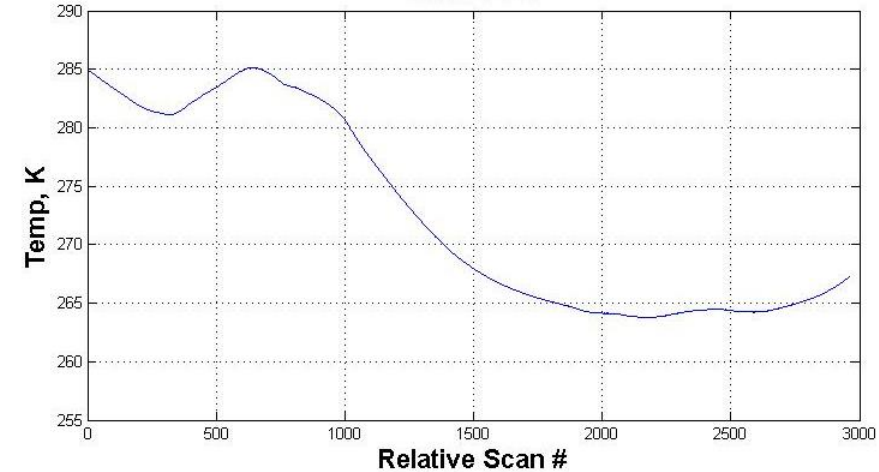
Orbit: 4425



Orbit: 1276-1277



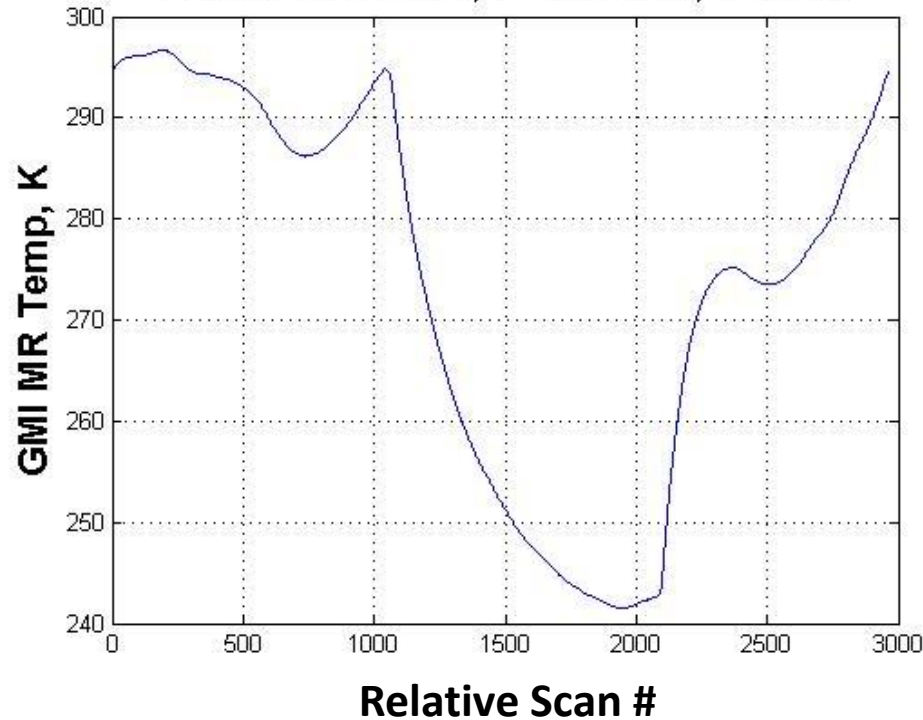
Orbit: 4425



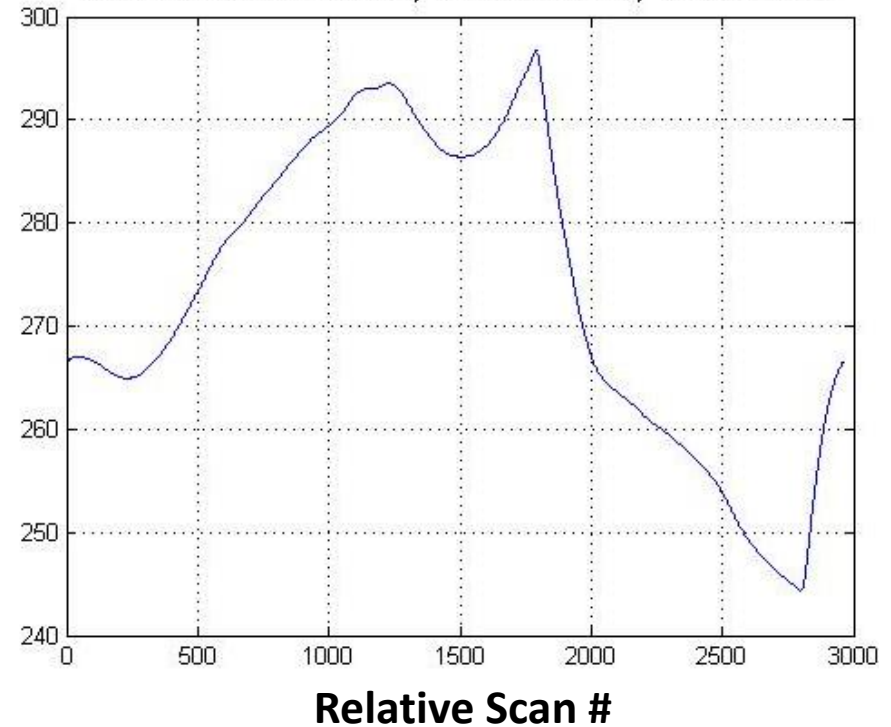
GMI MR Physical Temperature: Normal Orbit



For Beta of 44.33, Orbit: 5102, Yaw: 0



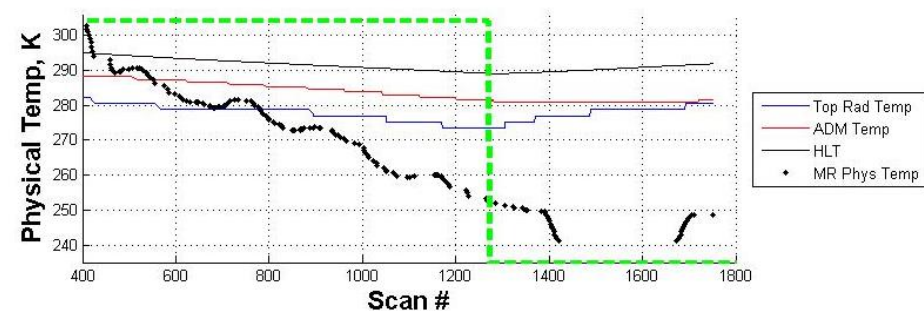
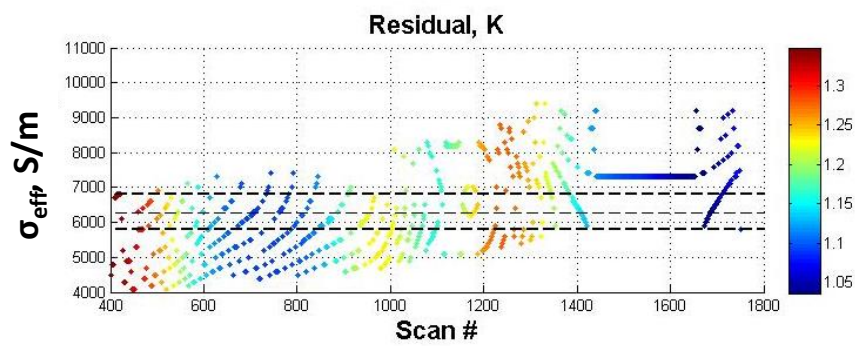
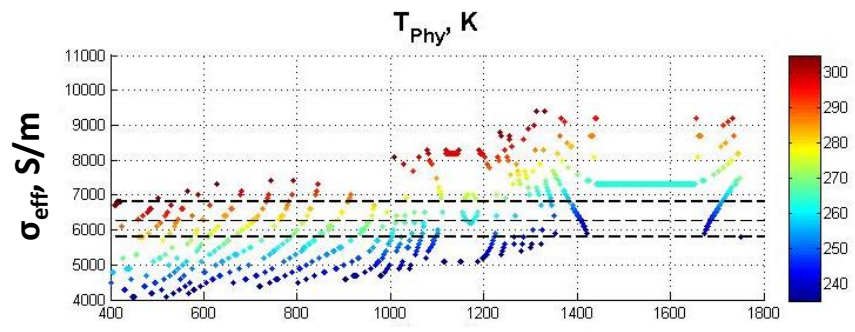
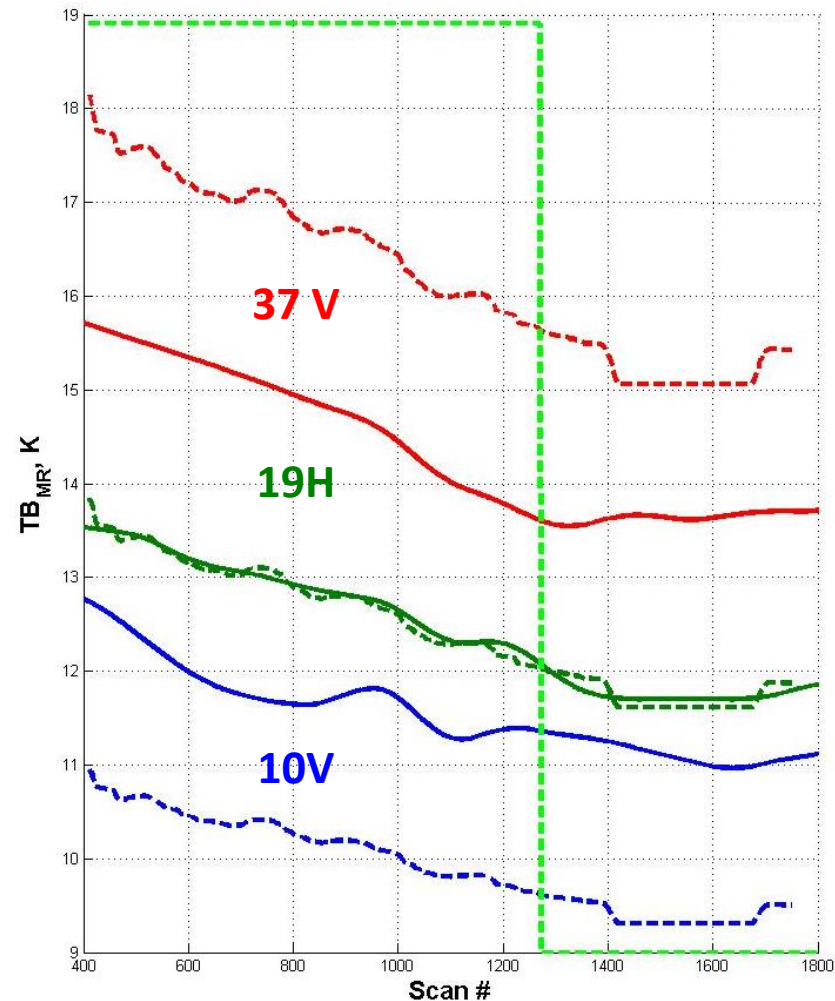
For Beta of -45.55, Orbit: 5548, Yaw: 180



Determining Conductivity

----- Lines: Is what I use determine σ_{eff}
 ——— Lines: Using σ_{eff} and $T_{\text{MR,Phys}}$ to recalculate TB,MR

Scan Bias Correction off

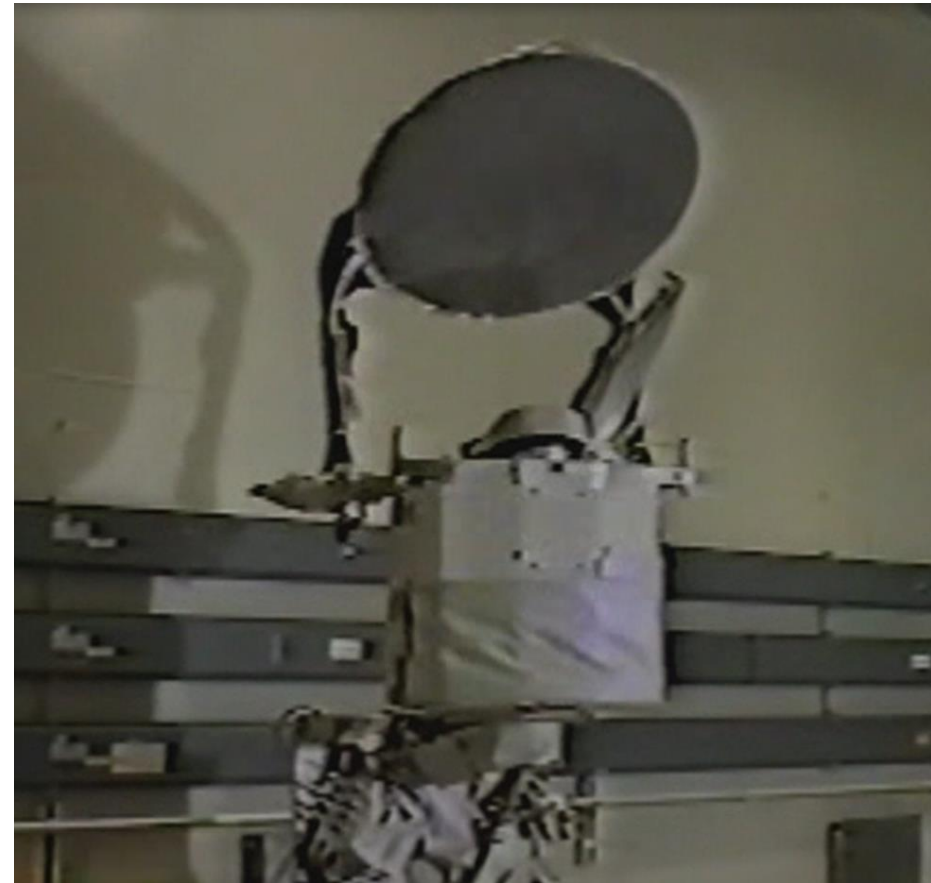
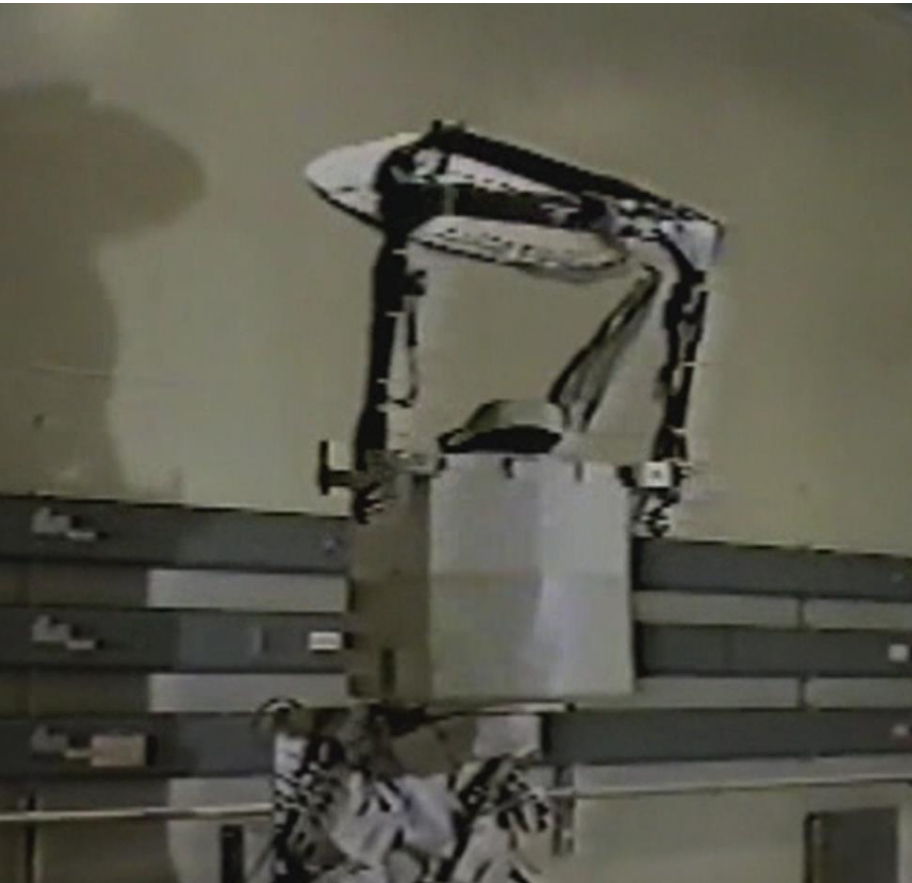


Reasons for Disagreement in Conductivity



- Reconstructed TA is imperfect
- Scan Angle Bias is not corrected for
- There can be an entire TB offset that we are not correcting for
- Imperfections in the Spillover Map – maybe use ERA-I
- Polarization Rotation should be corrected in while using the Spillover Map?
- Feed Horn Pattern is not correct
- 10 GHz feed horn squint angle is not applied

Why I Believe Sun Intrusion into the Warm Load Occurs

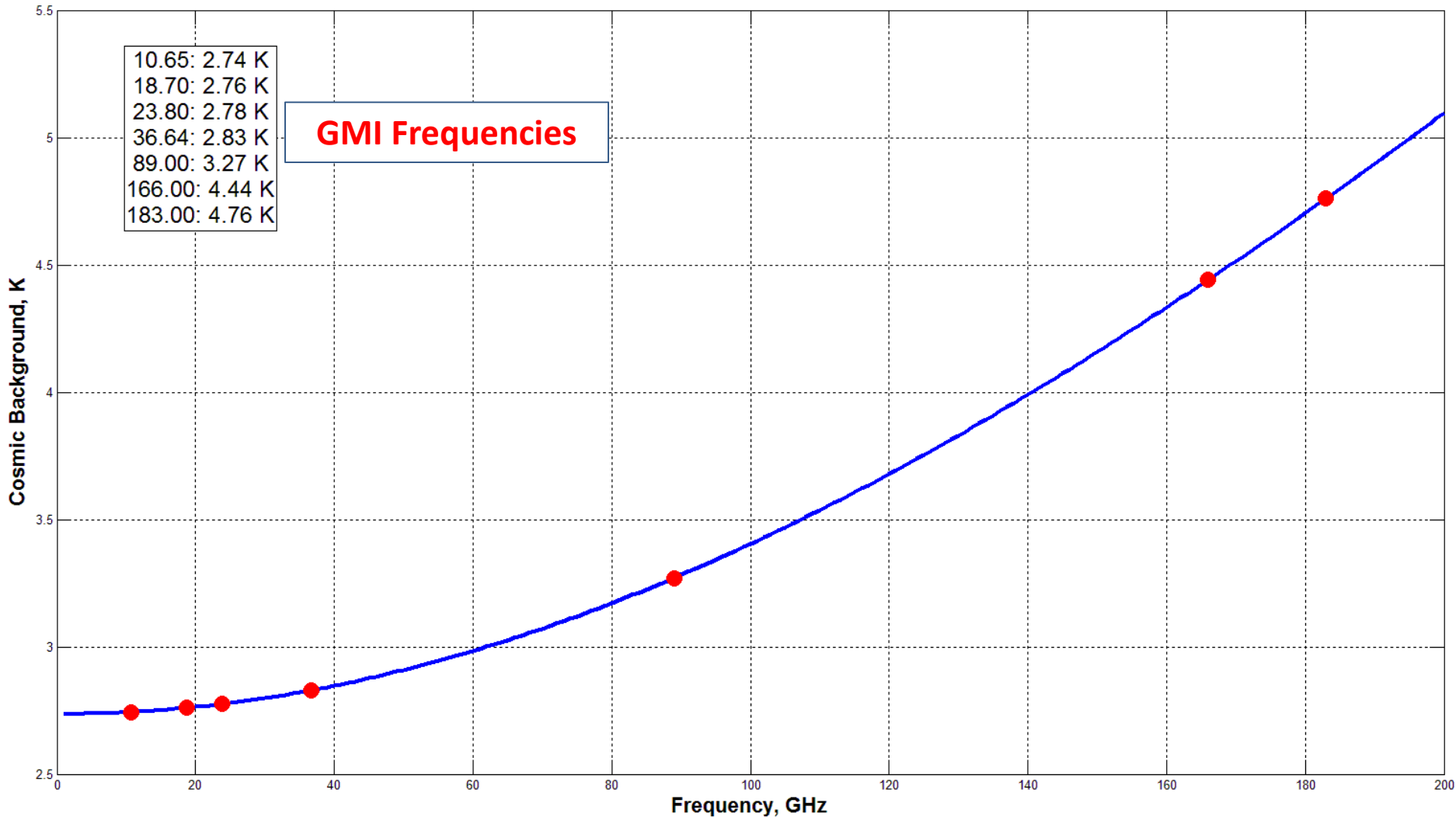


BackUps From Proposal

Cosmic Background



Rayleigh-Jeans Approximation of the Cosmic Background T_B



GMI Frequencies

Notes 2:

- Cosmic Microwave Background (CMB)
 - Thermal radiation left over from the Big Bang of cosmology, i.e., radiation left over from an early stage in the development of the universe
 - Is a cosmic background radiation that is fundamental to observational cosmology because it is the oldest light in the universe